Environmental Biosystems

Graduate Programs in Environmental Systems

Graduate School of Environmental Engineering

The University of Kitakyushu

PhD Thesis

Studies on the multi-biological functions of α-mangostin including inhibition of cancer metastasis, reduction of cell stiffness and activation of leukocytes

2017DAB402

PHAN THI KIEU TRANG

(June 2020)

Supervisor: Takanori Kihara

Abstract

In recent years, there is an increasing interest from scientists to plant derived compounds both in cosmetic and nutraceutical products. *Garcinia mangostana* Linn (Mangosteen) belongs family Guttiferae which is a tropical fruit and cultivated in many tropical rainforest countries such Thailand, Vietnam, Indonesia and Philippines. Mangosteen hull was used as a traditional medicine for skin infection, wounds, dysentery and diarrhea for hundreds of years in the Southeast Asia. The pericarp (peel) of Mangosteen fruit have been reported to contain tannin, xanthone, chrysanthemin, garcinone, gartanin and other bioactive substances.

α-Mangostin was found the most abundant in the major xanthones taken from the pericarps of the mangosteen fruit. This compound is a yellowish coloring matter and has been discovered with a wide range of biological activities both in *in vitro* and *in vivo* including anti-inflammatory, anti-tumor, cardioprotective and anti-obesity agents. It has been indicated that has verify function in biological activities. Therefore, the following chapters here deal with understanding the multi-biological functions of α-Mangostin with anti-metastasis, reduction of the cell stiffness and activation of leukocytes.

Chapter 2: α-Mangostin was first investigated to establish method to extracted this compound from the pericarp of Mangosteen fruit. There are several methods have been reported to extract α-Mangostin. In this study, α-Mangostin was extracted from the pericarp by using ethanol and silica gel, and optimized the condition and solvent to obtain the highest yield.

Chapter 3: The effect of α-Mangostin on cancer cell metastasis was indicated on human lung cancer cells. The metastasis of cancer is very completed, and almost the research of anti-metastasis of α-Mangostin were studied on mono-culture which is deficient in interaction between cancer cells and surrounding cells. Therefore, I developed a co-culture system that cultured cancer cells

and normal cells together in order to reflect the communication between cancer cells and normal cells. Then impacts of α-Mangostin were examined on this co-culture system.

Chapter 4: I found that α-Mangostin reduced the cell surface stiffness of various types of cells. The cell surface stiffness is mainly attributed by the actin cytoskeleton, so after treatment with α-Mangostin, these cells were stained their actin cytoskeleton to observe the change.

Chapter 5: The new biological function of α-Mangostin was found in activation of leukocytes. I found that α-Mangostin induced the adhesion of leukocytes and it also reduced the stiffness of leukocytes. In addition, the activation of protein kinase C (PKC) and protein phosphatase were necessary for α-Mangostin-activated leukocytes.

In this research, it was made clear that α-Mangostin presented its diversified biological functions, it was not only found with anti-cancer, but also has other effects with different cell types. The anti-metastasis of α-Mangostin has been found in several researches on cancer cells, but in this study, I found that α-Mangostin also had positive effect on normal cells which were surrounded cancer cells. This finding is important to optimize the conditions of this compound as a chemotherapeutic and chemopreventive agent for cancer treatment. In addition, α-Mangostin changed the mechanical properties which has been proposed to participate in regulation of cell state and fate. The mechanical properies is also play important role in leukocytes, α-Mangostin reduced the cell stiffness followed by induced the cell adhesion and activated leukocytes. These results contribute to complete the whole picture of the biological function of α-Mangostin, and these functions of α-Mangostin are useful for studies on the potential pharmacological principles as well as the preclinical applications of the α-Mangostin.

Table of Contents:

List of abbreviation:

AFM	Atomic force microscopy
AP	Activator protein
A23187	Calcium Ionophore
A549	Human lung adenocarcinoma cell line
BIM I	Bisindolylmaleimide I
BMMC	The bone marrow-derived mast cells
CA	Calyculin A
CCD-14Br	Human bronchogenic epithelioid cell line
CCK-8	Cell counting kit-8
CD	Cytochalasin D
Cdks	Cyclin-dependent kinases
COX	Cyclooxygenase
DAG	Diacylglycerol
DAPI	4′,6-diamidino-2-phenylindole
ECM	Extracellular matrix
ERK	Extracellular signal-regulated kinase
ERM	Ezrin/Radixin/Moesin
Dil	1,1’-Dioctadecyl-3,3,3’ ,3’-Tetramethylindocarbocynine perchlorate
Dio	3,3’-Dioctadecyl-oxacarbocyanine perchlonate
DMEM	Dulbecco’s Modified Eagle’s Medium-High glucose
DMSO	Dimethyl sulfoxide
FAK	Focal adhesion kinase
FBS	Fetal bovine serum
HGF	Hepatocyte growth factor
HEK293	Human embryonic kidney cells
IL	Interleukin
IR	Infrared spectroscopy
JNK/SAPK	c-Jun NH2-terminal kinase
LPS	Lipopolysaccharide
LDL	Human low-density lipoproteins

KG-1	Human myeloblasts cells
MG	α-Mangostin
MLC	Myosin light-chain
MLCK	Myosin light-chain kinase
MMP	Matrix metalloproteinase
MS	Mass spectrometry
NP	Nitropropionic acid
NF-κB	Nuclear factor kappa B
NMR	Nuclear magnetic resonance
PDGF	Platelet-derived growth factor
pERM	Phosphorylated ERM
PKA	Protein kinase
PKC	Protein kinase C
PMA	Phorbol 12-myristate 13-acetate
PPP1A	Protein phosphatase 1A
RAW 264.7	Mouse monocyte/macrophage-like cells
ROS	Reactive oxygen species
SDF	Stromal cell-derived factor
TBARS	Thiobarbituric reactive substances
TIG-1	Human lung fibroblast cells
TJ	Tight junction
TPA	12-O-tetradecanoylphorbol-13-acetate
VEGF	Vascular endothelial growth factor

Chapter 1: General Introduction

1 – 1. *Garcinia Mangostana* Linn and potential compounds

Garcinia Mangostana Linn, commonly known as mangosteen, is a tropical evergreen tree with edible fruit and native to nations of Southeast Asia. Its exact origins are unknown due to its widespread cultivation since ancient times, but it is believed to have been somewhere between the Sunda Island and the Moluccas, and mainly grows in Southeast Asia, southwest India and other tropical countries (Morton et al., 1987; Karp et al., 2006, 2007). Mangosteen is one the praised of tropical fruits, and certainly the most esteemed fruit in the family Guttiferae. There are numerous variations in nomenclature: among Spanish-speaking people, it is called "*mangostan*"; to the French, it is "*mangostanier*", "*mangoustanier*", "*mangouste"* or "*mangostier"*; in Dutch, it is "*manggis"* or "*manggistan"*; in Vietnamese, "*mang cut"*.

The place of origin of the mangosteen is unknown but they now grow almost in the Asian region as Malaysia, Myanmar, Thailand, Philippines, India and Vietnam. Especially, Vietnam used to be known the largest mangosteen gardens in the world. Mangosteen is a tropical tree, so it prefers hot and humid climate with temperate range from 25-35^{o}C with a relative humidity over 80% (Yaacob et al., 1995; Diczbalis, 2011). Therefore, in Vietnam, mangosteen is mainly distributed in the Mekong River Delta (Mekong Delta) and Southeast regions (Fig. 1.1). Mangosteen fruit are almost planted in Mekong Delta, the total mangosteen planting area is about 4.9 thousand hectares and giving a yield of 4.5 thousand tons per year. One mangosteen tree has normally about 80 kg mangosteen fruit for each harvest. According to current of the statistics, Ben Tre province has about 4.5 thousand hectares of mangosteen which accounts for 77% of the total mangosteen area. The distribution of mangosteen is shown in Figure 1.1.

The mangosteen tree is very slow-growing, erect with a pyramidal crown and attain 6-25 m in height. The tree trunk has dark-brown, flaking bark and the inner bark contain much yellow, gummy, bitter latex. The fruit is capped by the prominent calyx at the stem end and with 4 to 8 triangular, is round and dark-purple to re-purple and smooth externally, has 3.4-7.5 cm in diameter. The rind is 6-10 mm thick, red in cross-section, purplish-white on the inside. It contains bitter yellow latex and a purple, staining juice. There are 4 to 8 triangular segments of snow-white, juicy, soft flesh (actually the arils of the seed) (Fig. 1.2). The fruit may be seedless or have 1 to 5 fully developed seeds. The flesh is slightly acid and mild to distinctly acid in flavor and is acclaimed as exquisitely luscious and delicious.

Mangosteen fruit is moderately low calories (63 calories per 100 g) and contains no saturated fats or cholesterol, is a good source of nutrients, vitamins and minerals. Consuming 100 gram of mangosteen supplies, 17.91 g of Carbohydrate, 31 µg of Vitamin B9 (Folate, Folic acid), 0.069 mg of Copper, Cu, 1.8 g of Total dietary Fiber, 0.054 mg of Vitamin B1 (Thiamin), 0.102 mg of Manganese, Mn, 0.054 mg of Vitamin B2 (Riboflavin) and 0.3 mg of Iron, Fe. The detail nutritional value of Mangosteen is described in Table 1.

Some parts of mangosteen tree had a history of use in traditional medicine which has been reported almost in South Asia. It has been used to treat skin infections, wounds, dysentery, urinary tract infection and gastrointestinal complaints, although there is no high-quality clinical evidence for any of these effects (Morton, 1987; Obolskiy et al.,2009). Dried fruits are shipped from Singapore to Calcutta and to China for medicinal use. The sliced and dried rind is powdered and administered to overcome dysentery. Made into an ointment, it is applied on eczema and other skin disorders. The rind decoction is taken to relieve diarrhea and cystitis, gonorrhea and gleet and is applied externally as an astringent lotion. A portion of the rind is steeped in water overnight and

the infusion given as a remedy for chronic diarrhea in adults and children. Filipinos employ a decoction of the leaves and bark as a febrifuge and to treat thrush, diarrhea, dysentery and urinary disorders. A bark extract called "amibiasine", has been marketed for the treatment of amoebic dysentery ((Morton, 1987).

In addition, the rind of partially ripe fruits contains over 68 xanthone-type compounds, in which α-mangostin, β-mangostin, γ-mangostin, garcinone E, and gartanin are the most abundant (Ilyas et al., 1994) (Fig. 1.2). By far, the most studied xanthone is α-mangostin (α-MG) for which anti-oxidant, anti-proliferative, pro-apoptotic, anti-inflammatory, anti-carcinogenic, and anti-microbial activities have been reported.

1 – 2. α – Mangostin and its biological functions

α-Mangostin (Fig. 1.2) was found among the major xanthones taken from the pericarps of the mangosteen fruit in 1855 (Schmid, 1855). In 1855, α-mangostin was found among the major xanthones taken from the pericarps of the mangosteen fruit (Schmid, 1855). The compound is a yellowish coloring matter (Dragendorff, 1930), the structure of this xanthone was subsequently construed by Dragendorff and Murakami (Dragendorff, 1930; Murakami, 1932). The molecular formula, type and position of the substituent groups of α-mangostin were then determined by Yates and Stout in 1958.

α-Mangostin is extracted from the pericarp of the mangosteen fruit (*G. mangostana* Linn.) and is a metabolite of 1,3,6,7-tetrahydroxy-2,8-di(3-methyl-2-butenyl) xanthone. The α-mangostin is a derivative of xanthones that are widely present in the hull of the mangosteen fruit. The molecular formula of α-mangostin is $C_{24}H_{22}O_6$ with molecular weight 410.46 g/mol, and melting point 180-182°C (Peterson and Terrence, 2009).

Physical and chemical properties of α-mangostin: α-mangostin is a yellow amorphous crystal with melting point 180-182°C. This compound has a maximum wavelength at 215, 243, and 317 nm (Ee et al., 2008). α-Mangostin is soluble in methanol and has a water solubility 2.03×10^{-4} mg/L at 25°C. A qualitative analysis was performed by thin-layer chromatography (TLC) and detected by ultraviolet lamps with or without ammonia or using phenolic spray reagents. A quantitative analysis can be done with liquid chromatography (Walker et al., 2007; Tosa et al., 1997).

This compound has been discovered to possess a wide range of biological activities including anti-inflammatory, anti-tumor, cardioprotective, antidiabetic, antibacterial, antifungal, antiparasitic, antioxidant and anti-obesity activities (Fig. 1.3).

1 – 2. 1. Antioxidant properties

The antioxidant properties of α-mangostin were demonstrated through the ferric thiocyanate method (Fan and Su, 1997, Yoshikawa et al., 1994). α-Mangostin reduced copper- or peroxyl radicals-induced oxidation of the human low-density lipoproteins (LDL) (Williams et al., 1995). They also found that α-mangostin: (i) dose-dependently prolonged the lag time of conjugated dienes at 234 nm; (ii) decreases the production of thiobarbituric reactive substances (TBARS); and (iii) diminishes the consumption of α-tocopherol that is induced by LDL oxidation. In addition, nitric oxide (NO) was also significantly inhibited from lipopolysaccharide (LPS)-stimulated RAW 264.7 cells, and the inhibition showed an IC_{50} value of 12.4 μM (Chen et al., 2008). α-Mangostin scavenged singlet oxygen, superoxide anion and peroxynitrite anion in a concentration-dependent manner (Pérez-Rojas et al., 2009). On the contrary, the compound was unable to scavenge hydroxyl radicals and hydrogen peroxide. α-Mangostin was also able to improve the neuronal death induced by 3-nitropropionic acid (3-NP) in a concentration-dependent

manner. This protective effect of the α-mangostin was related to the amelioration of 3-NP-induced reactive oxygen species formation. The protective effect of α-mangostin on cardiac reperfusion damage was found (Buelna-Chontal et al., 2011). The findings indicate that α-mangostin preserves the mechanical work of the cardiac, reduces the area of infarct as well as prohibits the decrease in cardiac ATP and phosphocreatine levels in the re-perfused myocardium.

1 – 2.2. Anticancer and cytotoxic properties

α-Mangostin inhibited the cell growth of the human leukemia cell line HL60 (Matsumoto et al., 2003), induced cell death PC12 rat pheochromocytoma cells (Sato et al., 2004). Moreover, α-mangostin remarkably inhibited the sarco/endoplasmic reticulum Ca^{2+}-ATPase. The Ca^{2+}-ATPase inhibitory effects and the apoptotic effects of the xanthone derivatives showed a correlation with each other. On the contrary, α-mangostin treatment caused one of the signaling molecules of endoplasmic reticulum (ER) stress, c-Jun NH2-terminal kinase (JNK/SAPK), to be activated. These findings imply that α-mangostin inhibits Ca^{2+}-ATPase to bring about apoptosis through the mitochondrial pathway. α-Mangostin had exceptional apoptotic effects on the human head and neck squamous carcinoma cell lines, HN-22, HN-30 and HN-31, which induced the down-regulation of bcl-2, while on the other hand caused an up-regulation of bax and p53 in HN-22, HN-30 and HN-31 (Kaomongkolgit et al., 2011).

α-Mangostin strongly suppressed cell growth DLD-1 human colon cancer cells (Matsumoto et al., 2005). The antiproliferative effect of α-mangostin was attributable to cell-cycle arrest by affecting the cyclins, cdc2 and p27 expression. α-Mangostin was found that cytotoxicity against DLD-1 human colon cancer cells (Nakagawa et al., 2007), 20 μM of α-mangostin reduced the number of viable cells consistently, which largely due to apoptosis. The antiproliferation of canine osteosarcoma cells, D-17, induced by α-mangostin showed an IC_{50} value of 15 μg/ml

(Krajarng et al., 2012). Nuclear condensation and fragmentation, normally observed in apoptosis, were also induced by α-mangostin, as revealed through Hoechst 33342 nuclear staining and nucleosomal DNA-gel electrophoresis. α-Mangostin was also able to induce sub-G1 peak as demonstrated by cell-cycle analysis, as well as membrane flipping of the phosphatidylserine and the loss of mitochondrial membrane potential in D-17 cells.

The effectiveness of α-mangostin as an antimetastatic agent against the expressions of 12-O-tetradecanoylphorbol-13-acetate (TPA)-induced matrix metalloproteinase-2 (MMP-2) and matrix metalloproteinase-9 (MMP-9) was investigated in human breast adenocarcinoma cells, MCF-7 (Lee et al., 2010). Moreover, α-mangostin inhibited the activation of extracellular signal-regulated kinase 1 and 2 (ERK1/2) that takes place in the down-regulation of TPA-induced enzyme activities, protein, and MMP-2 and MMP-9 messenger RNA levels, as well as TPA-induced degradation of inhibitor of kappaBα (IκBα) and the nuclear levels of nuclear factor kappa B (NF-κB), c-Fos, and c-Jun. α-Mangostin treatment also resulted in a dose-dependent inhibition of the binding abilities of NF-κB and activator protein-1 (AP-1). Furthermore, MCF-7 cells treated with the specific inhibitor for ERK (U0126) could inhibit TPA-induced MMP-2 and MMP-9 expressions as well as cell invasion and migration. Results revealed the effectiveness of α-mangostin as a novel and effective antimetastatic agent that acts through the down-regulation of MMP-2 and MMP-9 gene expressions. It was also observed that α-mangostin treatment resulted in a dose-dependent inhibition on the binding abilities of NF-κB. The effect of α-mangostin is further potentiated in the reduction of FAK or ERK1/2 phosphorylation by FAK small interfering RNA (FAK siRNA) (Shih et al., 2010). α-Mangostin also suppressed the subsistence of lung cancer cells, A549 and displayed anti-metastatic activities by inhibiting the migration and invasion in co-culture condition, and reducing the actin cytoskeleton of cancer cells (Phan et al., 2018).

1 – 2.3. Anti-inflammatory, anti-allergy analgesic properties

α-Mangostin produced prominent anti-inflammatory activity in rats, via both intraperitoneal and oral routes. In fact, this anti-inflammatory activity was present in bilaterally adrenalectomized rats as well. Administration of α-mangostin in rats revealed considerable antiulcer activity of the compound (Shankaranarayan et al., 1979). α-Mangostin could also inhibit primary and secondary responses of adjuvant-induced arthritis in rats (Gopalakrishnan et al., 1980). In addition, α-mangostin significantly inhibited lipopolysaccharide-stimulated NO-production and cytotoxicity in mouse leukemic monocyte macrophage cell line (RAW 264.7 cells) (Chen et al., 2008). To prove the effect of this xanthone, the induction of inducible nitric oxide synthase as well as COX enzyme expressions was measured. α-Mangostin concentration was found to reduce iNOS induction in a dependent manner. Moreover, α-mangostin potently inhibited paw edema. α-Mangostin exhibited analgesic effects in the hot-plate and the results showed the potent peripheral and central antinociceptive effects exerted by α-mangostin in mice (Cui et al., 2010). α-Mangostin was shown to inhibit the production of Interleukin (IL)-6, prostaglandin D2 (PGD2) and leukotriene C4 (LTC4) as well as degranulation in bone marrow-derived mast cell (BMMC) induced by phorbol 12-myristate 13-acetate (PMA) plus A23187 (Chae et al., 2012). Another effect of α-mangostin that was observed was the repression of cyclooxygenase (COX)-2 expression. These results reflect the potential usefulness of α-mangostin in alleviating allergic inflammatory responses mediated by the mast cell.

1 – 3. Anticarcinogenic activities of α-Mangostin

Among the many studies showed, the anticancer and cytotoxic properties of α-mangostin have been the most interesting of scientists studied through a numerous of studies. The anti-cancer activities of include cell cycle arrest, suppression of tumor cell proliferation, induction of apoptosis

and differentiation, reduction of inflammation, and inhibition of adhesion, invasion, and metastasis (Akao et a;., 2008; Pedraza-Chaverri et a;., 2008; Hung et al., 2009). Figure 1.4 presents the molecular mechanism changed by α-mangostin.

1 – 3.1. Induction of Apoptosis

It has been reported that α-mangostin induces apoptosis in various cancer cell types by activating pro-apoptotic signaling molecules and by inhibiting anti-apoptotic molecules of the intracellular signal transduction pathways. The induction of apoptosis in human promyelocytic leukemia (HL-60) cells by α-mangostin was mediated by the activation of caspase-9 and caspase-3, but not caspase-8, indicating that α-mangostin may be involved in the mitochondrial apoptotic pathway (Matsumoto et al, 2004). PC12 cells treated with α-mangostin demonstrated typical apoptotic DNA fragmentation, caspase-3 cleavage, mitochondrial membrane depolarization, cytochrome c release, sarco-endoplasmic reticulum Ca^{2+}-ATPase inhibition, and c-Jun NH2-terminal kinase (JNK/SAPK) activation (Sato et al., 2004). The cytotoxic effect of α-mangostin on human colon cancer DLD-1 cells was found to be caused by apoptosis, but there is either activation of caspases or changes in Bax, Bcl-2 protein and apoptosis-inducing factor following α-mangostin treatment (Nakagawa et al., 2007). α-Mangostin-induced apoptosis may be involved the miR-143/ERK5/c-Myc pathway and mitochondrial factors endonuclease-G which is unique mechanisms of α-mangostin-induced apoptosis.

1 – 3.2. Induction of Cancer Cell Cycle Arrest

It is well known that the cell cycle is normally regulated by a number of proteins, including p53, p21waf, the cyclin-dependent kinases (cdks) and their activators, the cyclins. The dysregulation of cell cycle machinery and checkpoint signaling pathways is a hallmark of malignant cells (Collins and Garrett, 2005; Gali-Muhtasib and Bakkar, 2002). Thus, modulation

of cell cycle progression is one of the major strategies for both chemoprevention and chemotherapy. Treatment of α-mangostin results in a direct inhibition of the proliferation and viability of various cancer cell types in vitro, as manifested by the significant arrest of cells at various phases of the cell cycle (Akao et al., 2008). The antiproliferative effects of α-mangostin were associated with cell cycle arrest mediated by modulation of the expression of cyclin A, B1, D1, E1, cdc2 or p27 in human colon cancer DLD-1 cells (Matsumoto et al., 2004). The exposure of α-mangostin to DLD-1 cells resulted in G1 arrest (Han et al., 2009). These findings provide a rational basis for the development of α-mangostin as agent for cancer prevention or for use in combination with anti-cancer drugs; however, further experiments are required to explore the precise molecular mechanisms underlying the observed induction of cell cycle arrest.

1 – 3.3. Anti-Invasive and Anti-Metastatic Effects

Metastasis of cancer cells is a complex, multistage process that involves changes in cell adhesion, migration, invasion, rearrangement of the extracellular matrix (ECM), anoikis-suppression and reorganization of cytoskeletons (Brábek et al., 2010; Kargiotis et al., 2010; Sato et al., 2010; Mareel et al., 2010). α-Mangostin exhibited an inhibitory effect on adhesion, migration, and invasion of human prostate carcinoma cells (PC-3). This effect was associated with decreased expression of MMP-2, MMP-9, and urokinase-plasminogen activator (u-PA) mediated by suppression of the JNK1/2 signaling pathway and inhibition of NF-κB and AP-1 binding activity (HUng et al., 2009). α-Mangostin could inhibit invasion, and migration events of human breast adenocarcinoma cells, MCF-7 and human lung adenocarcinoma cells, A549 (Shih et al., 2010, Lee et al., 2010). α-Mangostin could inhibit the activation of extracellular signal-regulated kinase 1 and 2 (ERK1/2), and downregulate the enzyme activities, protein, and messenger RNA levels of MMP-2 and MMP-9; this compound could also inhibit the degradation of inhibitor of

kappaBα (IκBα) and the nuclear levels of NF-κB, c-Fos, and c-Jun. In A549 cells revealed that ERK1/2 inhibition occurred via blocking the activation of αvβ3 integrin and focal adhesion kinase (FAK). FAK is a non-receptor tyrosine kinase that is primarily localized to cell–matrix adhesions. It acts as a central regulator of focal adhesion, influencing cell survival, differentiation, proliferation, migration, and tissue remodeling. Briefly, α-mangostin is a novel, effective, antimetastatic agent that functions in regulating MMP-2 and MMP-9 gene expression.

Promisingly, the merely in vivo study about anti-metastatic activity of xanthones had been progressed in a BALB/c mice model with breast cancer cell, BJMC3879. The results showed that lung and Lymph node metastasis tended to decrease using 5000 ppm panaxanthone in their diet. These results suggest that the observed anti-metastatic activity of xanthone may be of clinical significance as adjuvant therapy in metastatic human breast cancer (Watanapokasin et al., 2010). Although the anti-invasive effect of xanthones has been observed, the underlying mechanism in the invasion process remains unclear. It is known that tumor growth is dependent upon angiogenesis and that for the process of metastasis to successfully occur to different organs, tumor cells must possess sufficient blood supply. Although the effect of xanthones exposure on angiogenesis and the regulation of HIF-1a and VEGF have yet to be reported, these areas warrant investigation.

References

Akao, Y., Nakagawa, Y., Iinuma, M., et al. Anti-cancer effects of xanthones from pericarps of mangosteen. Int J Mol Sci. 2008;9(3):355–70.

Collins, I., Garrett, M.D. Targeting the cell division cycle in cancer: CDK and cell cycle checkpoint kinase inhibitors. Curr Opin Pharmacol. 2005 Aug; 5(4):366-73.

Brábek, J., Mierke, C.T., Rösel, D., Veselý, P., Fabry, B. (2010). The role of the tissue microenvironment in the regulation of cancer cell motility and invasion. Cell communication and signaling : CCS, 8, 22.

Buelna-Chontal, M., Correa, F., Hernández-Reséndiz, S., Zazueta, C., Pedraza-Chaverri, J. Protective effect of α-mangostin on cardiac reperfusion damage by attenuation of oxidative stress. J. Med. Food, 14 (2011), pp. 1370-1374.

Chae, H.S., Oh, S.R., Lee, H.K., Joo, S.H., Chin, Y.W. Mangosteen xanthones, α-and γ-mangostins, inhibit allergic mediators in bone marrow-derived mast cell. Food Chem., 134 (2012), pp. 397-400

Chen, L.G., Yang, L.L., Wang, C.C. Anti-inflammatory activity of mangostins from (Garcinia mangostana). Food Chem. Toxicol., 46 (2008), pp. 688-693.

Cui, J., Hu, W., Cai, Z., Liu, Y., Li, S., Tao, W., Xiang, H. New medicinal properties of mangostins: analgesic activity and pharmacological characterization of active ingredients from the fruit hull of (Garcinia mangostana L.). Pharmacol. Biochem. Behav., 95 (2010), pp. 166-172.

Diczbalis, Y., (2011). "Farm and Forestry Production and Marketing for Mangosteen (Garcinia mangostana)".

Dragendorff, O., Über das Harz von Garcinia Mangostana L. Justus Liebigs Annalen Chem., 482 (1930), pp. 280-301.

Ee, GC., Daud, S., Izzaddin, SA., Rahmani, M. Garcinia mangostana: A source of potential anti-cancer lead compounds against CEM-SS cell line. J Asian Nat Prod Res 2008;10(5-6):475-9.

Fan, C.T., Su, J.D. Antioxidative mechanism of isolated components from methanol extract of fruit hulls of Garcinia mangostana L. J. Chin. Agric. Chem. Soc., 35 (1997), pp. 540-551.

Gali-Muhtasib, H., Bakkar, N. Modulating cell cycle: current applications and prospects for future drug development. Curr Cancer Drug Targets. 2002 Dec; 2(4):309-36.

Gopalakrishnan, C., Shankaranarayanan, D., Kameswaran, L., Nazimudeen, S. Effect of mangostin, a xanthone from Garcinia mangostana Linn. in immunopathological & Inflammatory reactions. Indian J. Exper. Biol., 18 (1980), pp. 843-846.

Han, A.R., Kim, J.A., Lantvit, D.D., Kardono, L.B., Riswan, S., Chai, H., Carcache de Blanco, E.J., Farnsworth, N.R., Swanson, S.M., Kinghorn, A.D. Cytotoxic xanthone constituents of the stem bark of Garcinia mangostana (mangosteen). J Nat Prod. 2009 Nov; 72(11):2028-31.

Hung, S.H., Shen, K.H., Wu, C.H., et al. Alpha-Mangostin suppresses PC-3 Human prostate carcinoma cell metastasis by inhibiting Matrix Metalloproteinase-2/9 and Urokinase-Plasminogen expression through the JNK signaling pathway. J Agr Food Chem. 2009;57(4):1291–8.

Ilyas, M., Kamil, M., Parveen, M., et al. Isoflavones from garcinia nervosa. Phytochemistry. 1994;36(3):807–9.

Kaomongkolgit, R., Chaisomboon, N., Pavasant, P. Apoptotic effect of alpha-mangostin on head and neck squamous carcinoma cells. Arch. Oral Biol., 56 (2011), pp. 483-490.

Kargiotis, O., Geka, A., Rao, J.S., et al. Effects of irradiation on tumor cell survival, invasion and angiogenesis. J Neuro-Oncol. 2010;100(3):323–38.

Krajarng, A., Nilwarankoon, S., Suksamrarn, S., Watanapokasin, R. Antiproliferative effect of α-mangostin on canine osteosarcoma cells. Res. Vet. Sci., 93 (2012), pp. 788-794.

Krajarng, A., Nilwarankoon, S., Suksamrarn, S., Watanapokasin, R. Antiproliferative effect of α-mangostin on canine osteosarcoma cells. Res. Vet. Sci., 93 (2012), pp. 788-794.

Karp, D., (9 August 2006). "Forbidden? Not the Mangosteen". The New York Times. Retrieved 22 May 2010.

Karp, D., (8 August 2007). "Mangosteens Arrive, but Be Prepared to Pay". The New York Times. Retrieved 22 May 2010.

Lee, Y.B., Ko, K.C., Shi, M.D., Liao, Y.C., Chiang, T.A., Wu, P.F., Shih, Y.X., Shih, Y.W. α-Mangostin, a novel dietary xanthone, suppresses TPA-mediated MMP-2 and MMP-9

expressions through the ERK signaling pathway in MCF-7 human breast adenocarcinoma cells. J. Food Sci., 75 (2010), pp. H13-H23.

Matsumoto, K., Akao, Y., Kobayashi, E., Ohguchi, K., Ito T., Tanaka, T., Iinuma, M., Nozawa, Y. Induction of apoptosis by xanthones from mangosteen in human leukemia cell lines. J. Nat. Prod., 66 (2003), pp. 1124-1127.

Mareel, M., Oliveira, M.J., Madani, I. Cancer invasion and metastasis: interacting ecosystems. Virchows Arch. 2009 Jun; 454(6):599-622.

Matsumoto, K., Akao, Y., Yi, H., Ohguchi, K., Ito, T., Tanaka, T., Kobayashi, E., Iinuma, M., Nozawa, Y. Preferential target is mitochondria in alpha-mangostin-induced apoptosis in human leukemia HL60 cells. Bioorg Med Chem. 2004 Nov 15; 12(22):5799-806.

Matsumoto, K., Akao, Y., Ohguchi, K., Ito T., Tanaka, T., Iinuma, M., Nozawa, Y. Xanthones induce cell-cycle arrest and apoptosis in human colon cancer DLD-1 cells. Bioorg. Med. Chem., 13 (2005), pp. 6064-6069.

Morton, JF., (1987). "Mangosteen". Fruits of warm climates. Purdue University. pp. 301–304. Retrieved 4 December 2012.

Murakami, M., Über die Konstitution des Mangostins Justus Liebigs Annalen Chem., 496 (1932), pp. 122-151.

Nakagawa, Y., Iinuma, M., Naoe, T., Nozawa, Y., Akao, Y. Characterized mechanism of α-mangostin-induced cell death: Caspase-independent apoptosis with release of endonuclease-G from mitochondria and increased miR-143 expression in human colorectal cancer DLD-1 cells. Bioorg. Med. Chem., 15 (2007), pp. 5620-5628.

Obolskiy, D., Pischel, I., Siriwatanametanon, N,. Heinrich, M., (August 2009). "Garcinia mangostana L.: a phytochemical and pharmacological review". Phytotherapy Research. 23 (8): 1047–65. doi:10.1002/ptr.2730. PMID 19172667.

Pedraza-Chaverri, .J, Cardenas-Rodriguez, N., Orozco-Ibarra, M., et al. Medicinal properties of mangosteen (garcinia mangostana) Food Chem Toxicol. 2008;46(10):3227–39.

Pérez-Rojas, J.M., Cruz, C., García-López, P., Sánchez-González, D.J., Martínez-Martínez, C.M., Ceballos, G., Espinosa, M., Meléndez-Zajgla, J., Pedraza-Chaverri, J. Renoprotection by α-mangostin is related to the attenuation in renal oxidative/nitrosative stress induced by cisplatin nephrotoxicity. Free Radical Res., 43 (2009), pp. 1122-1132.

Peterson, K.D., Terrence, E.D. The Shaping School Culture Field Book. Vol. 2. San Francisco: Jossey-Bass; 2009. p. 10-4.

Phan, T.K.T., Shahbazzadeh, F., Pham, T.T.H, Kihara, T. 2018. Alpha-mangostin inhibits the migration and invasion of A549 lung cancer cells. PeerJ 6:e5027.

Sato, A., Fujiwara, H., Oku, H., Ishiguro, K., Ohizumi, Y. ALPHA.-mangostin induces Ca^{2+}-ATPase-dependent apoptosis via mitochondrial pathway in PC12 cells. J Pharmacol. Sci., 95 (2004), pp. 33-40.

Sato, H., Takino, T. Coordinate action of membrane-type matrix metalloproteinase-1 (MT1-MMP) and MMP-2 enhances pericellular proteolysis and invasion. Cancer Sci. 2010;101(4):843–7.

Schmid, W., Ueber das mangostin. Justus Liebigs Annalen Chem., 93 (1855), pp. 83-88.

Shankaranarayan, D., Gopalakrishnan, C., Kameswaran, L. Pharmacological profile of mangostin and its derivatives. Arch. Int. Pharmacol. Ther., 239 (1979), pp. 257-269.

Shih, Y.W., Chien, S.T., Chen, P.S., Lee, J.H., Wu, S.H., Yin, L.T. α-Mangostin suppresses phorbol 12-myristate 13-acetate-induced MMP-2/MMP-9 expressions via αvβ3 integrin/FAK/ERK and NF-κB signaling pathway in human lung adenocarcinoma A549 cells. Cell Biochem. Biophys., 58 (2010), pp. 31-44.

Tosa, H., Iinuma, M., Tanaka, T., Nozaki, H., Ikeda, S., Tsutsui, K., et al. Anthraquinones from Neonauclea calycina and their inhibitory activity against DNA topoisomerase II. Chem Pharm Bull 1997;45:418-20.

Yaacob, O., Tindall, HD., (1995). Mangosteen cultivation. Rome: Food and Agriculture Organization of the United Nations. ISBN 92-5-103459-1.

Yates, P., Stout, G.H.The structure of mangostin1. J. Am. Chem. Soc., 80 (1958), pp. 1691-1700.

Watanapokasin, R., Jarinthanan, F., Jerusalmi, A., Suksamrarn, S., Nakamura, Y., Sukseree, S., Uthaisang-Tanethpongtamb, W., Ratananukul, P., Sano, T. Potential of xanthones from tropical fruit mangosteen as anti-cancer agents: caspase-dependent apoptosis induction in vitro and in mice. Appl Biochem Biotechnol. 2010 Oct; 162(4):1080-94.

Walker, EB. HPLC analysis of selected xanthones in mangosteen fruit. J Sep Sci 2007;30(9):1229-34.

Williams, P., Ongsakul, M., Proudfoot, J., Croft, K., Beilin, L. Mangostin inhibits the oxidative modification of human low density lipoprotein. Free Radical Res., 23 (1995), pp. 175-184.

Figures

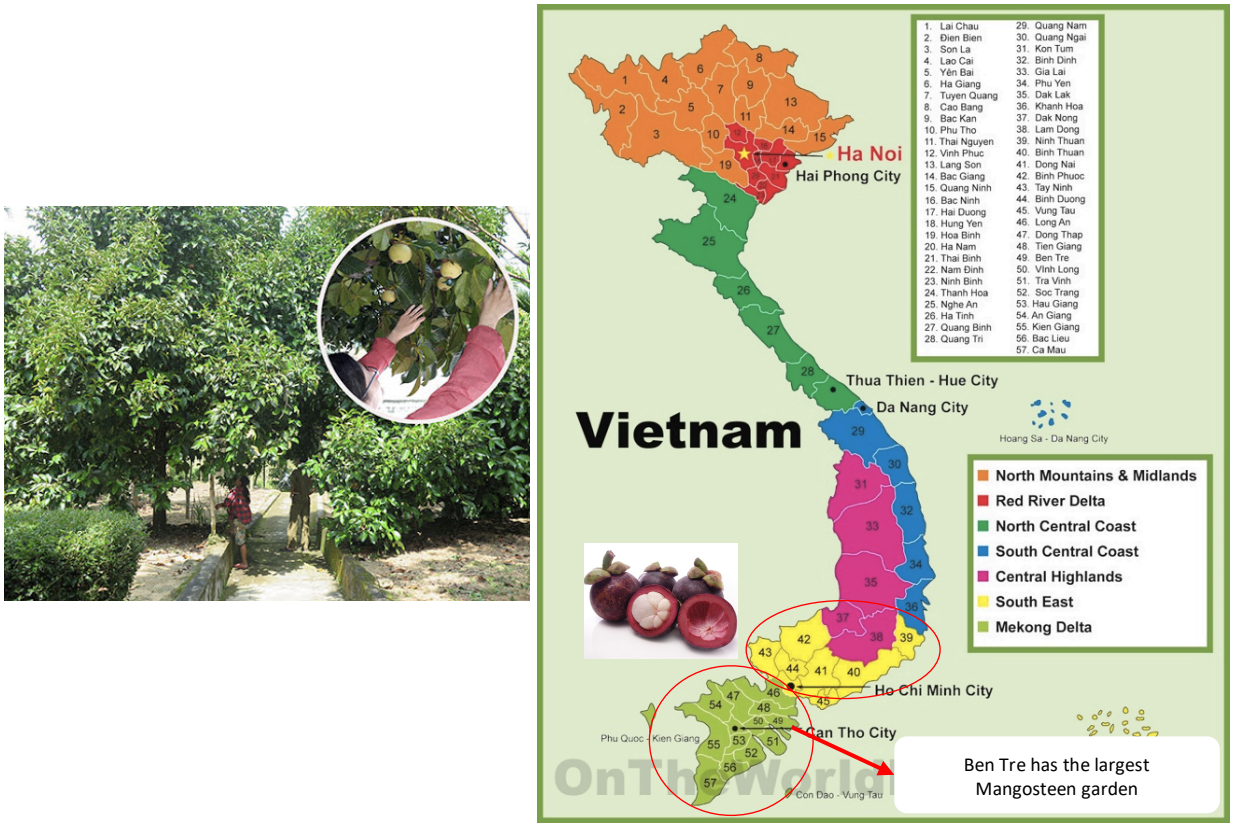

Figure 1.1. Mangosteen tree *Garcinia mangostana* Linn and its distribution in Vietnam. Mangosteen are planted almost in Mekong Delta and Southeast of Vietnam. Especially, Ben Tre is province where has the largest Mangosteen garden and contributes above 70% Mangosteen fruit yield every year.

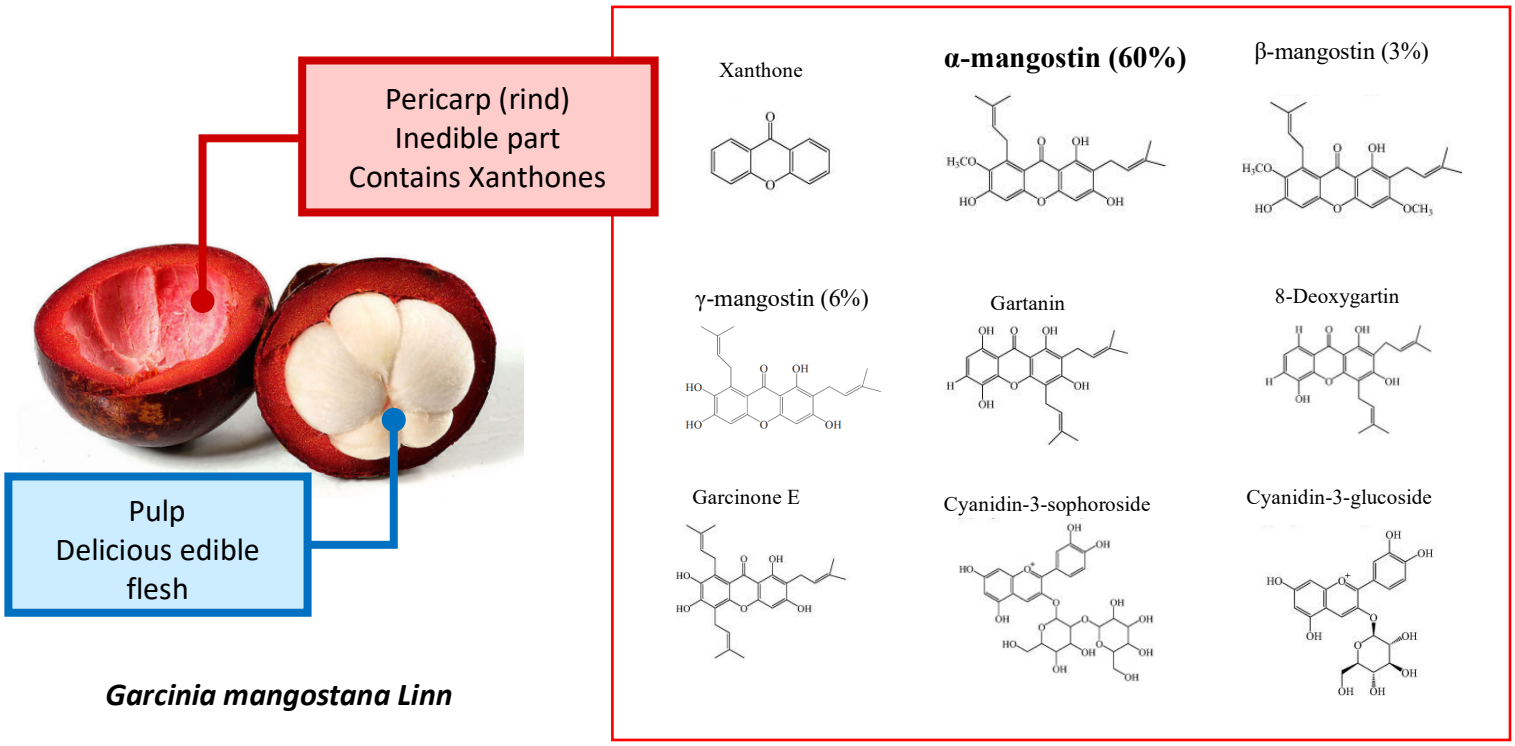

Figure 1.2. Mangosteen fruit and the chemical structure of the main xanthones found in its pericarp. α-mangostin, β-mangostin, γ-mangostin are the main xanthone extracted from the pericarp and they are the most studied.

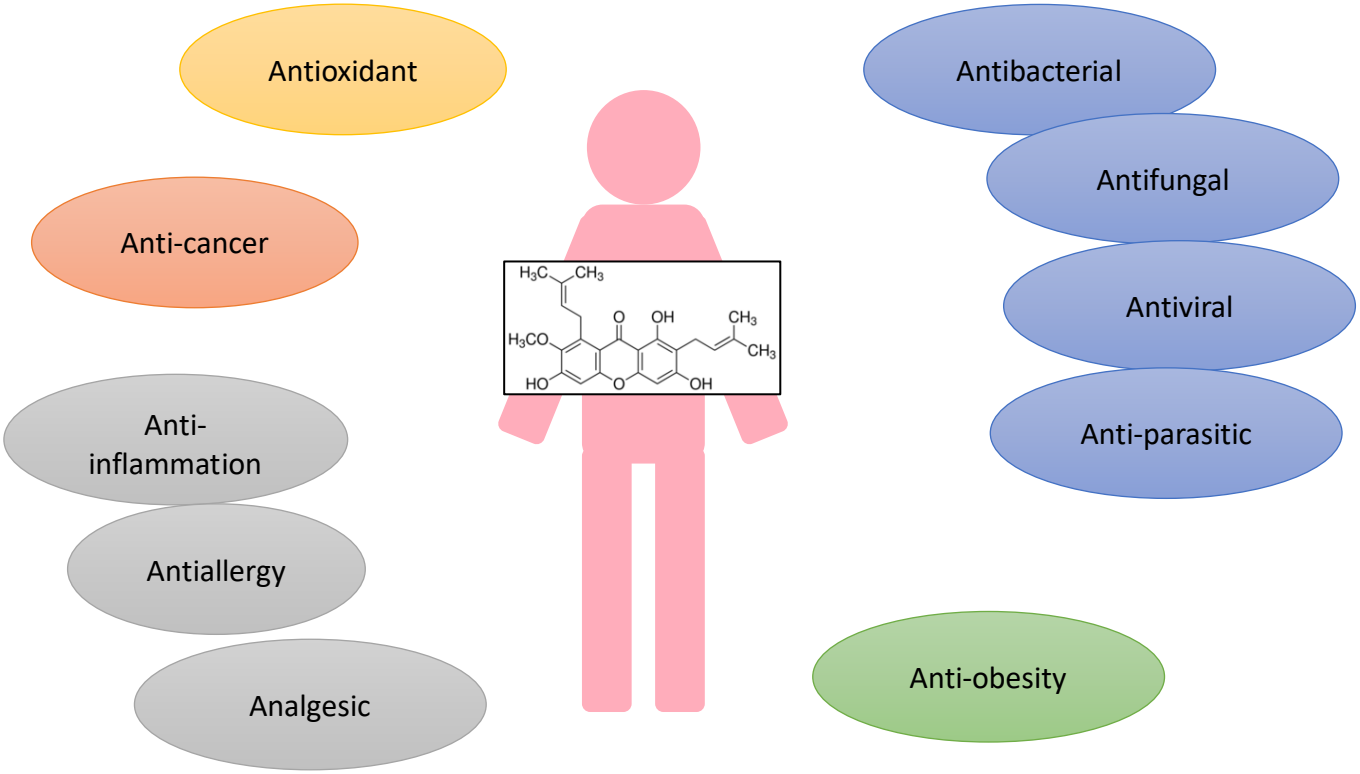

Figure 1.3: Pharmacological properties of α-mangostin

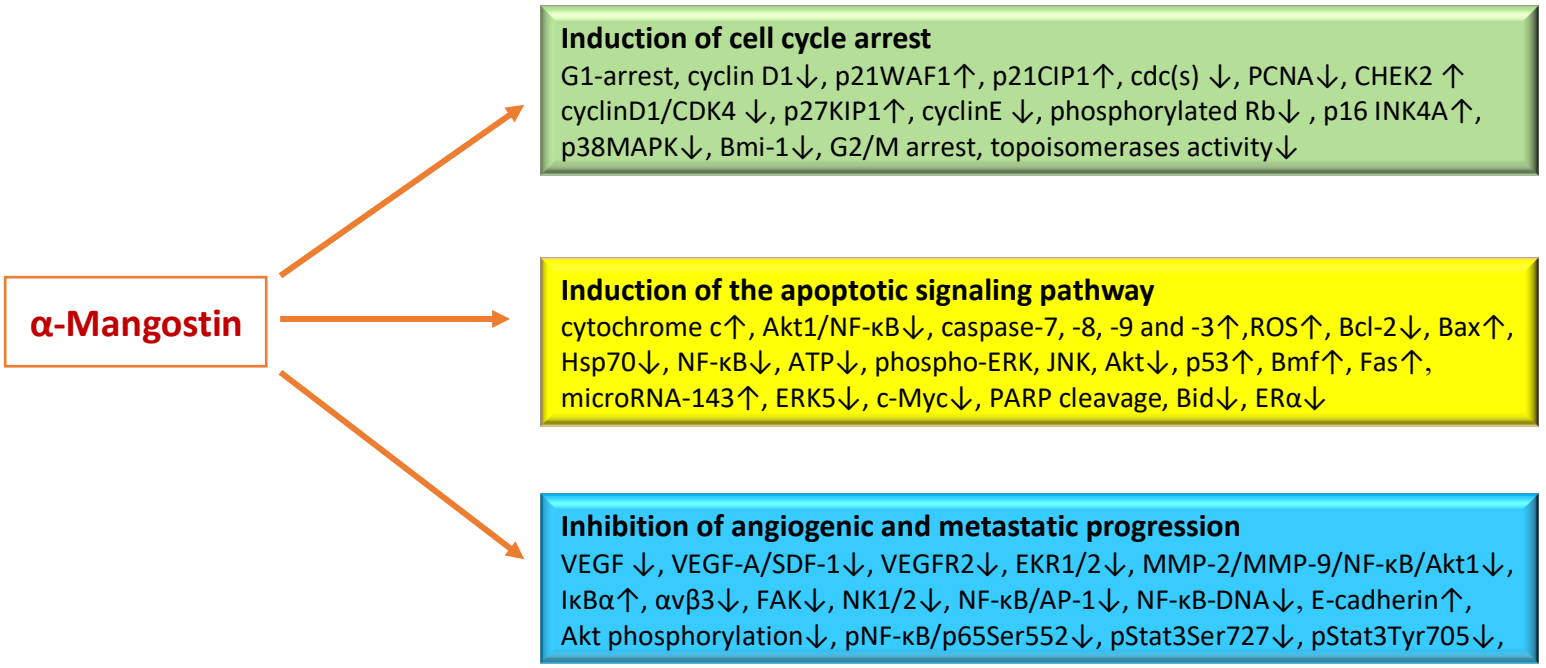

Figure 1.4: Molecular mechanisms behind the anticarcinogenic activities of α-Mangostin

Table 1: Nutritional value of Mangosteen fruit

(Source: USDA National Nutrient database)

Serving Size: 1 Cup (100 g) **Calories** 73 Kcal. **Calories from Fat** 5.22 Kcal.

Proximity	**Amount**	**% DV**
Water	80.94 g	
Energy	73 Kcal	
Energy	305 kJ	
Protein	0.41 g	0.82%
Total Fat (lipid)	0.58 g	1.66%
Ash	0.16 g	
Carbohydrate	17.91 g	13.78%
Total dietary Fiber	1.8 g	4.74%
Minerals	**Amount**	**% DV**
Copper, Cu	0.069 mg	7.67%
Manganese, Mn	0.102 mg	4.43%
Iron, Fe	0.3 mg	3.75%
Magnesium, Mg	13 mg	3.10%
Zinc, Zn	0.21 mg	1.91%
Calcium, Ca	12 mg	1.20%
Phosphorus, P	8 mg	1.14%
Potassium, K	48 mg	1.02%
Sodium, Na	7 mg	0.47%
Vitamins	**Amount**	**% DV**
Vitamin B9 (Folate, Folic acid)	31 µg	7.75%
Vitamin B1 (Thiamin)	0.054 mg	4.50%
Vitamin B2 (Riboflavin)	0.054 mg	4.15%
Vitamin C (Ascorbic acid)	2.9 mg	3.22%
Vitamin B3 (Niacin)	0.286 mg	1.79%

Vitamin B6 (Pyridoxine)	0.018 mg	1.38%
Vitamin B5 (Pantothenic acid)	0.032 mg	0.64%
Vitamin A	2 µg	0.29%
Beta Carotene	16 µg	
alpha Carotene	1 µg	
Beta Cryptoxanthin	9 µg	

*Above mentioned Percent Daily Values (%DVs) are based on 2,000 calorie diet intake. Daily values (DVs) may be different depending upon your daily calorie needs. Mentioned values are recommended by a U.S. Department of Agriculture. They are not healthbenefitstimes.com recommendations. Calculations are based on average age of 19 to 50

Chapter 2: Extraction of α – Mangostin

2 – 1. Overview

A huge number of compounds are widely distributed in nature and many of these possess medicinal/biological/pharmacological activity. α-Mangostin, a natural xanthone isolated from the pericarps of mangosteen, represents one of the most studied chemopreventive agents. This compound has been reported to interfere with all the major stages of carcinogenesis: initiation, promotion, and progression. A number of mechanisms have been proposed for its anticarcinogenic activities. Therefore, in order to obtain the biological active compound, the present study was designed for the extraction of this compound from the fruit pericarp of Garcinia mangostana L.). The extraction condition and solvent were optimized, the dried pericarp powder was extracted with ethanol and loaded on silica gel. A high yield of α - mangostin was extracted from dry pericarp. The verification of experimental results under optimized conditions showed that α - mangostin value for mangostin pericarp was 18.65g/kg dry matter. The chemical structure of α-mangostin was then verified by mass spectrometry (MS), nuclear magnetic resonance (1H NMR and 13C NMR), and infrared spectroscopy (IR).

2 – 1. Introduction

Mangosteen (Garcinia mangostana L.) belongs the Garcinia genus which is mainly cultivated in Thailand, Vietnam, Indonesia and other tropical countries. The pericarp of G. mangostana has been used as traditional medicines for diarrhea, skin infection, cholera, purulence and other diseases (Chopra, Nayar & Chopra, 1965; Garnett & Sturton, 1932; Mahabusarakam, Wlriyachitra & Taylor, 1987). A variety of active ingredients, including xanthones, polysaccharides, phenolic acids and pigments has been extracted from mangosteen pericarp and α-mangostin is one of the most important natural xanthone derivative (Zarena, 2015; Weecharangsan, 2006; Moongkarndi, 2014; Yu LM, 2014; Kosem, 2013, Ketsa, 2011; Zhang, 2011).

Extraction is an important process for the preparation of medically useful extracts that contain an optimum level of active constituents. An appropriate extraction method as well as a suitable solvent for extraction is the first requirement for producing an appropriate yield of active constituents in the extracts. There have been some reports on obtaining preparations of mangosteen pericarp extraction that have increased amounts of α-mangostin, for example, an extraction of the pericarps with (95%) ethanol using the Soxhlet apparatus produced the highest yield of an extract (26.60% dry weight) and the highest content of α-mangostin (13.51% w/w of crude extract). This yield was much higher than when other extraction methods were used, such as maceration, percolation, ultrasonic extraction and extraction using a magnetic stirrer, and the use of other extraction solvents (70% and 50% ethanol). Recently, dichloromethane has been reported that was the most suitable solvent for extraction of α-mangostin from G. mangostana pericarps, and yielded α-mangostin content of up to 46.2% w/w (Pothitirat et al., 2010). However, the use of dichloromethane, a halogenated hydrocarbon, as a solvent for extraction may be harmful due to its

toxicity including the possibility of the onset of dizziness, headache, nausea, irritation or intense burning in the skin, eyes and respiratory tract. There are also reports that dichloromethane can induce pancreatic, liver, biliary passages, breast and brain cancers (Ames et al., 2000). Moreover, dichloromethane is expensive and must be completely removed by evaporation before use. Obviously, this results in an increased cost for producing the product. Recent trends in extraction techniques have largely focused on finding solutions that could minimize the use of potentially toxic solvents.

Therefore, in the present study, I have focused on investigating an extraction method of α-mangostin based on the design of extraction produces that can prevent waste, less use hazardous chemical solvent, and ensures a safe, cheap and high-quality extract.

2 – 2. Experiment results

α-Mangostin was isolated from the ethyl acetate extract using silica gel column separation as a yellow amorphous powder with melting point 180-181°C (Lit. 181.6-182.6°C). MS and NMR spectroscopy was utilized to identify the recrystallized α-mangostin. The results of mass spectra, ^{1}H- NMR (deuterated chloroform), ^{13}C - NMR (deuterated chloroform), IR- spectra are shown as follows: A total of 24 carbons were observed in the ^{13}C NMR spectrum where the signal at δ 131.3 comprises two overlapped carbons (Fig. 2.1).

The DEPT spectrum indicated five methyls (δ 17.8, 18.2, 25.8, 25.9, 61.1), two methylenes (δ 21.9, 26.8), four methines (δ 93.0, 102.6,123.4, 124.7) and thirteen quaternary carbons (δ 182.8 (C-9), 163.1 (C-3), 161.6 (C-1), 157.5 (C-6), 156.1 (C-5a), 155.6 (C-4a), 144.4 (C-7), 138.0 (C-8), 131.3 (C-3'), 131.3 (C-3"), 111.8 (C-8a), 111.0 (C-2), 103.5 (C-9a)) in the molecule (Fig. 2.2). Further, the mass spectrum showed the presence of a molecular ion peak at m/z 410 which validated a molecular formula $C_{24}H_{26}O_6$.

Analysis of the IR spectrum is indicated in Fig. 2.3, an absorption at 3422 cm^{-1} indicated the presence of a phenolic group. Meanwhile the presence of a chelated carbonyl group in the middle ring and a methoxy group were proved by a strong absorption at δ 1642 cm^{-1} and 1284 cm^{-1}. The absorptions at 2926 cm^{-1} and 2344 cm^{-1} indicated the presence of CH_2 and CH_3. Besides this, the absorption peak at 1459 cm^{-1} was due to the C=C aromatic stretching of the xanthone skeleton.

From the ^{1}H NMR spectrum (Fig. 2.1), a sharp singlet was observed in the down field region at δ 13.80 (1-OH) which indicated the presence of an intra-molecular hydrogen bonded hydroxyl group. Two singlet signals at δ 6.25 and δ 6.72 were assigned to the two isolated aromatic protons at positions C-4 and C-5 respectively. Meanwhile the presence of 3-methylbut-2-enyl groups was

confirmed by the following characteristic signals. Two doublet signals at δ 3.37 (J=7.3 Hz) and δ 4.10 (J=7.3 Hz) were attributed to the benzylic methylene groups at C-11 and C-16. A triplet at δ 5.26 which integrated to two protons were due the vinylic protons at C-12 and C-17. Meanwhile, four singlet signals at δ 1.71, δ 1.82, δ 1.68, and δ 1.84 were assigned to H-14, H-15, H-19 and H-20, respectively. The extracted α-Mangostin was therefore identified as α-mangostin as shown in Figure 2.1 and the spectral data are summarized in Table 2.

The final total amount of total α-mangostin which extracted from 1 kg dry pericarp of *G. mangostana* fruit was 18.62 g.

$$\text{Yield} = \frac{18.62}{1000} \times 100 = 1.862\ \%\ \text{(with dry pericarp)}$$

$$\text{Yield} = \frac{18.62}{4863} \times 100 = 0.383\ \%\ \text{(with fresh fruit)}$$

Through the analysis, we confirmed that the crystallized sample is α-mangostin of high purity. The IR, MS and NMR spectral results were in accordance with those previously reported (Sen AK et al., 1982; Ee GCL et al., 2006). The IR- and NMR-spectral results conclusively confirmed the structure of the sample.

2 – 3. Conclusion and discussion

In this paper, α-mangostin of relatively high purity was extracted successfully using silica gel fraction, and the extraction process engineering is simple, inexpensive with high yields. The mainly way to extract mangosteen pericarp is the novel extraction technique – subcritical ethanol extraction. According to this method for extracting the alpha-mangostin from the *Garcinia mangostana* pericarp, water extraction and alcohol extraction are used for obtaining the crude extract first in the extracting process, the content of the α-mangostin of the crude extract is 70%-80%, then subcritical extraction is conducted, and the content of the alpha-mangostin is further made to reach 98%. The method is short in time, small in dosage of reagents, simple in step and high in yield and content, a subcritical extraction agent is volatilized directly to obtain a product, and thus the method is more suitable for industrial production.

In the extraction process of bioactive compounds from plant, organic solvents such as methanol, ethanol, chloroform and ethyl acetate are known as solvents. However, due to their toxicity and volatility these organic solvents are considered contributing the environmental pollution and health hazard (Fig. 2.6) (Bi et al., 2013; Duan et al., 2016; Azmir et al., 2013). Therefore, it is needed to optimize the extraction method in order to give minimum negative impact to the environment and human health which is emerging become the focus of many researchers now days for the conventional organic solvents.

In addition, the sample to solvent ratio significantly affected to the extraction yield (Scheme 1). For the experiment, ethanol, hexane and ethyl acetate were applied to investigate this affect to the extraction yield. The extraction was carried out in the laboratory equipment. Xanthone extraction was increased with increasing of percent ethanol and extraction time. The increasing of percent ethanol, extraction time and temperature increased solubility of xanthone in solvent

(Nuttawan Yoswathana and M. N. Eshtiaghi, 2015). It was found the extraction constant conditions were at extraction time 2 days and room temperature in 95% ethanol. The solvent ratio of hexane and ethyl acetate were investigated 10:0, 10:1, 5:1, 2:1 (v/v) as shown in scheme 1. The yellow crystallized was found only in the fraction of 5:1, this crystallized was then determined as α-mangostin. The uncrystallize was chromatographed with isocratic solvent n – hexane/EtOAc 5:1 and 3:1, the yield of α-mangostin were collected 12.16 g and 4.26 g, respectively. This result indicated that the maximum extraction yield was obtained at the ratio of hexane and ethyl acetate of 5:1 (v/v). In addition, nearly no increasing of α-mangostin within 0.5 to 2 h could be detected with increasing of extraction time. Therefore, α-mangostin was increased with increasing of extraction time that means 30 min extraction time was long enough to extract xanthone at applied technique conditions.

In conclusion, in this study I successfully extracted α-mangostin based the traditional method using ethanol. I investigated to optimize the extraction condition to save the solvent and decreased the process cost. In addition, it is more important that this method minimized the impacts from used solvents to human and environment, by using minimized the ratio of hexane and ethyl acetate with highest yield of α-mangostin.

2 – 4. Material and experimental method

Materials

Mangosteen fruit pericarp were collected at Cau Giay district, Hanoi province, Vietnam in April, 2019. The pericarp of mangosteen fruit were then dried and milled to be fine powder before extraction. n – Hexane and ethyl acetate solvents were obtained from Thermo Fisher Scientific (Waltham, MA, USA). Dioleoylphosphatidylcholine (DOPC), cholesterol (Chol) and polycarbonate membranes (100 nm) were purchased from Avanti® Polar Lipids (Alabaster, AL, USA). Phosphate buffered solution (PBS) was obtained from Sigma

Extraction of α-mangostin

The pericarp powder of mangosteen fruit (1kg) was extracted by maceration with EtOH (2L x 3 times) at room temperature in 2 days each. The combined extracts were filtrated and evaporated the solvent under reduced pressure to form 144.9 g of dark brown residue. Purified water H_2O (400 ml) was used to disperse the extract then followed by extraction with n – hexane (2 x 250ml), EtOAc (4 x 250 ml) and H_2O – soluble extracts.

The n – hexane and ethyl acetate (EtOAc) extracts were pre-adsorbed on SiO_2, that was chromatographed by silicagel column with n – hexane/EtOAc (from 10:0 to 2:1), to give 4 fractions (E1 – E4). Fraction E3 (38g) was recrystallized to give α-mangostin (2.2 g) and 2 fractions (E-3.3; E-3.4). The crystallinity E-3.3 fraction (7.15 g) was chromatographed with isocratic solvent n – hexane/EtOAc (3: 1) to give more of α-mangostin (4.26 g). E-3.4 fraction was splitted by silicagel column with hexane - Acetone (5: 1) to give α-mangostin more (12.16 g). The extraction scheme was shown in Scheme 1.

References

Ames, R., Brown, J. and Wang, Y. 2000. Dichloromethane in drinking water. Office of Environmental Health Hazard Assessment.

Azmir, J., Zaidul, I.S.M., Rahman, M.M., Sharif, K.M., Mohamed, A., Sahenab, F., Jahurul, M.H.A., Ghafoor, K., Norulaini, N.A.N., Omar, A.K.M. (2013). Techniques for Extraction of Bioactive Compounds from Plant Materials: A Review. Journal of Food Engineering, 117 , 4, 426–436.

Bi, W., Tian, M., Row, K.H. (2013). Evaluation of Alcohol-based Deep Eutectic Solvent in Extraction and Determination of Flavonoids with Response Surface Methodology Optimization. Journal of Chromatography A, 1285, 22–30.

Chopra, R.N., Nayar, S.L., Chopra, I.C. 1965. Glossary of Indian medicinal plants. Nueva Delhi: the National Institute of Science Communication and Information Resources.

Duan, L., Dou L-L., Guo, L., Li, P., Liu, E-H. (2016). Comprehensive Evaluation of Deep Eutectic Solvents in Extraction of Bioactive Natural Products, ACS Sustainable Chemistry & Engineering, 4, 2405-2411.

Ee, G.C.L., Daud, S., Taufiq-Yap Y.H., Ismail, N.H., Rahmani, M. Xanthones from Garcinia mangostana (Guttiferae). J Nat Prod Res. 2006; 20: 1067–1073.

Garnett, M., Sturton, S.D. 1932. Garcinia Mangostana in the treatment of amoebic dysentery. Chinese Medical Journal 46:969–973.

Ketsa S, Paull RE. Mangosteen (Garcinia mangostana L.). In Yahia EM, editor. Postharvest biologyand technology of tropical and subtropical fruits, Vol. 4. Woodhead Publishing Ltd: Cambridge; 2011 pp. 1–30.

Kosem, N., Ichikawa, K., Utsumi, H., Moongkarndi, P. In vivo toxicity and antitumor activity of mangosteen extract. J Nat Med. 2013; 67: 255–263. doi: 10.1007/s11418-012-0673-8 PMID: 22622784.

Mahabusarakam, W., Wlriyachitra, P., Taylor, W.C. 1987. Chemical constituents of garcinia mangostana. Journal of Natural Products 50:474–478 DOI 10.1021/np50051a021.

Moongkarndi, .P, Jaisupa, N., Samer, J., Kosem, N., Konlata, J., Rodpai, E., Pongpan, N. Comparison of the biological activity of two different isolates from mangosteen. J Pharm Pharmacol. 2014; 66: 1171–1179. doi: 10.1111/jphp.12239 PMID: 24641353

Pothitirat, W., Chomnawang, M.T., Supabphol, R. and Gritsanapan, W. 2010. Free radical scavenging and anti-acne activities of mangosteen fruit rind extracts prepared by different extraction methods. Pharmaceutical Biology. 48: 182-186.

Sen, A.K., Sarkar, K.K., Mazumder, P.C., Banerji, N., Uusvuori, R., Hase, T.A. The structures of garcinones a, b and c: Three new xanthones from Garcinia mangostana. J Phytochem. 1982; 21: 1747–1750.

Weecharangsan, W., Opanasopit, P., Sukma, M., Ngawhirunpat, T., Sotanaphun, U., Siripong, P. Antioxidative and neuroprotective activities of extracts from the fruit hull of mangosteen (Garcinia mangostana L.). Med Prin Pract. 2006; 15: 281–287.

Zhang, C.Z. The effect of α-mangostin on metabolic disease. M. Sci. Thesis, Jilin Agriculture University, 2011.

Zarena AS, Sankar KU. Synthesis of α−mangostin-D-glucoside in supercritical carbon dioxide media. J Food Sci Technol. 2015;52(10):6547–6555. doi:10.1007/s13197-014-1705-z.

Yu L.M., Liu J.M., Feng W.H., Bai W.D. Changes of the active ingredients of Mangostana wine during fermentation and aroma components of finished wine. Mod Food Sci Technol. 2014; 30: 287–291,296.

Yoswathana Nuttawan, Eshtiaghi Mohammad. Optimization of Subcritical Ethanol Extraction for Xanthone from Mangosteen Pericarp. International Journal of Chemical Engineering and Applications. 2015. 10.7763/IJCEA.2015.V6.463.

Figures

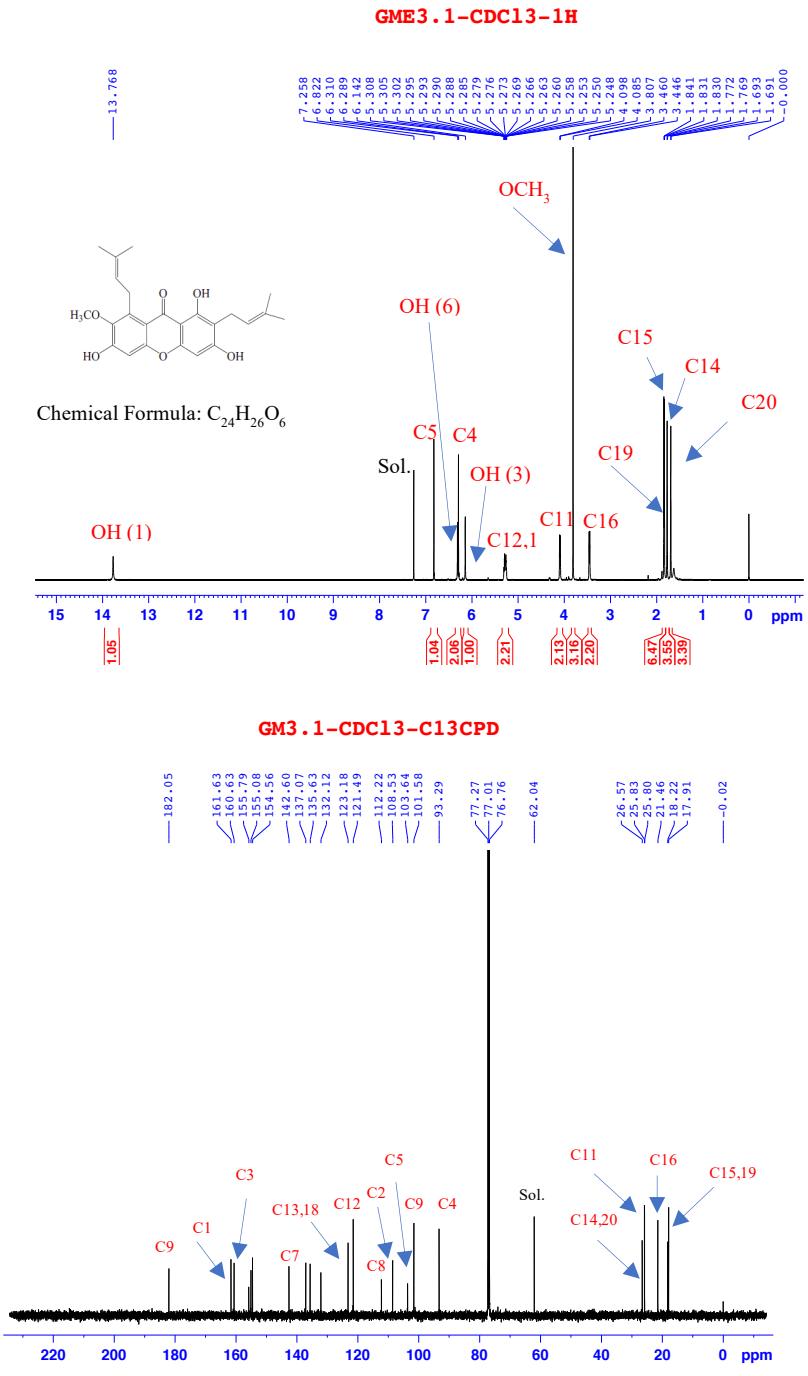

Figure 2.1. ^{1}H NMR and ^{13}C NMR spectra of α-mangostin in deuterated chloroform $CDCl_3$

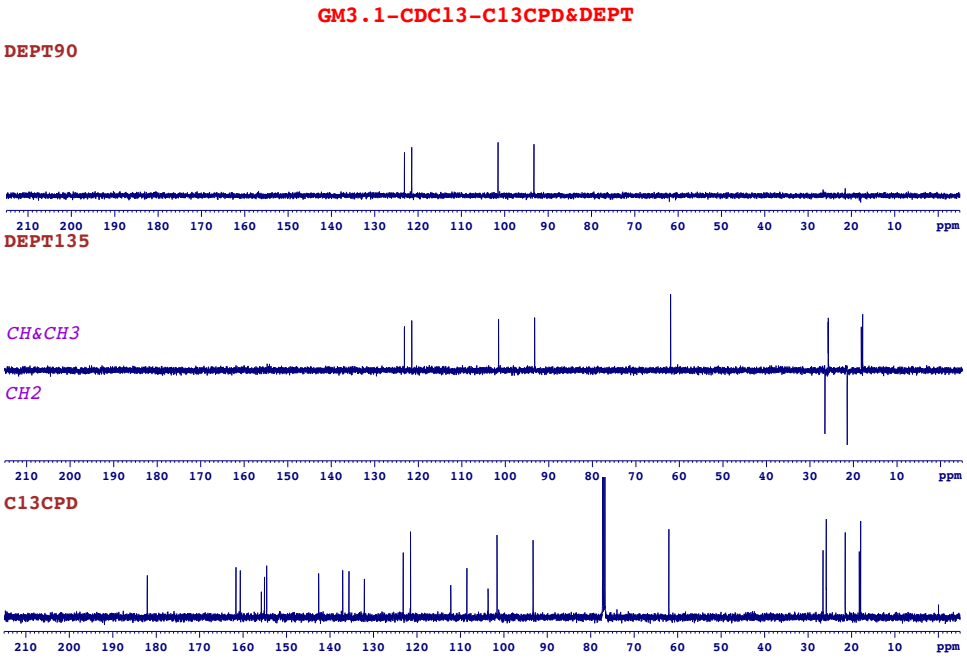

Figure 2.2. DEPT spectrum of α-mangostin

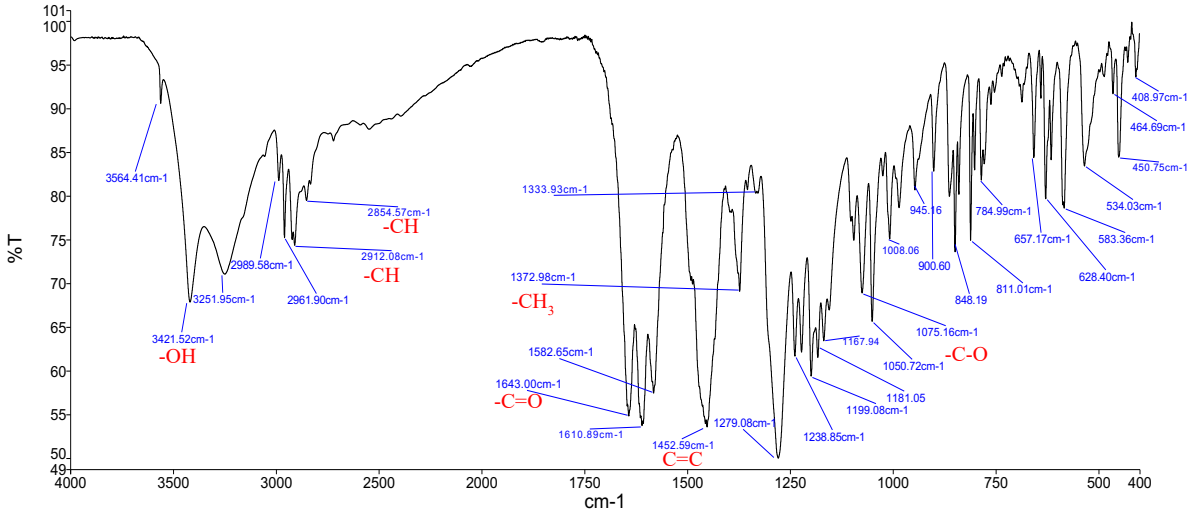

Figure 2.3: The results of IR spectra of α-mangostin

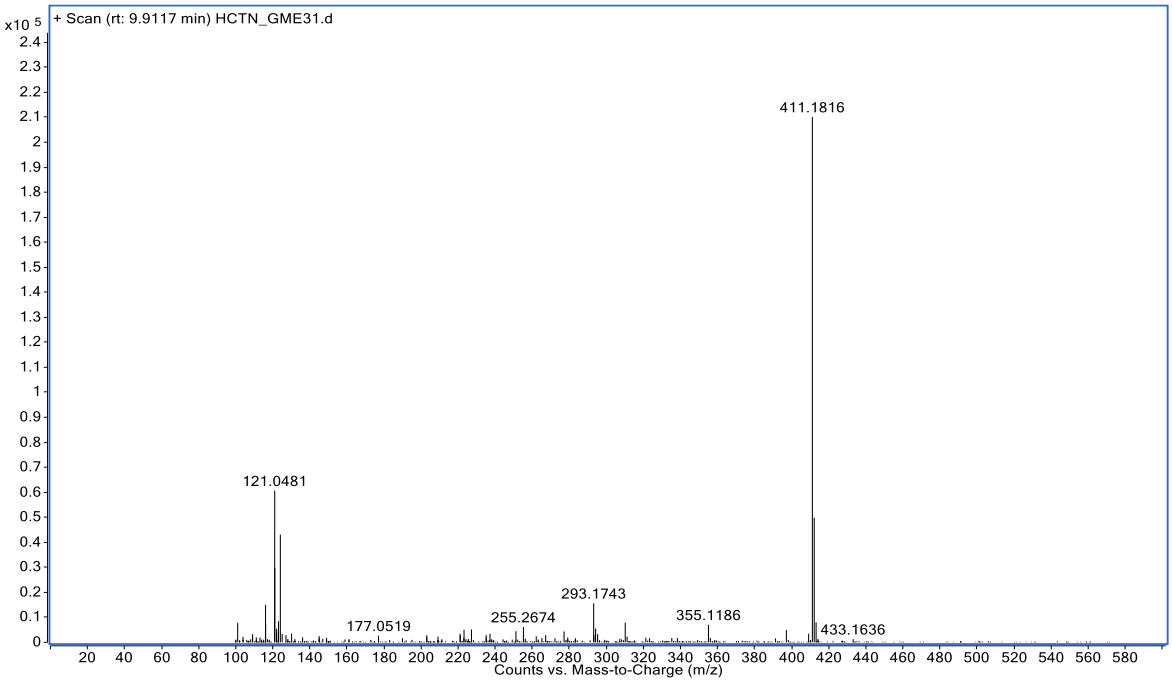

Figure 2.4. Mass spectrometry of α-mangostin

Figure 2.5. α-Mangostin is collected after extraction. A yellow crystalline powder of α-Mangostin was obtained after extraction process.

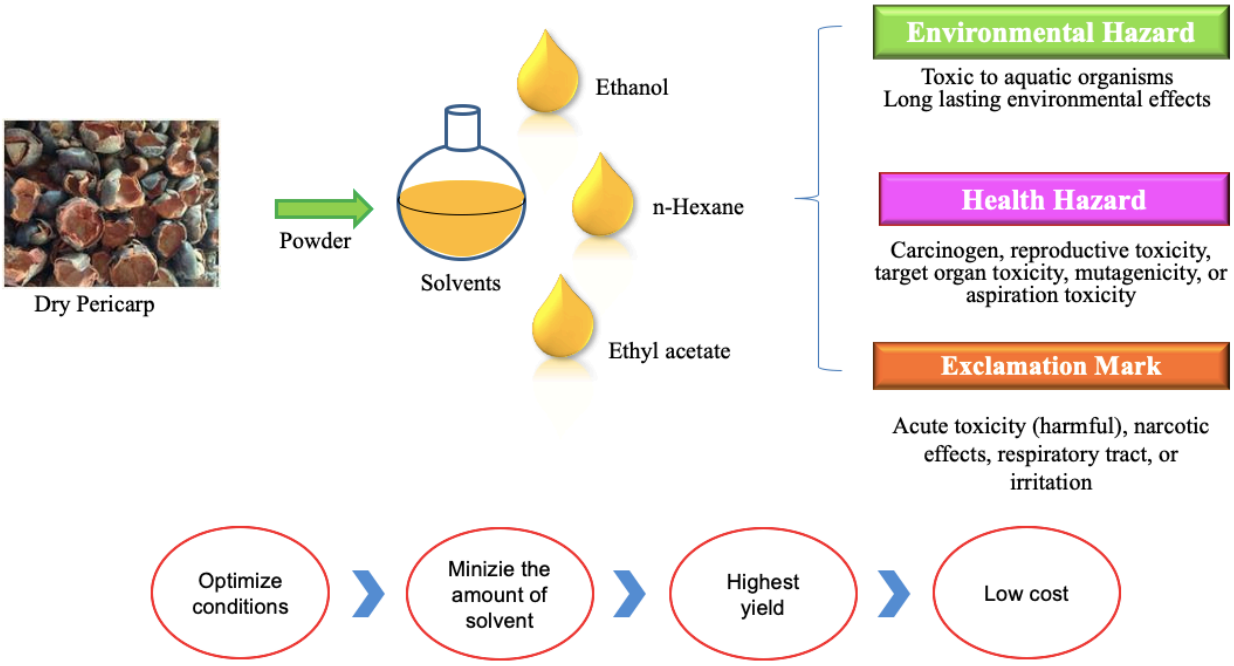

Figure 2.6: The solvents using for extraction process and their hazard.

Table 2. **NMR data for α-mangostin in deuterated chloroform $CDCl_3$; 500 Hz**

	$\delta_{H;}$ ppm (mult., J in Hz)	δ_H (500MHz, $CDCl_3$ [1]
1	-	-
2	-	-
3	-	-
4	6.29 (s; 1H)	6.3 (s)
4a	-	
5	6.82 (s; 1H)	6.83(s)
6	-	-
7	-	-
8	-	-
8a	-	-
9	-	-
9a	-	-
10	-	-
11	3.46 (d;J= 7Hz; 2H)	3,46 (d; J= 7.5 Hz)
12	5.3 (m, 1H)	5.29 (t; J=7Hz)
13	-	-
14	1.77 (d; CH_3)	1.77 (s)
15	1.83 (d; CH_3)	1.83 (s)
16	4.09 (d; J=6.5 Hz, 2H)	4.09 (d; J=6.5 Hz)
17	5.3 (m; 1H)	5.29 (t; J=7Hz)
18	-	-
19	1.84 (s; CH_3)	1.84 (s; CH_3)
20	1.69 (d; CH_3)	1.69 (s; CH_3)
OCH_3 (7)	3.8 (s,3H)	3.8 (s,3H)
OH (1)	13.77 (s)	13.78 (s)
OH (3)	6.14 (s)	6.15 (s)
OH (6)	6.3 (s)	6.31 (s)

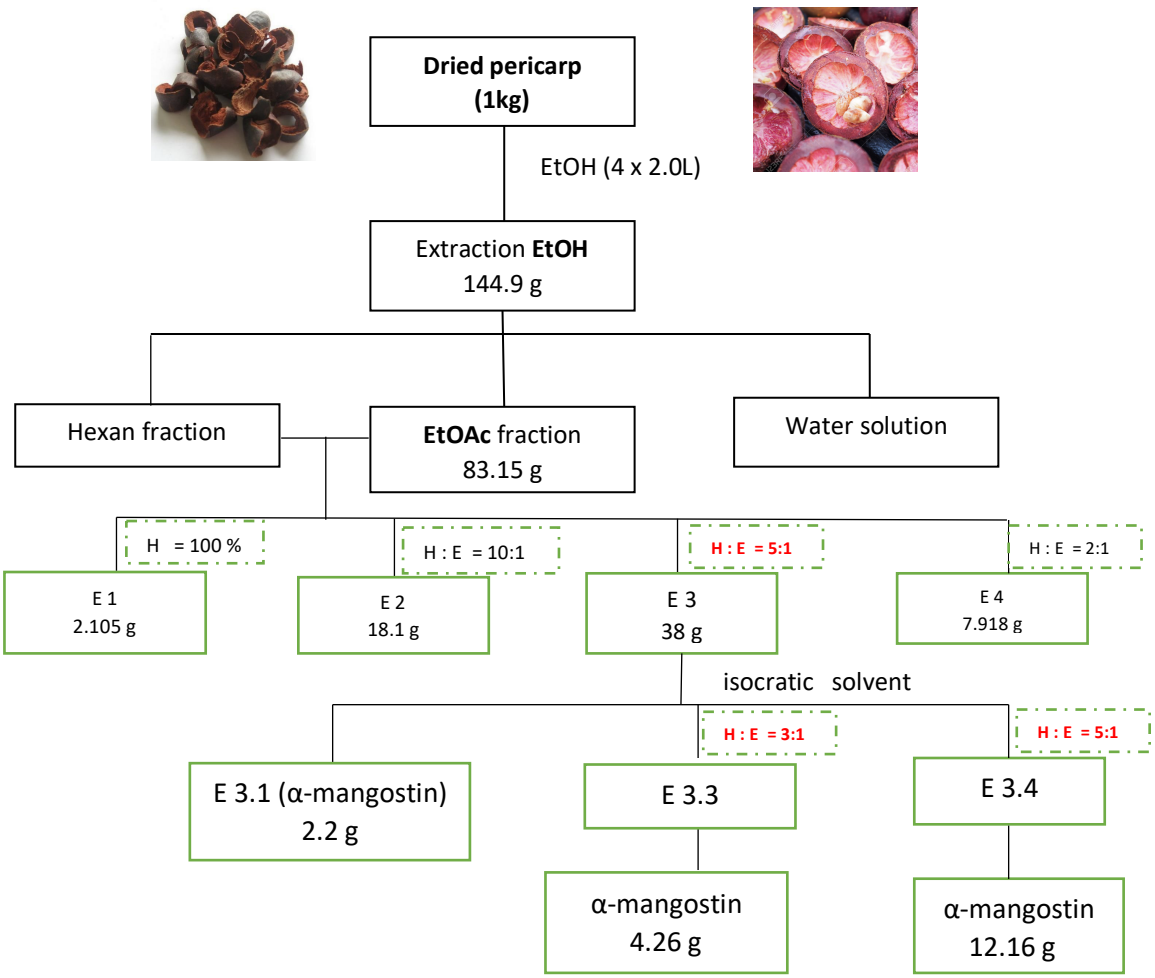

Scheme 1: The isolation of α-mangostin

Chapter 3: α – Mangostin inhibits metastasis of lung cancer cells

3 – 1. Overview

Several studies have indicated that α-mangostin exerts anti-metastasis and anti- subsistence effects on several types of cancer cells. Especially, the anti-metastatic effect of α-mangostin on cancer cells is a prospective function in cancer treatment. However, the metastasis process is complicated, and includes migration, invasion, intravasation, and extravasation; thus, the main target of anti-metastatic effect of α-mangostin is not known. In this study, I investigated the effects of α-mangostin on the invasion, subsistence, and migration of lung cancer cells under co-culture conditions with normal cells and regular mono-culture conditions. I found that α-mangostin killed the lung cancer and normal cells in a dose-dependent manner. Furthermore, the alteration in the surface mechanical properties of cells was examined by using atomic force microscopy. Although the α-mangostin concentrations of 5 and 10 μM did not affect the short- term cell viability, they considerably decreased the Young's modulus of lung cancer cells implying a decline in cell surface actin cytoskeletal properties. Additionally, these concentrations of α-mangostin inhibited the migration of lung cancer cells. In co- culture conditions (cancer cells with normal cells), the invasive activities of cancer cells on normal cells were discernibly observed, and was inhibited after treatment with 5 and 10 μM of α-mangostin. Taken together, α-mangostin suppressed the subsistence of lung cancer cells and displayed anti-metastatic activities by inhibiting the migration and invasion, and reducing the actin cytoskeleton of cancer cells. Our findings suggest that α-mangostin could be a potential therapeutic agent for cancer treatment.

3 – 2. Introduction

3 – 2.1. Cancer metastasis

Cancer metastasis is the propagation of cancer cells from their original location (the primary tumor) to distant organs and locations to form secondary tumors (Fig. 3.1). This is the result of a series of molecular events involving not only through their association with the ECM and invasion of adjacent tissues. The process is composed of a number of sequential events which must be completed in order to the tumor cell to successfully metastasize, the so called metastatic cascade (Chambers et al., 2002).

The metastatic cascade can be divided into three main processes which includes invasion, intravasation and extravasation. Once cancer cells lose cell-cell adhesion capacity which allows them to dissociate from the primary tumor mass and changes in cell-matrix interaction enable the cells to invade the surrounding stroma, this called invasion. The abnormalities such as mutation or dysregulation can lead to the dissociation of the primary tumor and enhanced potential for dissemination of cancer cells. The regulators of cell-cell adhesion which are play important role are tight junction (TJ), gap junction, E-cadherin (Jiang et al., 2015). In epithelial cell, the TJ functions in an adhesive manner and can prevent cell dissociation. A change in cancer cells by upregulation or downregulation of TJ protein results in loss of cell-cell association, cell contact inhibition, leading to uncontrolled growth, loss of adhesion to and degradation of the basement, then help cancer cells passages through this barrier. Beside, E-cadherin is essential in weakening of cell-cell adhesion occurs to allow cells become motile and metastasis and modification in the adhesive properties of cells (Tracey A. Martin et al., 2013; Jiang et al., 2015).

The tumour will not develop if lack of angiogenesis process, it is necessary to local diffusion for transport of nutrients to and removal of waste products. The blood vessel within the

tumour's vicinity can then provide a route for the detached cells to enter the circulatory system and metastasize to distant sites called the process of intravasation (Tracey A. Martin el at., 2013). Cancer cells breach the basement membrane and invade nearby blood vessels to gain access to the circulation and are subsequently transported to a distant site. The cancer cells take in use blood vessel tissue to product pro-angiogenic factors such as vascular endothelial growth factor (VEGF) family, FGF, hepatocyte growth factor (HGF), then bind to and activate endothelial cells of a neighboring blood vessel begin to produce enzyme that break down the basement membrane of the blood vessel creating tiny pore (Jiang et al., 2015). Endothelial proliferated and migrate through this pores, toward the angiogenic source, then undergo a tubule formation phase, and recruit additional cell types to support the vessel and allowing blood follow to the angiogenic source.

The tumour cell has arrived at a likely point of intravasation, it interacts with the endothelial cells to form stronger bonds, and penetrates the endothelium and the basement membrane, it called extravasation (Don X. Nguyen et al., 2009). Cancer cell contact to mesothelial cells is followed consequently by adhesion, invasion and growth of tumor cells at such a new site. Factors released from tumor cells or adjacent stroma provide a favorable environment for the interaction between cancer cells and mesothelial such as IL-1β or TGF-β1 from cancer cells which can act on the mesothelial cells and adjacent stroma to promote peritoneal dissemination (Tracey A. Martin et al., 2013).

3 – 2.2. The anticancer properties of α-Mangostin

α-Mangostin is the major xanthone extracted from the pericarp of mangosteen (Garcinia mangostana Linn) fruit. Mangosteen is a prevalent fruit in the tropical rainforests of Southeast Asian nations, and its pericarp has had a long history of medicinal value in this region (Pedraza-Chaverri, 2008). The dried pericarp powder has been used as a medicinal agent for treatment of

skin-related diseases, wounds, and amoebic dysentery (Chopra, Nayar & Chopra, 1965; Garnett & Sturton, 1932; Mahabusarakam, Wlriyachitra & Taylor, 1987). The pericarp of mangosteen fruit contains a variety of secondary metabolites such as prenylated and oxygenated xanthones (Govindachari et al., 1971; Peres, Nagem & De Oliveira, 2000; Sultanbawa, 1980). Exudates from the mangosteen pericarp include α-, β, and γ-mangostin, garcinone B and E, along with mangostinone, tannins, and a flavonoid called epicatechin (Wexler, 2007). Especially, α-mangostin is the most abundant prenylated xanthone present in the pericarp.

α-Mangostin displays strong pharmacological effects (Ibrahim et al., 2016); specifically, its potential in cancer treatment has attracted increasing attention from scientists. Several studies have indicated that α-mangostin is effective against various types of cancer. α-Mangostin has been shown to induce apoptosis in rat pheochromocytoma (Sato et al., 2004) and human head and neck squamous carcinoma cells (Kaomongkolgit, Chaisomboon & Pavasant, 2011). The anti-proliferative effects of α-mangostin were discovered in human colon cancer (Matsumoto et al., 2005) and canine osteosarcoma cells (Krajarng et al., 2012). The anti-metastatic properties of α-mangostin were found in human prostate carcinoma (Hung et al., 2009), breast adenocarcinoma (Lee et al., 2010), and lung adenocarcinoma cells (Shih et al., 2010). Studies in in vivo experiments revealed that α-mangostin reduced the tumor growth and lymph node metastasis (Aisha et al., 2012; Shibata et al., 2011). Thus, α-mangostin is considered to be able to prevent cancer cell metastasis as well as subsistence.

3 – 2.2. The purpose of this study

Although a broad range of biological and pharmacological activities of α-mangostin have been reported, the mechanism behind its anti-metastatic effects is not fully understood. In the metastasis process, the cancer cells undergo multiple steps including migration, invasion,

intravasation, as well as extravasation (Sahai, 2007). These steps are probable targets for the inhibition of metastasis, especially invasion, which is an early and important target for the inhibition of metastatic process. In this study, I focused on the invasion process of cancer cells and examined the effects of α-mangostin on the progression of initial invasion of cancer cells that come in contact with normal cells (Fig. 3.2). In order to reflect the anti-invasion activities of α-mangostin more accurately in cancer treatment, I established a co-culture system of cancer and normal cells that imitated the initial invasive progression of cancer cells. Lung cancer is one of the most aggressive cancers with a five-year overall survival rate in 10–15% of the patients. This is attributable to the early metastatic process of lung cancer cells via the rapid spread to many distant sites within the body. Therefore, in this study, I employed non-small cell lung cancer A549 cells along with one normal bronchus diploid cell line CCD-14Br and used them in co-culturing experiments.

3– 3. Experimental results

3 – 3.1. Cytotoxicity of α – Mangostin on lung cells

The cytotoxicity of α-mangostin on A549 cells was evident by a dose- and time-dependent inhibition of cell viability and growth (Shih et al., 2010). I first evaluated the cytotoxicity of α-mangostin by treatment of both the non-small cell lung cancer A549 and pulmonary normal diploid CCD-14Br cell lines with various concentrations of α-mangostin for 24 h. The cell viability was evaluated by the reduction of formazan dye produced from WST-8 in the presence of an electron mediator by the activities of dehydrogenases in cells. α-Mangostin exhibited cytotoxic effects on A549 and CCD-14Br cells at higher concentrations (Fig. 3.3A). The half-maximal effective concentration (EC50) values of α-mangostin for the cytotoxicity of A549 and CCD-14Br cells were 19 μM and 22 μM, respectively (Fig. 3.3). Furthermore, I examined the cytotoxic effects of α-mangostin on these cells in time course experiments (24–96 h culture). The EC50 values of α-mangostin for the cytotoxic effects for A549 and CCD-14Br cells decreased in a time-dependent manner (Figs. 3.3B and 3.3C). The EC50 values of α-mangostin for the cytotoxic effects for A549 cells almost plateaued at 48 h of culturing and was about 10 μM (Fig. 3.3B). On the other hand, the EC50 values of α-mangostin for the cytotoxic effects for CCD-14Br cells gradually decreased (Fig. 3.3C). Thus, CCD-14Br cells were less sensitive to the cytotoxic effects of α-mangostin than the A549 cells. Compared with the untreated control, A549 and CCD-14Br cells treated with α-mangostin at concentrations below 5 μM were not significantly different, proving that these dosages are non-toxic to these cells. However, those treated with more than 10 μM of α-mangostin displayed some cytotoxicity in both A549 and CCD-14Br cells (Fig. 3.3). Therefore, I used less than 10 μM of α-mangostin for subsequent experiments.

3 – 3.2. α – Mangostin decreases the cell surface stiffness

I then examined the effect of α-mangostin on the mechanical properties of cells using AFM. Alterations in cell activities or states often entail a change in the mechanical properties of cells (Haghparast et al., 2013; Shimizu et al., 2012), and the mechanical alterations are largely attributable to the actin cytoskeleton (Dai & Sheetz, 1995; Sugitate et al., 2009). Thus, analyzing the alteration in mechanical properties of cells can reveal the changes in characteristics of their underlying actin networks as well as their states (Haghparast, Kihara & Miyake, 2015; Haghparast et al., 2013; Kihara et al., 2011). AFM indentation is a sensitive method for analyzing the surface mechanical properties of cells (Haghparast, Kihara & Miyake, 2015; Haghparast et al., 2013). Figure 3.4 shows the distribution of the Young's modulus of the cells treated with α-mangostin. The distribution of Young's modulus of normal CCD-14Br cells (fibroblast-like morphology) has a logarithmic average value of 8.9 kPa, which was clearly higher than that of cancerous A549 cells with logarithmic average value of 3.6 kPa (Fig. 3.4). The difference in mechanical properties of normal and cancer cells is based on the difference in F-actin structures at the apical surface of these cell types (Cross et al., 2007; Haghparast et al., 2013; Lekka et al., 2012).

Addition of 5 μM or 10 μM of α-mangostin to the cells reduced the distribution of the Young's moduli in A549 as well as CCD-14Br cells in a dose-dependent manner (Fig. 3.4). Particularly, the Young's modulus of A549 cells significantly decreased (Fig. 3.4). Thus, even though its concentration does not affect cell viability in a short-time period, α-mangostin clearly reduced the surface rigidity of cells. Furthermore, A549 cells, whose surface stiffness was originally soft, were more sensitive to the effect of α-mangostin than the CCD-14Br cells. Lung cancer cells A549 are more sensitive with α-mangostin compared with normal cells CCD-14Br in changing the mechanical properties.

3 – 3.3. α-Mangostin inhibit cell migration

The effect of α-mangostin on lung cancer A549 cell motility was measured by the wound healing assay (Liu et al., 2013), an established method for studying directional cell migration in vitro. The migration of several types of cancer cells was reportedly inhibited after treatment with α-mangostin (Shih et al., 2010; Wang, Sanderson & Zhang, 2012; Yuan, Wu & Lu, 2013). In the untreated control group, cells exhibited marked cell migration in the wounded area, whereas the wounds treated with α-mangostin showed a delayed healing (Fig. 3.5). The ratio of recovered area of wound closure in the untreated cells was about 0.47 at 12 h and almost 0.98 after 24 h (Fig. 3.5B). On the other hand, α-mangostin, at 5 and 10 μM, reduced the ratio of recovered area of wound closure to approximately 0.36 after 12 h, and 0.87 after 24 h (Fig. 3.5B). This result indicated that α-mangostin inhibited the migration of A549 cells in vitro.

3 – 3.4. Impacts of α – Mangostin on metastasis of lung cancer cells

The co-culturing system of A549 and CCD-14Br cells was used as a model for evaluating cancer cell invasiveness, which imitate the initial invasive progress of cancer cells. Then I examined the potential effects of α-mangostin on cancer cell invasion (Fig. 3.7A). Besides, the monoculture of each cell type was also conducted to compare their results with those of the co-culture (Fig. 3.6).

When only cancerous A549 cells were cultured, the cells grew and covered almost all of the plate surface after six days under α-mangostin concentration of less than 5 μM; however, the cells treated with 10 μM of α-mangostin showed a gradual decrease in the area covered by cells (Fig. 3.6, A549 and Fig. 3.7B, A549 mono-culture). Conversely, when CCD-14Br cells were cultured under α-mangostin condition, the cells gradually proliferated (Fig. 3.6, CCD-14Br and Fig. 3.7B, CCD-14Br mono-culture). These results suggest that A549 cells were relatively sensitive to high

concentration of α-mangostin and showed gradual cell death at 10 μM of α-mangostin after three days culture. These results are roughly corresponding to our cytotoxic experiments (Figs. 3.3B and 3.3C).

After A549 and CCD-14Br cells were co-cultured, the A549 cells gradually grew and almost covered the whole area at six days (Figs. 3.7A, ctrl and 3.7B, Co-culture of control condition). Conversely, the covered area of CCD-14Br cells increased within several days, and after coming in contact with A549 cells, the area of CCD-14Br cells gradually decreased (Figs. 3.7A, control and 3.7B, Co-culture of ctrl condition). A549 cancer cells killed and eroded the normal CCD-14Br cells and resulted in a decline in the area of the CCD-14Br cells. In contrast, in the presence of α-mangostin, A549 cells could not cover the whole surface area of the culture plate, and the coverage area of the CCD-14Br cells did not decrease (Fig. 3.7A, 5 μM of α-mangostin and 10 μM of α-mangostin and 3.7B, Co-culture of 5 and 10 μM of α-mangostin conditions). Thus, invasive activities of A549 cells on CCD-14Br cells were inhibited by treatment with α-mangostin. Furthermore, in the presence of 10 μM of α-mangostin, A549 cells proliferated gradually but did not show any cell death as seen with the monoculture (Fig. 3.7B, 10 μM of α-mangostin).

Thus, normal CCD-14Br cells probably rescue A549 cells from the cytotoxic effects of highly concentrated α- mangostin. These results demonstrate that by using a co-culturing system, I can conspicuously observe the invasive activities of cancer cells acting on normal cells and α-mangostin exhibited its potential effect in repressing cancer cell invasion.

3 – 4. Conclusion and Discussion

Metastasis is a critical biological process in cancer pathophysiology and is a therapeutic target for treating active cancer. Previous studies have shown that α-mangostin displays anti-metastatic properties in many carcinoma cells and lymph node metastasis (Hung et al., 2009; Lee et al., 2010; Shibata et al., 2011; Shih et al., 2010). Although it has been demonstrated that α-mangostin decreased the expression of many cancer-related signal transductions and matrix metalloproteases (Fang et al., 2016; Hung et al., 2009; Krajarng et al., 2011; Shih et al., 2010), the detailed anti-metastatic mechanism of α-mangostin remains unclear. One of the reasons is that the metastatic process consists of multiple biological steps including migration, invasion, intravasation, and extravasation; thus, it is difficult to determine which steps are the targets of α-mangostin. Previous studies have been conducted only in a monoculture condition, where normal and cancer cells were cultured in isolation. Cancer development, progression, and invasion are positively and negatively affected from the tumor microenvironment, in which cancer cells interact with associated stroma (Quail & Joyce, 2013). Interaction between the cancer cells and the associated stroma present a powerful relationship that influences disease initiation and procession and patient prognosis. However, the monoculture condition alone cannot reproduce the cell responses associated with the cell–cell interactions. In this study, I established a 2D co-culturing system using cancer and normal cells; this model was devised to explore the interactions during the process of lung cancer invasion. Indeed, previous studies demonstrated that the co-culturing system showed dramatically different cellular properties in terms of morphology, proliferation, and cellular function (Angelucci et al., 2012; Furukawa et al., 2015).

Thus, the co-culturing system better simulates the living environment and cellular interactions that occur under in vivo conditions. However, our co-culturing system is based on a

2D culture system and thus I are unable to ascertain cancer cell-extracellular matrix interactions. If I want to simulate the whole invasion process of cancer cells, I may have to develop a 3D co-culture system using cancer cells and normal cells in the future. In this study, I demonstrated that α-mangostin exerts pharmacological effects in lung cancer treatment, by using not only the monoculture but also co-culture conditions with non-small cell lung cancer A549 cells and normal bronchus diploid CCD-14Br cells.

Our results indicated that A549 cells, which are highly invasive carcinoma cells, invaded and caused serious damage to normal CCD-14Br cells. However, the invasive and erosive activities of A549 cells declined following treatment with α-mangostin, which could rescue the CCD-14Br cells from the invaded damage. Another interesting finding was that the A549 cells gradually died when treated for a long time period with high concentration of α-mangostin under the monoculture condition, meanwhile the cancer cells survived under co-culture with normal cells. Communication between cancer and surrounding cells is probably mediated by secreted proteins, including growth factors and cytokines (Mueller & Fusenig, 2004; Polyak, Haviv & Campbell, 2009; Quail & Joyce, 2013). In previous study, α-mangostin was indicated that inhibited some growth factors (PDGF), cytokines (TGF, MCP1), proteases which are released from cancer cells and send to surrounding cells (cancer-associated fibroblast, stroma cells) in order to recruit other factors for cancer growth and metastasis (Fig. 3.8). Therefore, α-mangostin inhibited cancer-released signals following by breaking down the communication between cancer cells and normal cells. In addition, I consider that the surrounding normal cells support the cancer cell subsistence by secreting cytokines. I believe that co-culturing of cancer cells with normal cells provides an environment similar to the tumor microenvironment (Quail & Joyce, 2013) and a more accurate characterization of the invasive ability of cancer cells.

α-Mangostin affected cell surface stiffness of A549 and CCD-14Br cells, especially the Young's modulus of A549 cells, which clearly declined by treatment with 10 μM α-mangostin. The surface stiffness of cells reflects their underlying actin networks as well as their states (Haghparast, Kihara & Miyake, 2015; Haghparast et al., 2013; Kihara et al., 2011). Therefore, α-mangostin clearly altered the actin network of A549 cancer cells. It is known that the stiffness of cancer cells is lesser than that of the corresponding normal cells (Cross et al., 2008; Guck et al., 2005; Lekka, 2016), and softer cancer cells show higher malignant properties than stiffer cancer cells (Cross et al., 2011; Ramos et al., 2014). On the other hand, F-actin modification reagents usually decrease cell migration (Yamaguchi & Condeelis, 2007), and apoptotic cells are less stiff than normal cells (Kihara et al., 2009; Kim et al., 2012). α-Mangostin-treated cancer cells presented a decrease in their migration and invasion properties. Thus, α-mangostin probably affects the F-actin structures or mass, and this change has negative effects on cancer cell properties.

Finally, I discuss the pharmacological potential of α-mangostin. I suggest that α-mangostin shows an ability to suppress cancer cells at concentrations about 10 μM, which could effectively inhibit cancer progression by inhibiting cell growth, migration, and invasion. Using this dosage of α-mangostin, I aim to treat cancer by turning off the growth and development of cancer cells. However, only low levels of α-mangostin are adsorbed through the gastrointestinal tract in treated mice and the bioavailability F value of α-mangostin from oral administration is about 0.8% (Choi et al., 2014). The terminal half time of α-mangostin after intravenous administration is about 3 h in mice (Choi et al., 2014). For further research and effective application of α-mangostin in cancer treatment, it is necessary to develop an efficient system to deliver the optimal amount of α-mangostin to the cancer-affected area in our body.

I demonstrated that α-mangostin exerts pharmacological effects in lung cancer treatment, by using monoculture and co-culture conditions with non-small cell lung cancer A549 cells and normal bronchus diploid CCD-14Br cells. The EC50 values of α-mangostin cytotoxicity on A549 cells were lower than those of CCD-14Br cells. Although the dosages below 10 μM of α-mangostin did not show significant toxicity in an early 24-h cell culture, the treatment clearly affected A549 cancer cell properties. α-Mangostin decreased surface stiffness and inhibited the migration of A549 cells. Furthermore, α-mangostin repressed cancer cell invasion in normal cells. Our findings thus suggest that α-mangostin could be a potential therapeutic agent for cancer treatment. Furthermore, I established a co-culturing system using cancer and normal cells; and this model was devised to explore the interactions involving the cancer cell and normal cell as cancer invades.

3 – 5. Materials and experimental methods

Material

Human lung adenocarcinoma cell line A549 cells and normal human bronchogenic epithelioid cell line CCD-14Br cells were purchased from Japanese Collection of Research Bioresources (JCRB) cell bank (Osaka, Japan). 3,3'-Dioctadecyloxacarbocyanine perchlorate (DiO), 1,1'-Dioctadecyl-3,3,3',3'-tetramethylindocarbocyanine perchlorate (DiI), and antibiotics were purchased from Sigma-Aldrich (St. Louis, MO). Cell harvesting solution TrypLE express and fetal bovine serum (FBS) were purchased from Life Technologies Japan Ltd. (Tokyo, Japan). α-Mangostin was purchased from Wako Pure Chemical Industries Ltd. (Osaka, Japan). Cell counting kit-8 was purchased from Dojindo Molecular Technologies, Inc. (Kumamoto, Japan). The cone probe (BL-AC-40TS-C2; spring constant: around 0.05 N/m) was purchased from Olympus (Tokyo, Japan). Other reagents were purchased from Sigma-Aldrich, Wako Pure Chemical Industries Ltd., or Life Technologies Japan Ltd.

Cell culture

The cells were cultured in DMEM containing 10% FBS and antibiotics (100 units/mL penicillin G and 100 μg/mL streptomycin sulfate) in humidified atmosphere of 95% air and 5% CO_2 at 37 °C

Determination of cell viability

The viability of cells after treatment with various concentrations of α-mangostin was evaluated by the cell counting kit-8 as recommended by the manufacturer. Briefly, cells were seeded on a 96-well-plate at 10^4 cells/well with 100 μL medium and cultured for 24 h, so as to allow the cells to adhere to the plate. The culture medium was replaced by 100 μL of fresh culture medium diluted with various concentrations of α-mangostin for a 24-h treatment. The medium

was replaced by adding 100 μL fresh medium diluted with 10 μL of cell counting kit-8 solution to each well. The cells were cultured for suitable time periods for each cell type. The plate absorbance was then measured at 450 nm using a microplate reader. Ratio of cell viability V_c was calculated as:

$$V_c = \frac{Abs_{target} - Abs_{background}}{Abs_{ctrl} - Abs_{background}}$$

where V_c is the cell viability ratio, Abs_{target} is the absorbance of α-mangostin-treated cells, Abs_{ctrl} is the absorbance of control cells, $Abs_{background}$ is the absorbance of the background.

Measurement of mechanical properties of cells

The cultured cells treated with α-mangostin for 24 h were manipulated by atomic force microscopy (AFM) (Nanowizard III; JPK Instruments AG, Berlin, Germany) at room temperature. Combining optical microscopy (IX-71; Olympus) and AFM allows the probe to be placed on a particular region of the cell surface. In this study, the AFM probe was indented at the top of the cell surface with a loading force of up to 0.5 nN and velocity of 5 μm/s. The Young's modulus of the cell was calculated using the Hertz model (Hertz, 1882). The force-distance curve for a region up to about 1 μm of cell surface indentation was fitted using JPK data processing software (JPK instruments AG) as:

$$F = \frac{E}{1 - \nu^2} \frac{2tan\alpha}{\pi} \delta^2$$

Where F = force, δ = depth of the probe indentation, ν = Poisson's ratio (0.5), α = half-angle of the cone probe (9º), and E = Young's modulus. More than 25 cells were used per experiment, and 25 points were examined on the surface of each cell. The logarithmic Young's modulus values for each group were compared by analysis of variance followed by Mann-Whitney U test. Young's

modulus of the polystyrene tissue culture surface was more than 1×10^7 Pa (Haghparast, 2015). The range of Young's moduli of cell surface was in the order of about 10^2 to 10^4 Pa. Thus, I were convinced that the surface stiffness of the cells could be measured by this method without affecting the rigidity of culture surface.

Invasion assay

In order to evaluate the invasion ability of cancer cells, a co-culture system was established by culturing both cancer and normal cell lines together. Briefly, cells were trypsinized, spun, and resuspended with fresh medium. Then, the cell suspension was fluorescently labeled with DiI for A549 cells or DiO for CCD-14Br cells for their membrane at 37 °C for 1 h in the dark. Cells were then spun at 200 × *g* for 5 min; the medium was then removed, and cells were resuspended with fresh medium and spun one more time. The labeled cells were cultured in 12-well-plates at a density of 2×10^4 and 4×10^4cells/well with CCD-14Br and A549 cells, respectively. For monoculture, A549 or CCD-14Br cells were prepared separately at the same density. After incubation for 24 h, the cells were exposed to α-mangostin at 0, 5, and 10 μM concentrations. The cells were observed and image acquisition was done by using fluorescence microscopy at the first time point (t = day 0). Then, the cells were cultured for 1, 2, 3, 4, 5, and 6 days and image acquisition was done for each day.

The fluorescence images were analyzed by ImageJ software. After binarization of each fluorescent color image, the cell area estimated by DiI or DiO fluorescence was calculated. Finally, I evaluated the cell area as cell coverage ratio, A_c:

$$A_c = \frac{Fluorescence\ detectable\ pixels}{Total\ image\ pixels}$$

References

Aisha, A.F., Abu-Salah, K.M., Ismail, Z., Majid, A.M. 2012. In vitro and in vivo anti-colon cancer effects of Garcinia mangostana xanthones extract. BMC Complementary and Alternative Medicine 12:104 DOI 10.1186/1472-6882-12-S1-P104.

Angelucci, C., Maulucci, G., Lama, G., Proietti, G., Colabianchi, A., Papi, M., Maiorana, A., De Spirito, M., Micera, A., Balzamino, O.B., Di Leone, A., Masetti, R., Sica, G. 2012. Epithelial-stromal interactions in human breast cancer: effects on adhesion, plasma membrane fluidity and migration speed and directness. PLOS ONE 7:e50804

Chambers, A.F., Groom, A.C., and MacDonald, I.C. (2002). Dissemination and growth of cancer cells in metastatic sites. Nature reviews Cancer 2, 563-572.

Choi, Y.H., Han, S.Y., Kim, Y.J., Kim, Y.M., Chin, Y.W. 2014. Absorption, tissue distribution, tissue metabolism and safety of alpha-mangostin in mangosteen extract using mouse models. Food and Chemical Toxicology 66:140–146 DOI 10.1016/j.fct.2014.01.028.

Chopra, R.N., Nayar, S.L., Chopra, I.C. 1965. Glossary of Indian medicinal plants. Nueva Delhi: the National Institute of Science Communication and Information Resources.

Cross, S.E., Jin, Y.S., Lu, Q.Y., Rao, J., Gimzewski, J.K. 2011. Green tea extract selectively targets nanomechanics of live metastatic cancer cells. Nanotechnology 22:Article 215101 DOI 10.1088/0957-4484/22/21/215101.

Cross, S.E., Jin, Y.S., Rao, J., Gimzewski, J.K. 2007. Nanomechanical analysis of cells from cancer patients. Nature Nanotechnology 2:780–783 DOI 10.1038/nnano.2007.388.

Cross, S.E., Jin, Y.S., Tondre, J., Wong, R., Rao, J., Gimzewski, J.K. 2008. AFM-based analysis of human metastatic cancer cells. Nanotechnology 19:Article 384003 DOI 10.1088/0957-4484/19/38/384003.

Dai, J., Sheetz, M.P. 1995. Mechanical properties of neuronal growth cone membranes studied by tether formation with laser optical tweezers. Biophysical Journal 68:988–996 DOI 10.1016/S0006-3495(95)80274-2.

Don X. Nguyen, Paula D. Bos and Joan Massague, 2009. Reviews: Metastasis from dissemination to organ-specific colonization. Nature Reviews Cancer 9, 274-284.

Fang, Y., Su, T., Qiu, X., Mao, P., Xu, Y., Hu, Z., Zhang, Y., Zheng, X., Xie, P., Liu, Q. 2016. Protective effect of alpha-mangostin against oxidative stress induced-retinal cell death. Scientific Reports 6:21018 DOI 10.1038/srep21018.

Furukawa, M., Wheeler, S,. Clark, A.M., Wells, A. 2015. Lung epithelial cells induce both phenotype alteration and senescence in breast cancer cells. PLOS ONE 10:e0118060 DOI 10.1371/journal.pone.0118060.

Garnett, M., Sturton, S.D. 1932. Garcinia Mangostana in the treatment of amoebic dysentery. Chinese Medical Journal 46:969–973.

Govindachari, T.R., Kalyanaraman, P.S., Muthukumaraswamy, N., Pai, B.R. 1971. Xanthones of Garcinia mangostana Linn. Tetrahedron 27:3919–3926 DOI 10.1016/S0040-4020(01)98253-5.

Guck, J., Schinkinger, S., Lincoln, B., Wottawah, F., Ebert ,S., Romeyke, M., Lenz, D., Erickson, H.M., Ananthakrishnan, R., Mitchell, D., Kas, J., Ulvick, S., Bilby, C. 2005. Optical deformability as an inherent cell marker for testing malignant trans- formation and metastatic competence. Biophysical Journal 88:3689–3698 DOI 10.1529/biophysj.104.045476.

Haghparast, S.M., Kihara, T., Miyake, J. 2015. Distinct mechanical behavior of HEK293 cells in adherent and suspended states. PeerJ 3:e1131 DOI 10.7717/peerj.1131.

Haghparast, S.M., Kihara, T., Shimizu, Y., Yuba, S., Miyake, J. 2013. Actin-based biome- chanical features of suspended normal and cancer cells. Journal of Bioscience and Bioengineering 116:380–385 DOI 10.1016/j.jbiosc.2013.03.003.

Hertz, H. 1881. Über die berührung fester elastischer Körper. Journal für die reine und angewandte Mathematik 92:156–171.

Hung, S.H., Shen, K.H., Wu, C.H., Liu, C.L., Shih, Y.W. 2009. Alpha-mangostin suppresses PC-3 human prostate carcinoma cell metastasis by inhibiting matrix metalloproteinase-2/9 and urokinase-plasminogen expression through the JNK signaling pathway. Journal of Agricultural and Food Chemistry 57:1291–1298 DOI 10.1021/jf8032683.

Ibrahim, M.Y., Hashim, N.M., Mariod, A.A., Mohan, S., Abdulla, M.A., Abdelwahab, S.I., Arbab, I.A. 2016. α-Mangostin from Garcinia mangostana Linn: an updated review of its pharmacological properties. Arabian Journal of Chemistry 9:317–329 DOI 10.1016/j.arabjc.2014.02.011.

Jiang, W.G. , Sanders, A.J., Katoh, M., et al., 2015. Review: Tissue invasion and metastasis: Molecular, biological and clinical perspectives. Seminars in Cancer Biology, Volume 35, Issue null, Pages S244-S275.

Kaomongkolgit, R., Chaisomboon, N., Pavasant, P. 2011. Apoptotic effect of alpha- mangostin on head and neck squamous carcinoma cells. Archives of Oral Biology 56:483–490 DOI 10.1016/j.archoralbio.2010.10.023.

Kihara, T., Haghparast, S.M., Shimizu, Y., Yuba, S., Miyake, J. 2011. Physical properties of mesenchymal stem cells are coordinated by the perinuclear actin cap. Biochemical and Biophysical Research Communications 409:1–6 DOI 10.1016/j.bbrc.2011.04.022.

Kihara, T., Nakamura, C., Suzuki, M., Han, S.W., Fukazawa, K., Ishihara, K., Miyake, J. 2009. Development of a method to evaluate caspase-3 activity in a single cell using a nanoneedle and a fluorescent probe. Biosensors and Bioelectronics 25:22–27 DOI 10.1016/j.bios.2009.05.036.

Kim, K.S., Cho, C.H., Park, E.K., Jung, M.H., Yoon, K.S., Park, H.K. 2012. AFM-detected apoptotic changes in morphology and biophysical property caused by paclitaxel in Ishikawa and HeLa cells. PLOS ONE 7:e30066 DOI 10.1371/journal.pone.0030066.

Krajarng, A., Nakamura, Y., Suksamrarn, S., Watanapokasin, R. 2011. alpha-Mangostin induces apoptosis in human chondrosarcoma cells through downregulation of ERK/JNK and Akt signaling pathway. Journal of Agricultural and Food Chemistry 59:5746–5754 DOI 10.1021/jf200620n.

Krajarng, A., Nilwarankoon, S., Suksamrarn, S., Watanapokasin, R. 2012. Antiproliferative effect of alpha-mangostin on canine osteosarcoma cells. Research in Veterinary Science 93:788–794 DOI 10.1016/j.rvsc.2012.01.015.

Lee, Y.B., Ko, K.C., Shi, M.D., Liao, Y.C., Chiang, T.A., Wu, P.F., Shih, Y.X., Shih, Y.W. 2010. alpha-Mangostin, a novel dietary xanthone, suppresses TPA-mediated MMP- 2 and MMP-9 expressions through the ERK signaling pathway in MCF-7 human breast adenocarcinoma cells. Journal of Food Science 75:h13–h23 DOI 10.1111/j.1750-3841.2009.01407.x.

Lekka, M. 2016. Discrimination Between Normal and Cancerous Cells Using AFM. Bionanoscience 6:65–80 DOI 10.1007/s12668-016-0191-3.

Lekka. M., Pogoda, K., Gostek, J., Klymenko, O., Prauzner-Bechcicki, S., Wiltowska-Zuber, J., Jaczewska, J., Lekki, J., Stachura, Z. 2012. Cancer cell recognition - Mechanical phenotype. Micron 43:1259–1266 DOI 10.1016/j.micron.2012.01.019.

Liu, N., Li, Y., Su, S., Wang, N., Wang, H., Li, J. 2013. Inhibition of cell migration by ouabain in the A549 human lung cancer cell line. Oncology Letters 6:475–479 DOI 10.3892/ol.2013.1406.

Mahabusarakam, W., Wlriyachitra, P., Taylor, W.C. 1987. Chemical constituents of garcinia mangostana. Journal of Natural Products 50:474–478 DOI 10.1021/np50051a021.

Matsumoto, K., Akao, Y., Ohguchi, K., Ito, T., Tanaka, T., Iinuma, M., Nozawa, Y. 2005. Xanthones induce cell-cycle arrest and apoptosis in human colon cancer DLD-1 cells. Bioorganic and Medicinal Chemistry 13:6064–6069 DOI 10.1016/j.bmc.2005.06.065.

Mueller, M.M., Fusenig, N.E. 2004. Friends or foes—bipolar effects of the tumour stroma in cancer. Nature Reviews Cancer 4:839–849 DOI 10.1038/nrc1477.

Pedraza-Chaverri J., Cárdenas-Rodríguez N,. Orozco-Ibarra M., Pérez-Rojas J.M. 2008. Medicinal properties of mangosteen (Garcinia mangostana). Food and Chemical Toxicology 46:3227–3239 DOI 10.1016/j.fct.2008.07.024.

Peres, V., Nagem, T.J,. De Oliveira, F.F. 2000. Tetraoxygenated naturally occurring xanthones. Phytochemistry 55:683–710 DOI 10.1016/S0031-9422(00)00303-4.

Polyak, K., Haviv, I., Campbell, I.G. 2009. Co-evolution of tumor cells and their microenvironment. Trends in Genetics 25:30–38 DOI 10.1016/j.tig.2008.10.012.

Quail, D.F., Joyce, J.A. 2013. Microenvironmental regulation of tumor progression and metastasis. Nature Medicine 19:1423–1437 DOI 10.1038/nm.3394.

Ramos, J.R, Pabijan, J., Garcia, R., Lekka, M. 2014. The softening of human bladder cancer cells happens at an early stage of the malignancy process. Beilstein Journal of Nanotechnology 5:447–457 DOI 10.3762/bjnano.5.52.

Sahai, E. 2007. Illuminating the metastatic process. Nature Reviews Cancer 7:737–749 DOI 10.1038/nrc2229.

Sato, A., Fujiwara, H., Oku, H., Ishiguro, K., Ohizumi, Y. 2004. Alpha-mangostin induces Ca^{2+}-ATPase-dependent apoptosis via mitochondrial pathway in PC12 cells. Journal of Pharmacological Sciences 95:33–40 DOI 10.1254/jphs.95.33.

Shibata, M.A., Iinuma, M., Morimoto, J., Kurose, H., Akamatsu, K., Okuno, Y., Akao, Y., Otsuki, Y. 2011. Alpha-Mangostin extracted from the pericarp of the mangosteen (Garcinia mangostana Linn) reduces tumor growth and lymph node metastasis in an immunocompetent xenograft model of metastatic mammary cancer carrying a p53 mutation. BMC Medicine 9:69 DOI 10.1186/1741-7015-9-69.

Shih, Y.W., Chien, S.T., Chen, P.S., Lee, J.H., Wu, S.H., Yin, L.T. 2010. Alpha-mangostin suppresses phorbol 12-myristate 13-acetate-induced MMP-2/MMP-9 expressions via alphavbeta3 integrin/FAK/ERK and NF-kappaB signaling pathway in human lung adenocarcinoma A549 cells. Cell Biochemistry and Biophysics 58:31–44 DOI 10.1007/s12013-010-9091-2.

Shimizu, Y., Haghparast, S.M., Kihara, T., Miyake, J. 2012. Cortical rigidity of round cells in mitotic phase and suspended state. Micron 43:1246–1251 DOI 10.1016/j.micron.2012.03.011.

Sugitate, T., Kihara, T., Liu, X.Y., Miyake, J. 2009. Mechanical role of the nucleus in a cell in terms of elastic modulus. Current Applied Physics 9:e291–e293 DOI 10.1016/j.cap.2009.06.020.

Sultanbawa, M.U.S. 1980. Xanthonoids of tropical plants. Tetrahedron 36:1465–1506 DOI 10.1016/S0040-4020(01)83114-8.

Tracey A. martin, Lin Ye, Andrew J. Sanders, Jane Lane, and Wen G. Jiang, 2013. Cancer Invasion and metastasis: molecular and cellular perspective. Metastatic Cancer: Clinical and Biological Perespectives. Landes Bioscience.

Wang, J.J., Sanderson, B.J., Zhang, W. 2012. Significant anti-invasive activities of alpha-mangostin from the mangosteen pericarp on two human skin cancer cell lines. Anticancer Research 32:3805–3816.

Wexler, B. 2007. Mangosteen. Utah: Woodland Publishing.

Yamaguchi, H., Condeelis, J. 2007. Regulation of the actin cytoskeleton in cancer cell migration and invasion. Biochimica et Biophysica Acta/General Subjects 1773:642–652 DOI 10.1016/j.bbamcr.2006.07.001.

Yuan, J., Wu, Y., Lu, G. 2013. alpha-Mangostin suppresses lipopolysaccharide-induced invasion by inhibiting matrix metalloproteinase-2/9 and increasing E-cadherin expression through extracellular signal-regulated kinase signaling in pancreatic cancer cells. Oncology Letters 5:1958–1964 DOI 10.3892/ol.2013.1290.

Figures

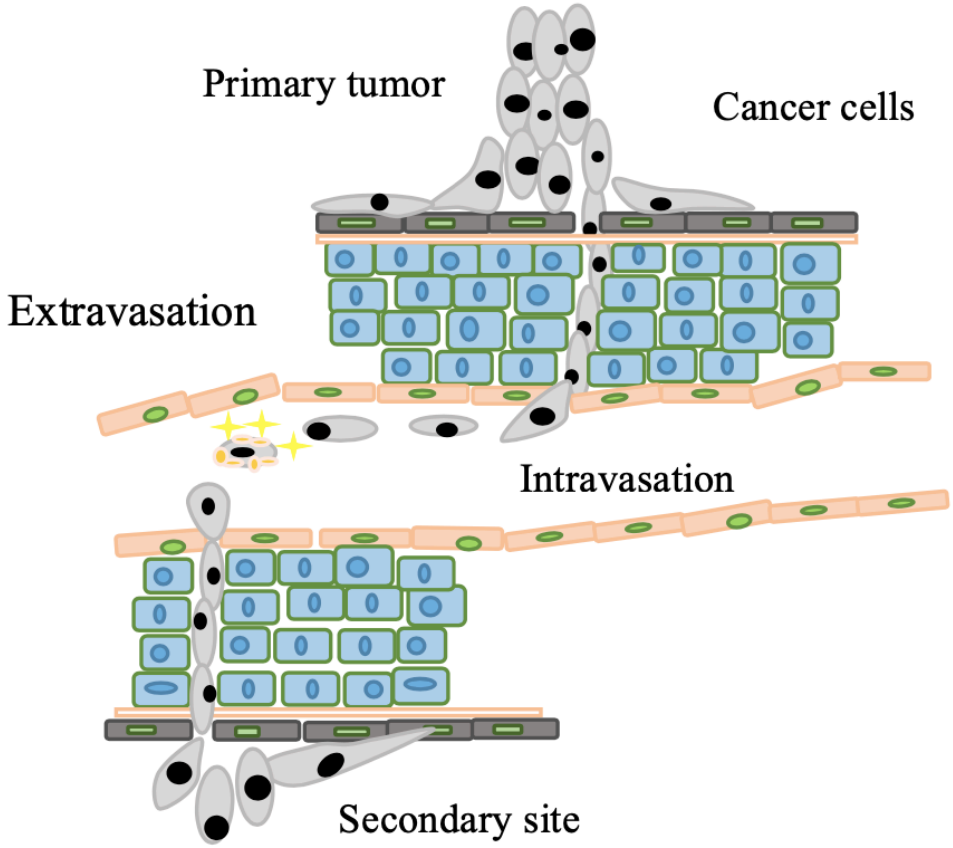

Figure 3.1: The metastatic cascade. Cancer cells in a primary tumor detach from adjacent cells in a tumor mass, they grow and then invade the basement membrane and traverse extracellular matrix surrounding tumor epithelium and subsequently invade endothelium of local blood vessel. The cells intravasate into blood vessel and are carried by the circulation.

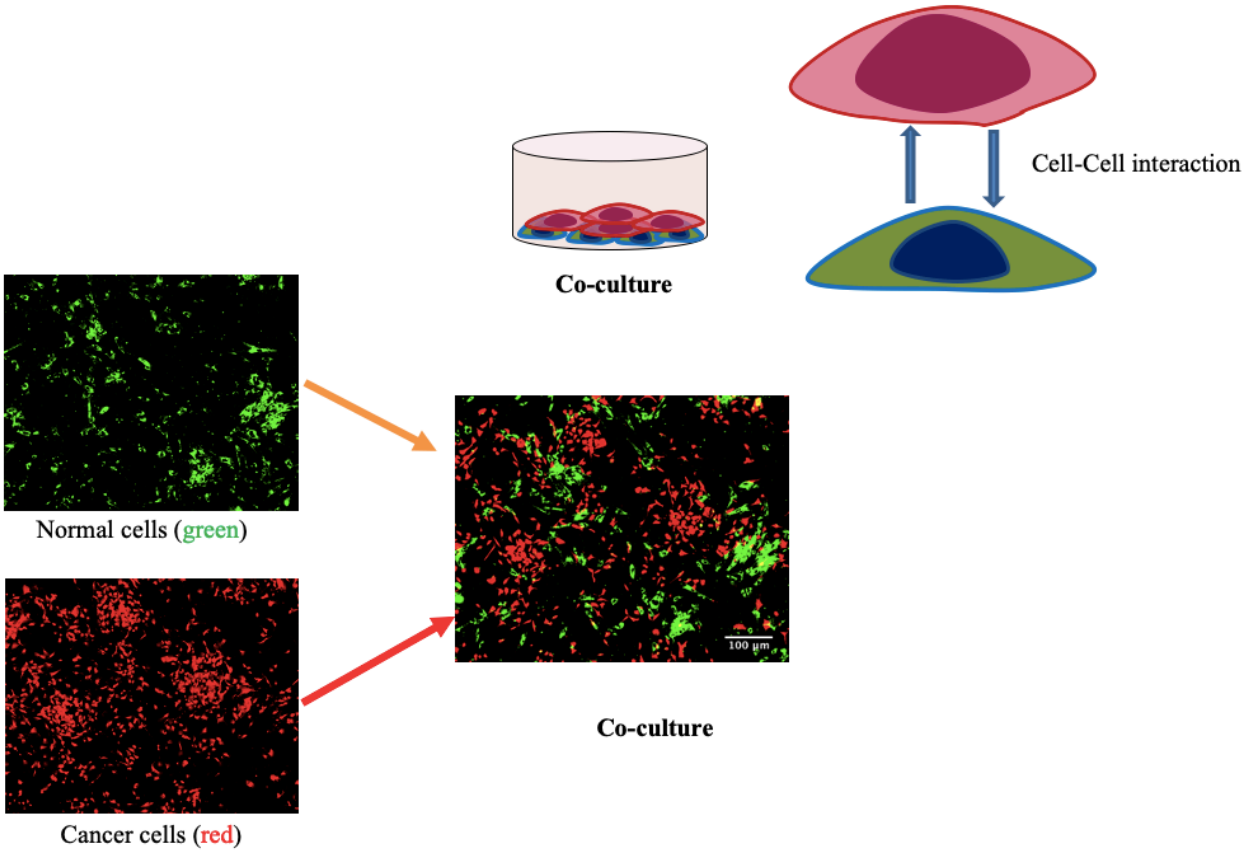

Figure 3.2: Co-culture definition and motivation. Co-culture compositions of at least two different type of cell (i.e., cancer/fibroblast, epithelial cell/lymphocyte, etc.) have been established in order to evaluate cell–cell interactions in cancer microenvironment through maximum simulation to in vivo microenvironment of human cancer.

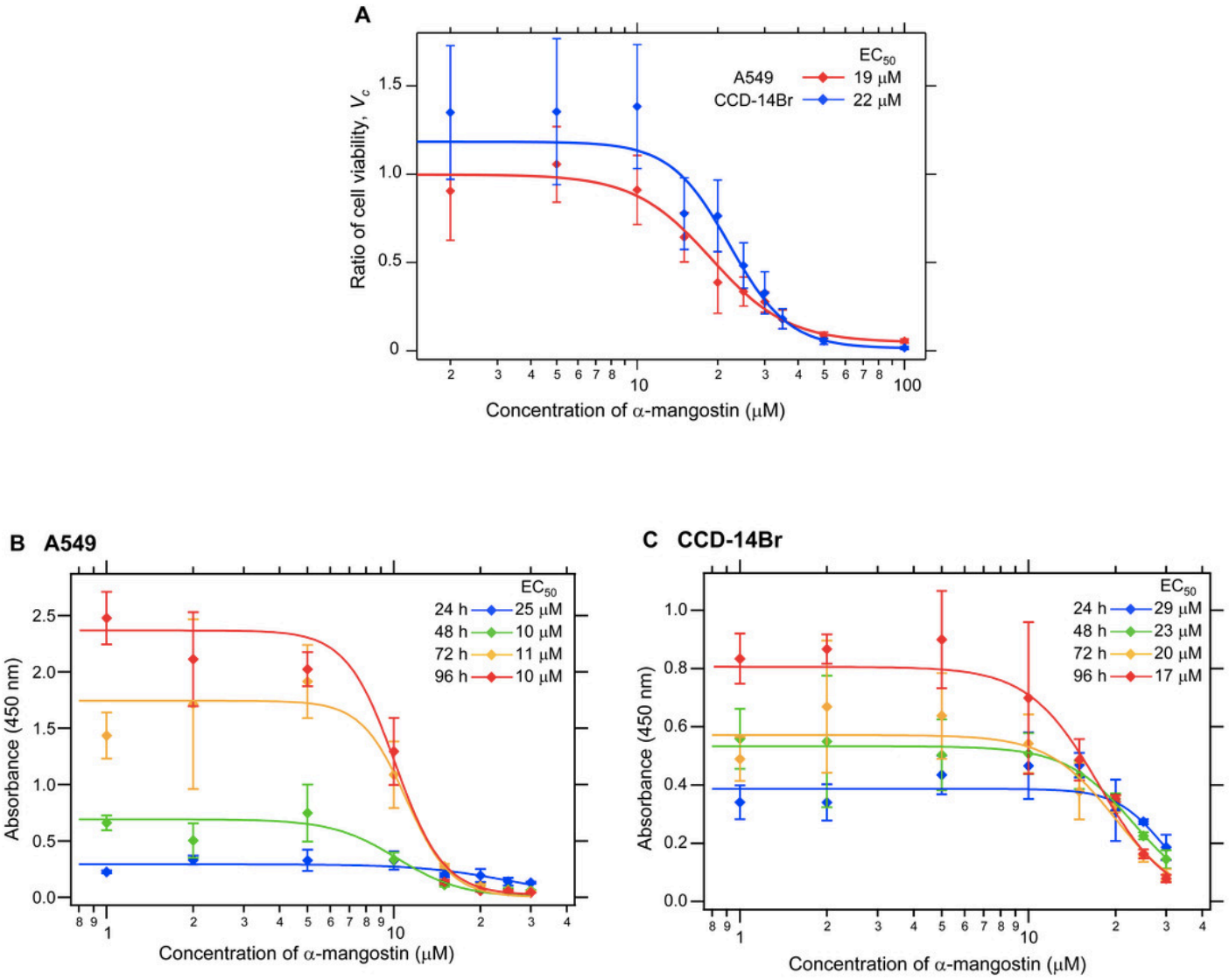

Figure 3.3. The cytotoxicity of α-mangostin on the human lung cell lines. Cells were treated with various concentration of α-mangostin (0-100 μM) incubated for 24 hours, then measured the O.D value using CCK-8 kit. The cell viability was expressed as a ratio of α-mangostin treated cells to that of the control.

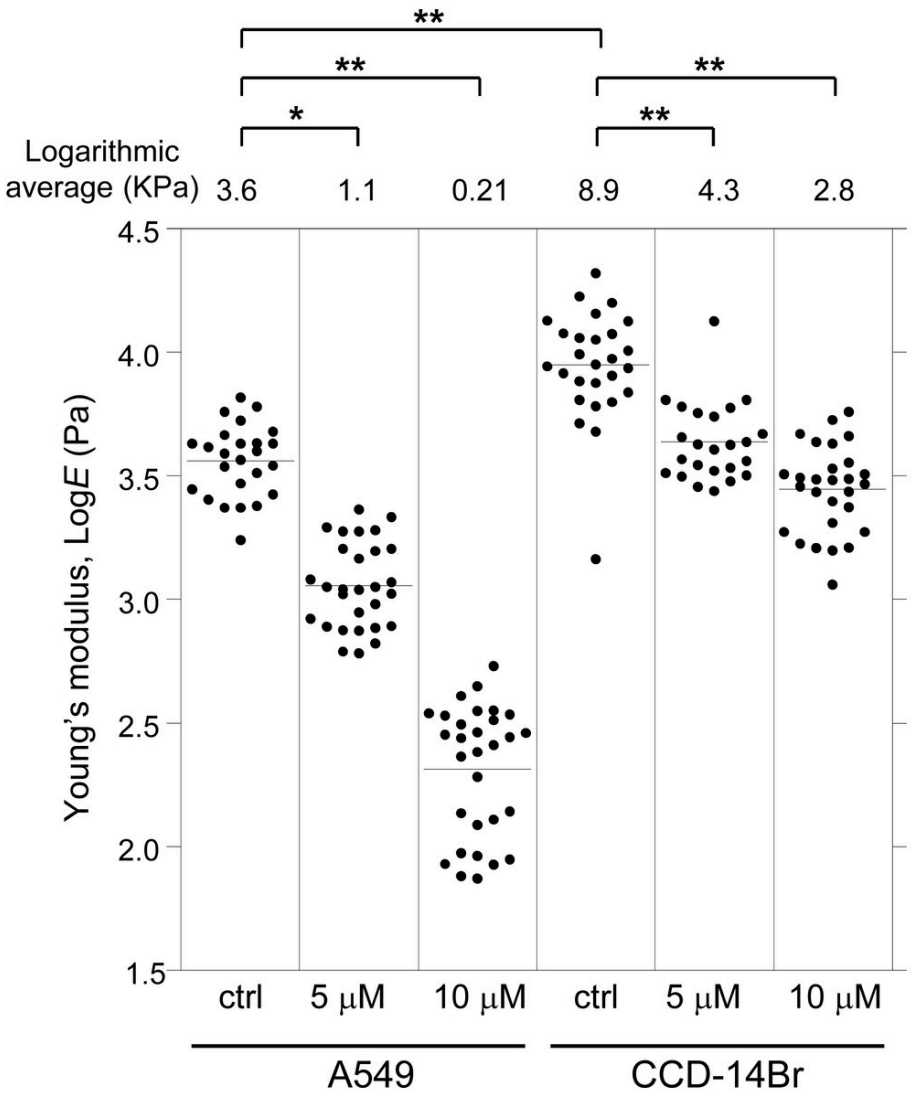

Figure 3.4. Young's modulus of A549 and CCD-14Br cells. The distributions of the Young's moduli of cells are shown as scatter plots in different concentration treatment of α-mangostin. Each condition displays the Young's modulus of more than 20 individual cells.

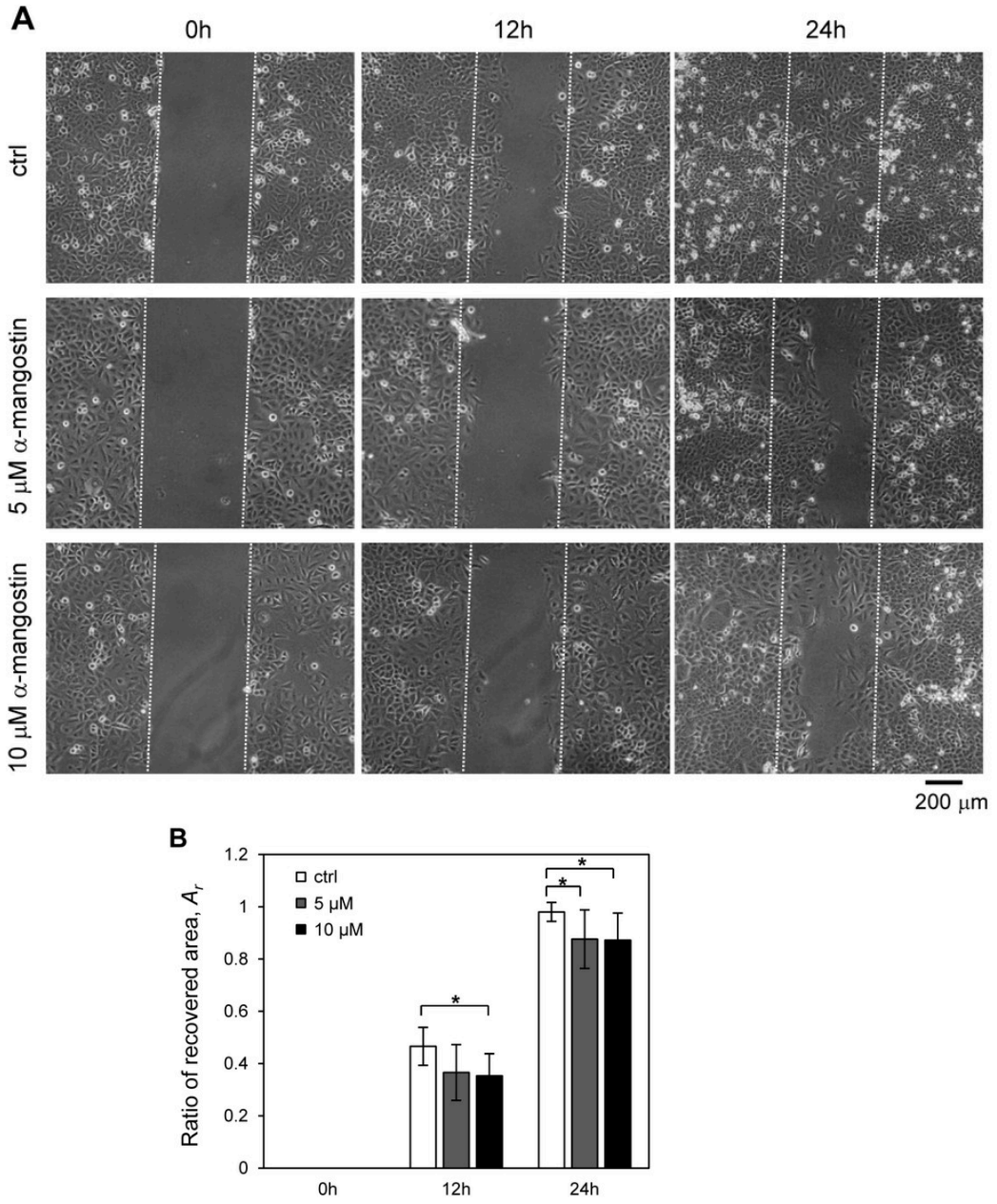

Figure 3.5. The effect of α-mangostin on migration of A549 cells. The cells were treated with 5 and 10 μM of α-mangostin for 24 h, and were subjected to analyser for cell migration. a) Images of migratory A549 cells were recorded at 0, 12, and 24 h by a microscope at x40 magnification, b) The percentage of the wound area by cell migration was calculated by using Fiji software. α-Mangostin displayed an inhibitory on cell migration for A549 after 12 h and 24 h.

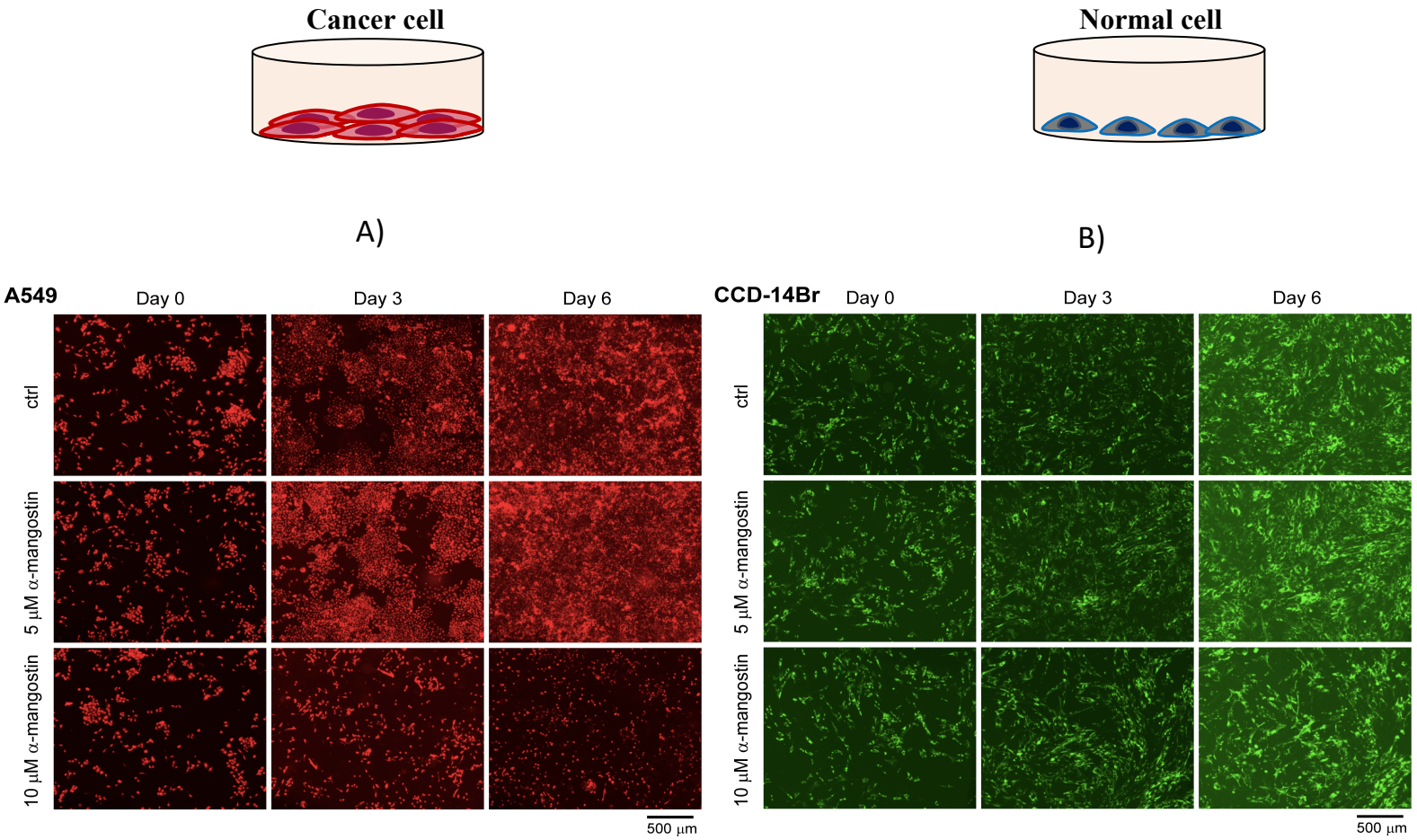

Figure 3.6. The effect of α-mangostin on migration of A549 cells. Cells were cultured in monoculture condition, then exposed with or without *α*-mangostin. (A) A549 cells were labeled with red fluorescence and (B) CCD-14Br cells were labeled with green fluorescence.

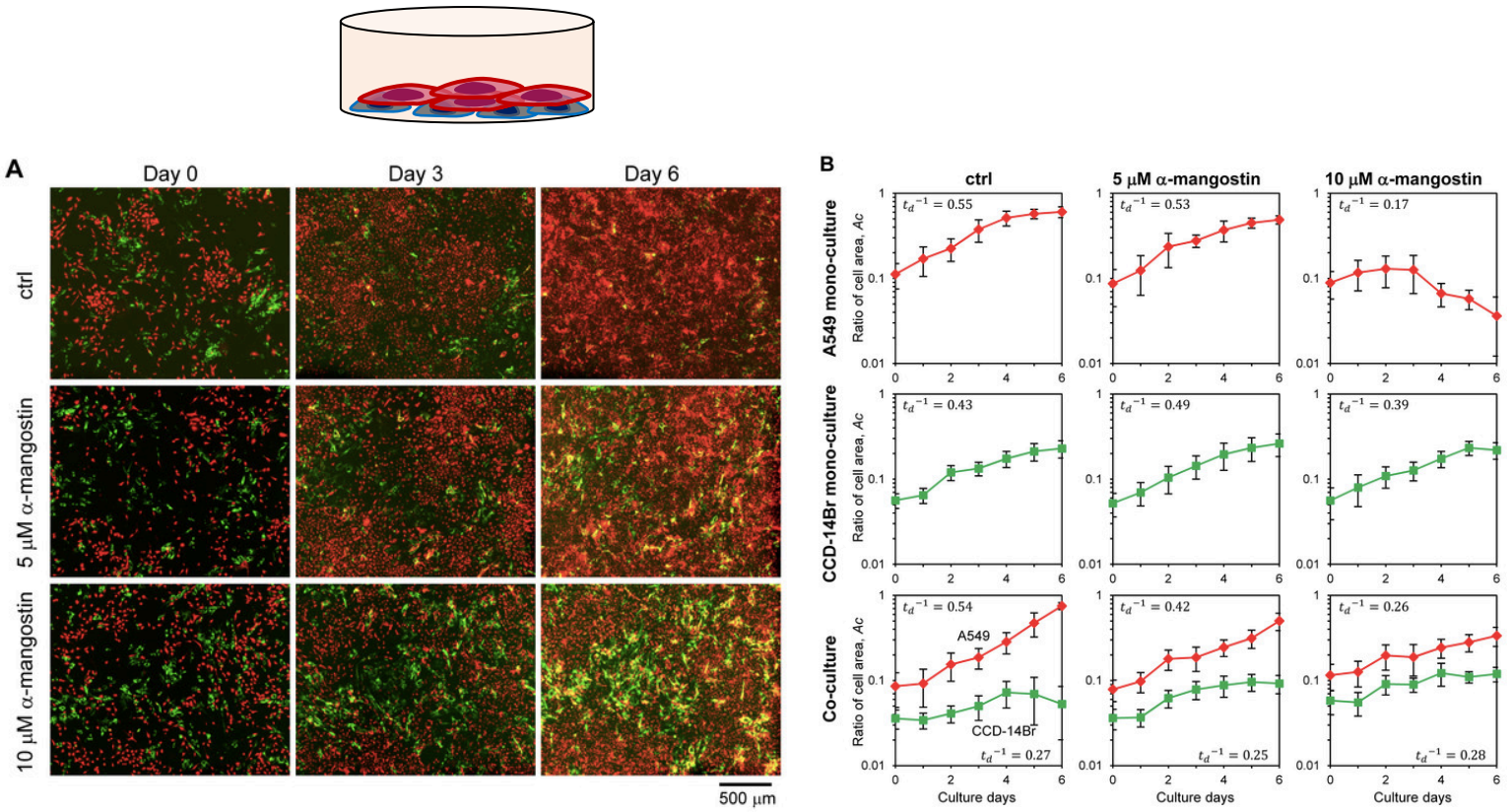

Figure 3.7. Invasion of cancer A549 to CCD-14Br cells in co-culture conditions treated with α-mangostin. Cells were cultured in co-culture condition, then exposed with or without α-mangostin. (A) Fluorescence images of co-cultured cells. A549 cells were labeled with red fluorescence and CCD-14Br cells were labeled with green fluorescence. (B) Ratio of each cell area, Ac, cultured in monoculture or co-culture with A549 and CCD-14Br cells. The cell area was calculated from more than seven fluorescence images in each condition. Inverse value of the doubling time of each culture condition, t−1d (d−1) is shown in each graph.

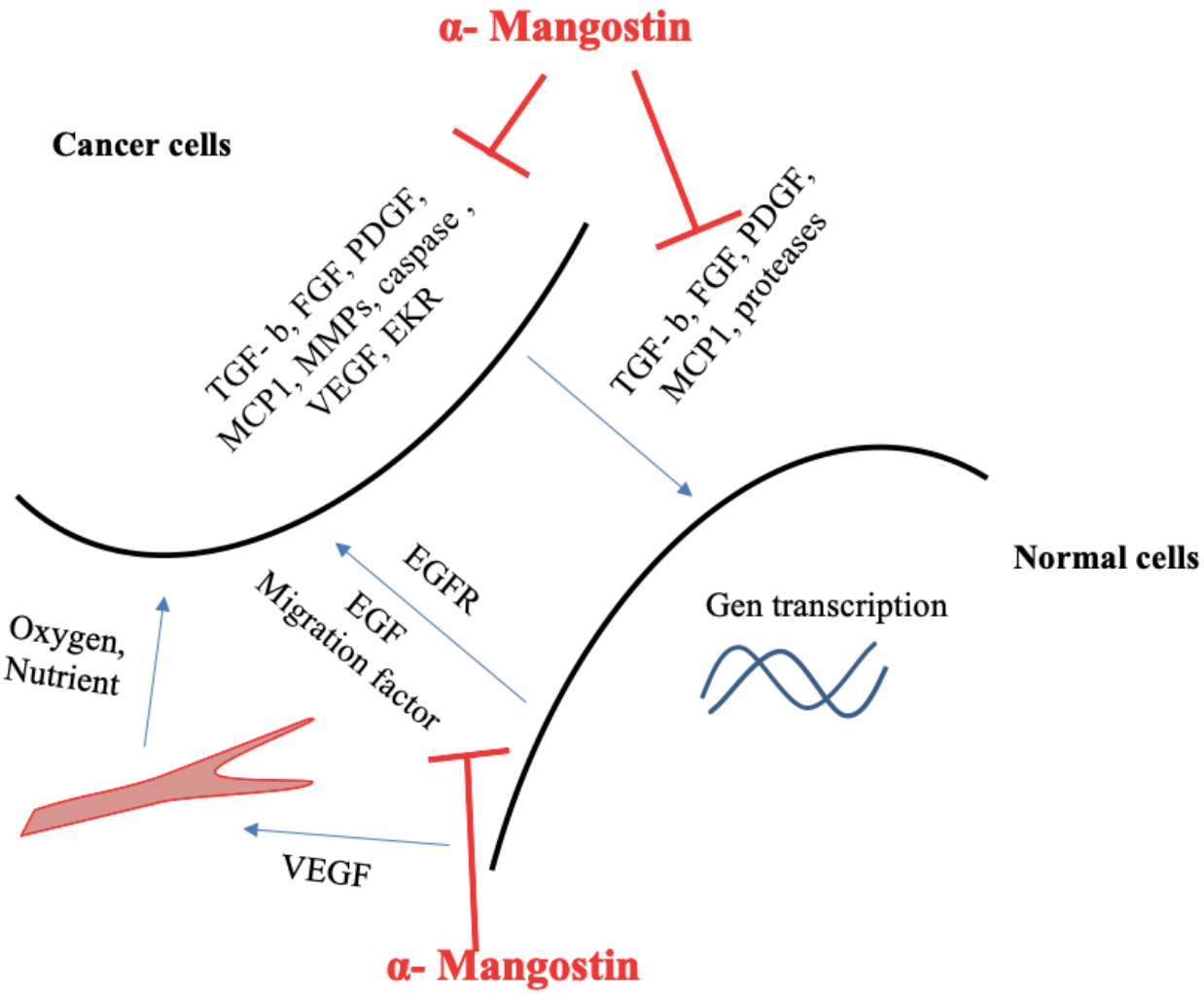

Figure 3.8: The interaction between cancer cell and surrounding cells. Cancer cells release some secreted protein, cytokines and growth factors to surrounding cells, then they response to secret the necessary cytokines to cancer cells. α-Mangostin was improved that inhibited some proteins, cytokines in cancer cells, so it may be break down the communication between cancer cells and normal cells in co-culture system. Therefore, α-mangostin inhibited the invasive activities of cancer cells and prevent cancer cells-damaged normal cells.

Chapter 4: α – Mangostin reduces the cell surface mechanical of various cell types

4 – 1. Overview

Alpha-mangostin (α-mangostin) has been identified as a naturally occurring compound with potential anticancer properties. α-Mangostin was found to reduce the mechanical stiffness of human lung cells. α-Mangostin was demonstrated that decreased the cell surface stiffness of lung cancer A549 cells and lung normal fibroblast-like CCD-14Br cells. Of these two cell types, the surface stiffness of A549 cells decreased significantly when treated with α-mangostin. The question is here that "Is the α-mangostin-induced reduction of surface stiffness in A549 cells related to the effects of α-mangostin on cancer cells?". The following cell types were examined: human fibroblast TIG-1 cells, human cancerous HeLa cells, human embryonic kidney HEK293 cells, mouse macrophage RAW 264.7 cells, and human myeloblasts KG-1 cells. Cells were treated with α-mangostin, and then examined for cell viability, actin cytoskeletal structures, and surface mechanical stiffness using atomic force microscopy. α-Mangostin demonstrated cytotoxicity against TIG-1, HeLa, HEK293, and KG-1 cells, but not against RAW 264.7 cells. The cytotoxic effect of α-mangostin varies according to cell type. On the other hand, α-mangostin reduced the mechanical stiffness of all cell types, including RAW 264.7 cells. Upon treatment with α-mangostin, F-actin was slightly reduced but the actin cytoskeletal structures were little altered in these cells. Thus, reducing mechanical stiffness of animal cells is an inherent effect of α-mangostin. Our results show that α-mangostin is a naturally occurring compound with potential to change the actin cytoskeletal micro-structures and reduce the surface stiffness of various cells.

4 – 2. Introduction

4 – 2.1. The mechanical properties of animal cells

Cells remain it phenotypes through combination of physiological functions, physical properties and gene expression (Figure 4.1). Physical properties refer to properties that can be observed or measured without changing the composition of the material. Mechanical property of simple materials depends on their material characters. Cell mechanics is a sub-field of biophysics that focuses on the mechanical properties and behavior of living cells and how it relates to cell function. It encompasses aspects of cell biophysics, biomechanics, soft matter physics and rheology, mechanobiology and cell biology (Moeendarbary et al, 2014). The mechanical properties of individual cells have been supposed as unique indicators of their states, which could constantly change in accordance with cellular events and diseases. Alterations in biological activities and transformation of cell states often entail a change in the mechanical behavior of cells. In particular, alterations in cell stiffness/elasticity have emerged as a marker for cellular phenotypic events and diseases.

Cell surface stiffness is attributed to the actin cytoskeleton (Dai, 1995; Collinsworth, 2002; Guilak, 2002; Trickey, 2004), and reflects the cell surface actin architectures (Haghparast, 2013; Haghparast, 2015) (Fig. 4.2). Moreover, cell surface stiffness changes in accordance with cellular events related to the remodeling of the actin cytoskeleton (Matzke, 2001; Kunda, 2008; Fletcher, 2010; Shimizu, 2012). Therefore, analyzing cell surface stiffness may reveal changes of cell characteristics, and provide a better understanding of the actin cytoskeleton remodeling process in certain cellular events and disease states. The mechanical properties is possible to provide specific information about the different states, types of animal cells. In addition, the mechanical properties of cells have been showed to be a useful maker of cell states and is promising biomarker indicative

of various cells disease processes and changes in cell state. Examples include changes in red blood cell stiffness in cytoskeletal disorders such as spherocytosis (Li et al., 2007; Lee et al., 2007), increased cell deformability of invasive cancer cells compared to benign or normal cells of the same origin, malignant cancer cells exhibit lower stiffness than normal cells (Cross et al., 2007; Guck et al., 2005; Haghparast et al., 2013; Suresh et al., 2007, 2005), and changes in stiffness of leukocytes in response to activation with antigens or other signals (Khismatullin, 2009). The mechanical properties of mesenchymal stem cells are attributed to their diverse characteristics and states (Kihara et al., 2011; Maloney et al., 2010; Sugitate et al., 2009), an increased deformability has also been identified as a potential biomarker for pluripotent stem cells (Pajerowski et al., 2007; Chowdhru et al., 2010). The cortical stiffness changes during mitotic cell rounding (Kunda et al., 2008; Shimizu et al., 2012); and the stiffness of the retinal epithelium changes during optic-cup morphogenesis (Eiraku et al., 2011). Therefore, analyzing the mechanical features of cells can reveal the characteristics of their underlying actin networks. It is also possible to characterize the sub-membrane actin networks in each cell type as indicators of surface stiffness.

4 – 2.2. Atomic Force Microscopy (AFM) measures the cell surface stiffness

In order to measure the cell surface stiffness, multiples methods have been developed including particle-tracking micro-rheology (Hoffman et al., 2006, 2009; Lau et al., 2003; Liu et al., 2006), magnetic twisting cytometry (Deng et al., 2006), micropipette aspiration (Oh et al., 2012; Hochmuth, 2000) and micro-indentation (Levental et al., 2010; Mahaffy et al., 2004; Radmacher, 1997) have been developed to measure the elasticity of cells. Particle tracking micro-rheology traces the thermal vibrations of either submicron fluorescent particles injected into cells or fiducial markers inside the cell cytoskeleton (Crocker et al., 2007). Elastic and viscous properties of cells are calculated from the measured particle displacements using the fluctuation-

dissipation theorem (Hoffman et al., 2006; Crocker et al., 2007). The micropipette aspiration method applies negative pressure in a micropipette of diameter ranging from 1 to 5 μm to suck a small piece of cell membrane into the pipette. Cell stiffness is calculated from the applied negative pressure and cell membrane deformation (Oh et al., 2012). The indenting force and the resulting indentation in cells often follow the prediction of the Hertz model. Young's moduli of cells can be calculated from the force-indentation curves by fitting them to the Hertz model. This method has been widely applied to test the mechanical properties of tissue and cells despite of its limitations such as uncertainty in contact point determination, applicability of the Hertz model, and the potential to physically damage the cells. Among the many devices for micro-indentation, the Atomic Force Microscope (AFM) is commercially available and has been widely applied to characterize mechanical properties of living cells and tissues (Mahaffy et al., 2004; Liu, F. & Tschumperlin, D.J., 2011; Solon et al., 2007; Wu et al., 1998; Radmacher et al., 1996)

The Atomic Force Microscope (AFM), inventedin 1986 (Binnig et al., 1986) emerged within a few years into an important tool for various physical and biological applications. AFM is nowadays one of the most sensitive (∼1 pN) and spatial resolution (∼1 nm) techniques for examining cell mechanics under physiological cell culture conditions (Radmacher, 1996). The atomic force microscope is a high resolution surface characterization technique, that has become rapidly adopted for imaging and mechanical characterization of a range of biological samples (Müller DJ and Dufrêne YF., 2008). AFM contains a nano-sized probe which can determine cell surface stiffness by indentation (Rotsch, 1997; Matzke, 2001) (Fig.4.3). Furthermore, this method is used to analyze surface stiffness of both adherent cells and suspension cells by using a substrate coated with hydrophilic cell-anchoring molecules (Kato et al., 2003) (Fig. 4.4), can be used to measure the stiffness of suspended leukocytes and trypsinized cells (Haga, 2000; Matzke, 2001;

Kihara, 2011; Kagiwada, 2010; Shimizu, 2012; Shimizu, 2012). Thus, AFM can be a powerful tool for analyzing the mechanical stiffness and actin cytoskeleton states of various cells.

4 – 2.3. The purpose of this study

α-Mangostin is one of the major xanthone compounds extracted from the pericarp of mangosteen (*Garcinia mangostana* Linn.) fruit. It has been demonstrated to possess numerous bioactive functions, both *in vitro* and *in vivo,* against various diseases, including cancer, inflammation, allergy, and bacterial and viral infections (Chen, 2018}. α-Mangostin targets different cellular factors through various mechanisms such as inducing apoptosis in cancer cells by regulating Bcl-2, Bax, and p53 (Watanapokasin, 2011; Kaomongkolgit, 2011; Lee, 2017); preventing the metastatic activities of cancer cells via inhibition of MMP-2, MMP-9, and NF-κB (Hung, 2009; Lee, 2010; Shih, 2010); and directly scavenging reactive oxygen species (ROS), thereby preventing neurotoxicity and ROS production by 3-nitropropionic acid in cultured neurons (Pedraza-Chaverri, 2009). Furthermore, recent research has illustrated that α-mangostin reduces cell surface stiffness in lung cancer cells (Phan, 2018).

I recently reported that α-mangostin suppressed the subsistence, migration, and invasion of lung cancer cells (Phan, 2018). In that study, I demonstrated that α-mangostin decreased the cell surface stiffness of lung cancer A549 cells and lung normal fibroblast-like CCD-14Br cells. Of these two cell types, the surface stiffness of A549 cells decreased significantly when treated with α-mangostin (Phan, 2018). The mechanical changes in cancer cells are important indicators of cancer state and type: softer cancer cells show more invasive properties (Cross, 2011; Ramos, 2014; apoptotic cancer cells are softened (Kihara, 2009; Kim, 2012). Is the α-mangostin-induced reduction of surface stiffness in A549 cells related to the effects of α-mangostin on cancer cells? To answer this question, I have to first identify the range of cells on which α-mangostin has an

effect, and then to elucidate the mechanism of how α-mangostin reduces the surface stiffness of these cancer cells.

In the present study, I examined the cell types that were affected by α-mangostin with respect to cell surface stiffness. Identifying the range of cells that are impacted by the action of α-mangostin may help us to elucidate the mechanism. I used different cell types including normal human fibroblast TIG-1 cells, human cervical cancer HeLa cells, human embryonic kidney HEK293 cells, mouse leukemia macrophage RAW 264.7 cells, and human leukemia myeloblasts KG-1 cells. TIG-1, HeLa, HEK293, and RAW 264.7 cells are adherent cells and KG-1 cells are suspension cells. The morphologies of these cells vary, and the features of the actin cytoskeleton vary in these cell types. TIG-1 cells have an elongated morphology; HeLa and HEK293 cells have a shortly extended morphology; RAW 264.7 cells have weakly adhering morphology; and KG-1 cells are suspended and spherical shape. I examined the sensitivity of these cells to α-mangostin and the effects of α-mangostin on cell mechanics, actin cytoskeleton, and cell viability.

4 – 3. Experimental result

4 – 3.1. Cytotoxic sensitivity to α – Mangostin varies by cell types

Firstly, I examined the cytotoxic effects of α-mangostin on TIG-1, HeLa, HEK293, RAW 264.7, and KG-1 cells. TIG-1, HeLa, HEK293, and RAW 264.7 cells are adherent cells, and were seeded onto culture plates and pre-cultured for 24 h. They were then treated with α-mangostin for 24 h. KG-1 cells are suspension cells and were seeded onto culture plates and cultured with α-mangostin for 24 h. The survival cell number was evaluated by activity of living cells' mitochondrial tetrazolium reductase enzyme. α-Mangostin exhibited cytotoxic effects on TIG-1, HeLa, HEK293, and KG-1 cells at a concentration of 100 μM (Fig. 4.5). On the other hand, α-mangostin did not affect the cell viability of RAW 264.7 cells even at the concentration of 100 μM (Fig. 4.5). This result is in agreement with that of a previous study by Chen et al. (Chen, 2008). In Chen's study, the xanthones from mangosteen extracts, whose major component was α-mangostin, demonstrated no cytotoxicity on RAW 264.7 cells. The half-maximal effective concentration (EC_{50}) values of α-mangostin for the cytotoxicity of TIG-1, HeLa, HEK293, and KG-1 cells were estimated as 13, 16, 30, and 7.5 μM, respectively (Fig. 4.5). KG-1 cells were relatively sensitive but HEK293 cells were relatively resistant to the cytotoxic effects of α-mangostin. Thus, α-mangostin demonstrated cytotoxic effects on a number of different adherent cells and suspension leukemia myeloblasts. However, RAW 264.7 cells proved to be resistant to the cytotoxic effects of α-mangostin.

4 – 3.2. α-Mangostin reduces mechanical stiffness of various cells

Our previous study showed that α-mangostin suppressed the subsistence and decreased the mechanical properties of A549 cancer and CCD-14Br normal cells (Phan, 2018). Mechanical changes caused by α-mangostin appeared within 6 h, which was before the onset of cytotoxic

effects (Phan, 2018). I examined the impact of α-mangostin on cell mechanics in TIG-1, HeLa, HEK293, RAW 264.7, and KG-1 cells. These cells were exposed to α-mangostin for 6 h after which surface stiffness was examined using AFM. The morphologies of these cells are shown in Fig. 4.6. TIG-1, HeLa, and HEK293 cells adhered and extended on the dish. TIG-1 cells in particular showed a highly elongated morphology (Fig. 4.6). While these cells remained extended after the 6 h α-mangostin treatment, HeLa and HEK293 cells appeared somewhat shrunken (Fig. 4.6). RAW 264.7 cells adhered but did not extend significantly, and after treatment with α-mangostin for 6 h, their morphology appeared unchanged (Fig. 4.6). KG-1 cells were fixed on cell anchoring dishes to measure their surface stiffness using AFM. The morphology of KG-1 cells was spherical and they were unchanged by treatment with α-mangostin (Fig. 4.6).

The distribution of the elastic modulus (Young's modulus) of these cells is shown in Fig. 4.7. The values of Young's modulus are plotted in logarithmic scale as they were distributed in a log-normal pattern (Shimizu, 2012). With regard to the controls, the log-average values of the Young's moduli of TIG-1, HeLa, HEK293, RAW 264.7, and KG-1 cells were 5.4, 2.0, 0.28, 0.84, and 1.0 kPa, respectively (Fig. 4.7). TIG-1 fibroblasts had the highest surface stiffness of the cells tested, while HEK293 cells had the lowest. This result complements the data from our previous studies (Shimizu, 2012; Haghparast, 2013; Haghparast, 2015). The surface stiffness of suspension KG-1 myeloblasts was higher than that of adhered HEK293 and RAW 264.7 cells (Fig. 4.7). Thus, it appears that the actin cytoskeleton near the plasma membrane mechanically supports the surface of spherical KG-1 cells.

The Young’s modulus of these cells reduced following α-mangostin treatment (Fig. 4.7). The Young’s modulus of normal fibroblast TIG-1 cells was slightly reduced from 5.4 to 3.3 kPa following treatment with 10 μM of α-mangostin (Fig. 4.7). The Young’s modulus of cancerous

HeLa cells was markedly reduced from 2.0 to 0.68 kPa following treatment with 10 μM of α-mangostin (Fig. 4.7). This result demonstrates a similar trend to our previous analysis, such that normal fibroblast-like CCD-14Br cells softened slightly, and lung cancer A547 cells softened significantly following treatment with α-mangostin (Phan, 2018). The Young's modulus of HEK293 cells was too low and they had few mechanically supporting actin cytoskeletons, resulting in only a slight softening after treatment with α-mangostin (Fig. 4.7). RAW 264.7 cells, whose Young's modulus was relatively low, and which were resistant to the cytotoxic effects of α-mangostin, were also slightly softened by treatment with 10 and 20 μM α-mangostin (Fig. 4.7). Floating KG-1 cells, which had moderate stiffness and were sensitive to the cytotoxic effects of α-mangostin, were significantly softened by treatment with 5 and 10 μM α-mangostin (Fig. 4.7). Thus, although the impact of α-mangostin on cell mechanical properties varied by cell type, the mechanical stiffness of all cell types was reduced by the short-interval treatment with α-mangostin.

4 – 3.3. Actin cytoskeleton structures of α-mangostin-treated cells.

The mechanical stiffness of cells is largely attributed to the actin cytoskeleton (Dai, 1995; Collinsworth, 2002; Guilak, 2002; Trickey, 2004). Thus, the actin filaments of α-mangostin-treated cells were stained with rhodamine labeled-phalloidin and observed under the fluorescence microscope (Fig. 4.8). TIG-1 cells originally showed highly developed long actin stress fibers along the cell body. HeLa cells showed many weak actin fibers inside the cells and microvilli and protrusions on the edges. HEK293 and RAW 264.7 cells showed immature F-actin at the cell-cell border and many protrusions on the edges. KG-1 cells showed cortical F-actin and fine microvilli on the plasma membrane. Upon treatment with 10 μM α-mangostin, the F-actin amounts were slightly reduced and the actin cytoskeletal structures were little changed (Fig. 4.8). On the other hand, when these cells were treated with actin depolymerization reagent cytochalasin D, the F-

actin structures were significantly distorted (Fig. 4.8). Especially, the actin structures of TIG-1, HeLa, and HEK293 cells were fully destroyed, and in KG-1 cells, the cortical actin almost vanished and F-actin aggregates appeared (Fig. 4.8). Thus, the mechanism of mechanical alteration by α-mangostin clearly differed from that of actin depolymerization reagent cytochalasin D. Probably α-mangostin is involved in changing the actin cytoskeletal micro-structures or reducing the amount of the actin cytoskeleton gently, and then reduces the mechanical stiffness in various cells.

4 – 4. Conclusion and Discussion

In this study, the results indicate that α-mangostin has cytotoxic effects on some of the cell types and the ability to soften the mechanical properties of all the cell types that were analyzed. The impact of α-mangostin on cell mechanical properties varied in different cell types, and the sensitivity results also varied from that of the cytotoxic effect analysis.

First, I interpret our results from the perspective of actin cytoskeleton. The height of the value of Young's modulus reflects the structure and state of the actin cytoskeleton present near the cell surface. TIG-1 cells have well-developed actin stress fibers, and their surface stiffness is highly enhanced due to the developed actin stress fibers (Figs. 4.7 and 4.8). The surface stiffness of TIG-1 cells was slightly reduced and the elongated cell morphology and F-actin structures were unchanged upon treatment with α-mangostin (Figs, 4.6, 4.7 and 4.8). Thus, the developed stress fibers in TIG-1 cells are relatively stable against α-mangostin. HeLa cells have weak stress fibers and numerous protrusions and microvilli, and their surface stiffness is moderately enhanced by the presence of actin structures (Figs. 4.7 and 4.8). The surface stiffness of HeLa cells was markedly reduced, and the morphology appeared slightly shrunken, following the treatment with α-mangostin (Figs. 4.6 and 4.7). Thus, the weak actin structures with many protrusions and microvilli in HeLa cells were very sensitive to α-mangostin. HEK293 cells have immature actin cytoskeletons, and as such, the mechanical stiffness of HEK293 cells is very low (Figs. 4.7 and 4.8) (Haghparast, 2015). Although the surface stiffness of HEK293 cells is slightly reduced, it is difficult to evaluate the cell sensitivity to α-mangostin, since there is little room for decreasing the stiffness to begin with. However, the morphology of HEK293 cells was also somewhat shrunken upon treatment with α-mangostin, and therefore, they were most likely affected by α-mangostin (Fig. 4.8). RAW 264.7 cells did not display an extended morphology and exhibited F-actin at the

cell-cell border and cortical region with protrusions (Figs. 4.6 and 4.8). Also their surface stiffness was relatively low (Fig. 4.7). RAW 264.7 cells did not show any cell death after treatment with 100 μM of α-mangostin for 24 h (Fig. 4.5), and their surface stiffness was hardly reduced (Fig. 4.7). Thus, RAW 264.7 cells were resistant to not only cytotoxic, but also mechanical changes caused by of α-mangostin. The suspended KG-1 cells had cortical actin and microvilli at the plasma membrane (Fig. 4.8) (Ohnishi, 2013). These cells were very sensitive to the cytotoxic effects of α-mangostin and almost half of the cells died after treatment with 7.5 μM α-mangostin for 24 h (Fig. 4.5). Their mechanical stiffness also softened remarkably following the treatment with 5 and 10 μM of α-mangostin for 6 h (Fig. 4.7). Thus, KG-1 cells and their actin structures were very sensitive to α-mangostin.

The impact of α-mangostin on the surface stiffness of HeLa and KG-1 cells was high compared to other cell types (Fig. 4.7). On the other hand, the actin structures of these cells were different; for instance, HeLa cells had many fine actin fibers inside the cells and KG-1 cells had cortical actin (Fig. 4.8). These actin structures were not changed upon treatment with α-mangostin as observed in the images recorded by conventional fluorescence microscopy (Fig. 4.8). How does α-mangostin reduce the mechanical stiffness of these cells? Our previous study showed that the mechanical alteration determined by AFM is more sensitive method to determine the actin changes in the cells than by fluorescence microscopy (Shimizu, 2012). Thus, probably micro-structures of actin cytoskeleton are changed by treatment with α-mangostin. HeLa cells and cancer cells have many short microvillus and protrusions on their surface (Fig. 4.8) (Haghparast, 2013). KG-1 cells are also covered with short microvilli on the surface (Fig. 4.8) (Ohnishi, 2013; Tachibana, 2020). Thus, the short microvillus structure of actin cytoskeleton may be a sensitive target of α-mangostin. Microvilli structures are localized at the surface of leukocytes as well (von Andrian, 1995;

Majstoravich, 2004; Yamane, 2011). If the actin microvilli are sensitive targets of α-mangostin, α-mangostin may also affect the mechanical stiffness of circulating leukocytes.

Then, what kind of signal cascade or actin modulation molecules are the potential targets of α-mangostin with respect to its effect on mechanical stiffness? Previous research work indicates that α-mangostin has various contradictory functions on the molecules that affect the actin cytoskeleton; it inhibits myosin light-chain kinase (MLCK) and cyclic AMP-dependent protein kinase (PKA) (Jinsart, 1992); it increases myosin light-chain (MLC) phosphorylation and induces Ca^{2+} influx in platelets (Liu, 2015); it inhibits Ca^{2+}-ATPase in the sarcoplasmic reticulum (Furukawa, 1996); and it reduces Ca^{2+} elevation by suppressed Ca^{2+} influx (Itoh, 2008). These contradictory functions of α-mangostin can modulate the actin cytoskeleton positively and negatively. Thus, at present, it is difficult to assess the right targets of α-mangostin with respect to its effect on mechanical stiffness. But, recently, it has been reported that the mechanical stiffness and surface microvilli structures of KG-1 cells were related to cell adhesion and stimulation, and these were regulated by Ezrin/Radixin/Moesin (ERM) proteins that were linker proteins between membrane proteins and cortical actin (Tachibana, 2020). In future, further studies using KG-1 cells might reveal the molecules involved in the processes of mechanical change caused by α-mangostin. The research will definitely help to better understand the complex and diverse functions of α-mangostin on various cells, including cancer cells, and enhance the pharmaceutical potential of naturally occurring compound α-mangostin.

RAW 264.7 cells did not display any cell death but demonstrated slight mechanical change brought about by α-mangostin (Figs. 4.5 and 4.7). Other studies have also reported that α-mangostin has no cytotoxic effect on RAW 264.7 cells but does inhibit NO and PGE2 production from lipopolysaccharide (LPS)-stimulated RAW 264.7 cells (Chen, 2008). Furthermore, α-

mangostin suppressed TLR4/NF-κB mediated inflammation reactions in LPS-stimulated RAW 264.7 cells (Tao, 2018). Thus, although RAW 264.7 cells are completely resistant to the cytotoxic effects of α-mangostin, their intracellular molecules are affected by the multiple biological functions of α-mangostin.

In conclusion, I first reported that α-mangostin had a potential to reduce the mechanical properties of all cell types, including suspension cells, macrophages, and normal fibroblasts. The impact of α-mangostin on cell mechanical properties was found to be different from that of the cytotoxic effects on the cells. The surface stiffness of cancerous HeLa and floating KG-1 myeloblast cells was significantly softened by α-mangostin. In contrast, the surface stiffness of normal fibroblast TIG-1 and macrophage RAW 264.7 cells was slightly reduced by α-mangostin. Thus, the naturally occurring compound α-mangostin appears to modulate the common signal cascades of the actin cytoskeleton inside these cells but further studies are needed to confirm this. Our findings will aid in the use of the complex and multi-functional α-mangostin in future medical applications.

4 – 5. Materials and experimental methods

Material

Human fetal lung normal fibroblast TIG-1 cells, human cervical cancer HeLa cells, and human embryonic kidney HEK293 cells were obtained from the Japanese Collection of Research Bioresources (JCRB) cell bank (Osaka, Japan). Human leukemia myeloblast KG-1 cells and mouse leukemia macrophage RAW 264.7 cells were obtained from Riken Cell Bank (Ibaraki, Japan). α-Mangostin, rhodamine labeled- phalloidin, cytochalasin D, DMEM, and RPMI1640 medium were purchased from Wako Pure Chemical Industries Ltd. (Osaka, Japan). Cell anchoring molecule, SUNBRIGHT OE-020CS, was purchased from NOF Corporation (Tokyo, Japan). The cone probe (BL-AC-40TS-C2; spring constant: around 0.05 N/m) was purchased from Olympus (Tokyo, Japan). Cell counting kit-8 was purchased from Dojindo Molecular Technologies, Inc. (Kumamoto, Japan). Cell harvesting solution TrypLE express and fetal bovine serum (FBS) were purchased from Life Technologies Japan Ltd. (Tokyo, Japan). Antibiotics were purchased from Sigma- Aldrich (St. Louis, MO). Glass-based culture dishes were purchased from Matsunami Glass (Osaka, Japan). Other reagents were purchased from Sigma-Aldrich, Wako Pure Chemical Industries Ltd., or Life Technologies Japan Ltd.

Preparation of cell anchoring dishes

I coated cell anchoring molecule, SUNBRIGHT OE-020CS, on the culture dishes as described previously (Haghparast, 2013). Briefly, the polystyrene tissue culture dishes were coated with BSA, and then the surfaces were coated with SUNBRIGHT OE-020CS. SUNBRIGHT OE-020CS contains an oleyl group at one end and keeps a floating cell on the coated dish (Kato, 2003}. The anchored cells are fixed, and then the cell surface stiffness can be measured by AFM (Shimizu, 2012; Shimizu, 2012}.

Cell culture

TIG-1, HeLa, HEK293, and RAW 264.7 cells were cultured in DMEM containing 10% FBS and antibiotics (100 units/ mL penicillin G and 100 μg/mL streptomycin sulfate), and KG-1 cells were cultured in RPMI1640 medium containing 10% FBS and the antibiotics in humidified atmosphere of 95% air and 5% CO2 at 37 °C.

Cytotoxicity assay

The cytotoxicities of α-mangostin on various cells were evaluated by the cell counting kit-8 as recommended by the manufacturer. The adherent cells were seeded on a 96 well culture plate at 104 cells/well and cultured for 24 h, so as to allow the cells to adhere to the plate. The culture medium was replaced by 100 μL of fresh culture medium diluted with various concentrations of α-mangostin and cultured for further 24 h. The cell counting kit-8 solution (10 μL) was added to each well and incubated for 1 h. For KG-1 cells, the cells were seeded on a 96 well plate at 2 × 104 cells/well with 100 μL of culture medium containing with various concentrations of α-mangostin and cultured for 24 h. The cell counting kit-8 solution (10 μL) was added to each well and incubated for 2 h. The absorbance was then measured at 450 nm using a microplate reader. The absorbance values were fitted with the below Hill equation.

$$f(x) = a + \frac{b-a}{1+\left(\frac{x}{h}\right)^{r}}$$

Where x = concentration of α-mangostin, h = value of EC_{50}, r = Hill coefficient, a = base value of the absorbance, b = top value of the absorbance.

AFM measurements

The cells were manipulated by AFM (Nanowizard III; JPK Instruments AG, Berlin, Germany) at room temperature. TIG-1, Hela, HEK293, and RAW 264.7 cells were cultured on normal culture dishes for 24 h and then treated with α-mangostin for 6 h. KG-1 cells were plated on the cell anchoring dishes for 1 h in serum free medium, then washed with PBS to remove unattached cells, and cultured for 6 h in α-mangostin containing complete culture medium. The cone shaped AFM probe was indented 25 different points within 1 μm × 1 μm of cell top with a loading force of up to 0.5 nN and velocity of 5 μm/s. Young's modulus of the cell surface was calculated with the Hertz model (Hertz, 1881); the force-indentation curve for a region up to about 1 μm of indentation was fitted using JPK data processing software (JPK instruments AG) as:

$$F = \frac{E}{1-\nu^2}\frac{2\tan\alpha}{\pi}\delta^2$$

Where F = force, δ = depth of the probe indentation, ν = Poisson's ratio (0.5), α = half-angle of the cone probe (9°), and E = Young's modulus. The median value adopted for the Young's modulus of each cell (Kihara, 2011}. More than 21 cells and 525 force-distance curves were analyzed in each condition.

Actin filaments staining

TIG-1, Hela, HEK293, and RAW 264.7 cells were cultured on normal glass base dishes for 24 h and then treated with 10 μM α-mangostin for 6 h or 2 μg/mL cytochalasin D for 1.5 h. KG-1 cells were plated on the cell anchoring glass base dishes for 1 h in serum free medium, then washed with PBS to remove unattached cells, and cultured for 6 h in 10 μM α-mangostin or for 1.5 h in 2 μg/mL cytochalasin D containing complete culture medium. The cultured cells were fixed with 4% paraformaldehyde, permeabilized with 0.3% Triton X-100, and then stained with

rhodamine labeled-phalloidin for actin filaments. Specimens were observed by fluorescence microscopy (IX81, Olympus).

References

Allenspach, E.J., Cullinan, P., Tong, J., et al., ERM-dependent movement of CD43 defines a novel protein complex distal to the immune synapse. Immunity 15 (2001) 739e750.

Binnig, G., Quate, C.F., Gerber, C., 1986. Atomic force micro- scope. Phys Rev Lett 56: 930.

Brown, M.J., Nijhara, R., Hallam, J.A., et al., Chemokine stimulation of human peripheral blood T lymphocytes induces rapid dephosphorylation of ERM proteins, which facilitates loss of microvilli and polarization, Blood 102 (2003) 3890e3899.

Chen, L.G., Yang, L.L., Wang, C.C. Anti-inflammatory activity of mangostins from Garcinia mangostana. Food Chem Toxicol. 2008;46(2):688–93.

Chen, G., Li, Y., Wang, W., Deng, L. Bioactivity and pharmacological properties of alpha-mangostin from the mangosteen fruit: a review. Expert Opin Ther Pat. 2018;28(5):415–27.

Chowdhury, F., Na, S., Li, D., Poh, Y. C., Tanaka, T. S., Wang, F., Wang, N. Material Properties of the Cell Dictate Stress-Induced Spreading and Differentiation in Embryonic Stem Cells. Nat. Mater. 2010, 9(1), 82–88.

Collinsworth, A.M., Zhang, S., Kraus, W.E., Truskey, G.A. Appar- ent elastic modulus and hysteresis of skeletal muscle cells throughout differentiation. Am J Physiol Cell Physiol. 2002;283(4):C1219–C12271227.

Crocker, J.C. & Hoffman, B.D. Multiple-particle tracking and two-point microrheology in cells. Methods in Cell Biology. 83, 141-178, doi:10.1016/S0091-679X(07)83007-X (2007).

Cross, S.E., Jin, Y.S., Lu, Q.Y., Rao, J., Gimzewski, J.K. Green tea extract selectively targets nanomechanics of live metastatic cancer cells. Nanotechnology. 2011;22(21):215101.

Cross, S.E., Jin, Y.S., Rao, J., Gimzewski, J.K. 2007. Nanomechanical analysis of cells from cancer patients. Nature Nanotechnology 2:780–783 DOI 10.1038/nnano.2007.388.

Dai, J., Sheetz, M.P. Mechanical properties of neuronal growth cone membranes studied by tether formation with laser optical tweezers. Biophys J. 1995;68(3):988–96.

Delon, J., Kaibuchi, K., Germain, R.N., Exclusion of CD43 from the immunological synapse is mediated by phosphorylation-regulated relocation of the cytoskeletal adaptor moesin, Immunity 15 (2001) 691e701.

Deng, L., et al. Fast and slow dynamics of the cytoskeleton. Nature Materials. 5, 636-640, doi:10.1038/nmat1685 (2006).

Drake, B., Prater, C.B., Weisenhorn, A.L., Gould, S.A.C., Albrecht, T.R., Quate, C.F., Cannerll, D.S., Hansma, H.G., Hansma, P.K., 1989. Imaging crystals, polymers and biological processes in water with AFM. Science 243: 1586–1589.

Drew, E., Merzaban, J.S., Seo, W., et al., CD34 and CD43 inhibit mast cell adhesion and are required for optimal mast cell reconstitution, Immunity 22 (2005) 43e57.

Eiraku, M., Takata, N., Ishibashi, H., Kawada, M., Sakakura, E., Okuda, S., Sekiguchi, K., Adachi, T., Sasai, Y. 2011. Self-organizing optic-cup morphogenesis in three-dimensional culture. Nature 472:51 56 DOI 10.1038/nature09941.

Fletcher, D.A., Mullins, R.D. Cell mechanics and the cytoskeleton. Nature. 2010;463(7280):485–92.

Furukawa, K., Shibusawa, K., Chairungsrilerd, N., Ohta, T., Nozoe, S. Ohizumi, Y. The mode of inhibitory action of alpha-mango- stin, a novel inhibitor, on the sarcoplasmic reticulum Ca(2+)- pumping ATPase from rabbit skeletal muscle. Jpn J Pharmacol. 1996;71(4):337–40.

Guilak, F., Erickson, G.R., Ting-Beall, H.P. The effects of osmotic stress on the viscoelastic and physical properties of articular chon- drocytes. Biophys J. 2002;82(2):720–7.

Granger, D.N., Senchenkova, E. San Rafael (CA): Morgan & Claypool Life Sciences; 2010.

Guck, J., Schinkinger, S., Lincoln, B., Wottawah, F., Ebert, S., Romeyke, M., Lenz, D., Erickson, H.M., Ananthakrishnan, R., Mitchell, D., Kas, J., Ulvick, S., Bilby, C. 2005. Optical deformability as an inherent cell marker for testing malignant transformation and metastatic competence. Biophysical Journal 88:3689–3698 DOI 10.1529/biophysj.104.045476.

Itoh, T., Ohguchi, K., Iinuma, M., Nozawa, Y., Akao, Y. Inhibitory effect of xanthones isolated from the pericarp of Garcinia mango- stana L. on rat basophilic leukemia RBL-2H3 cell degranulation. Bioorg Med Chem. 2008;16(8):4500–8.

Jinsart, W., Ternai, B., Buddhasukh, D., Polya, G.M. Inhibition of wheat embryo calcium-dependent protein kinase and other kinases by mangostin and gamma-mangostin. Phytochemistry. 1992;31(11):3711–3.

Haga, H., Sasaki, S., Kawabata, K., Ito, E., Ushiki, T., Sambongi, T. Elasticity mapping of living fibroblasts by AFM and immunofluorescence observation of the cytoskeleton. Ultramicroscopy. 2000;82(1–4):253–8.

Haghparast, S.M., Kihara, T., Shimizu, Y., Yuba, S., Miyake, J. Actin-based biomechanical features of suspended normal and cancer cells. J Biosci Bioeng. 2013;116(3):380–5.

Haghparast, S.M., Kihara, T., Miyake, J. Distinct mechanical behavior of HEK293 cells in adherent and suspended states. PeerJ. 2015;3:e1131.

Henderson, E., Haydon, P.G., Sakaguchi, D.S., 1992. Actin filament dynamics in living glial cells imaged by atomic force microscopy. Science 257: 1944–1946.

Hertz, H. Über die berührung fester elastischer Körper. J Reine Angewandte Math. 1881;92:156–71.

Hochmuth, R.M. Micropipette aspiration of living cells. Journal of Biomechanics. 33, 15-22 (2000).

Hoffman, B.D. & Crocker, J.C. Cell mechanics: dissecting the physical responses of cells to force. Annual Review of Biomedical Engineering.11, 259-288, doi:10.1146/annurev.bioeng.10.061807.160511 (2009).

Hoffman, B.D., Massiera, G., Van Citters, K.M., & Crocker, J.C. The consensus mechanics of cultured mammalian cells. Proceedings of the National Academy of Sciences of the United States of America. 103, 10259-10264, doi:10.1073/pnas.0510348103 (2006).

Hung, S.H., Shen, K.H., Wu, C.H., Liu, C.L., Shih, Y.W. Alpha-mangostin suppresses PC-3 human prostate carcinoma cell metastasis by inhibiting matrix metalloproteinase-2/9 and urokinase-plasmino- gen expression through the JNK signaling pathway. J Agric Food Chem. 2009;57(4):1291–8.

Kagiwada, H., Nakamura, C., Kihara, T., Kamiishi, H., Kawano, K., Nakamura,. N, et al. The mechanical properties of a cell, as determined by its actin cytoskeleton, are important for nanon- eedle insertion into a living cell. Cytoskeleton (Hoboken). 2010;67(8):496–503.

Kaomongkolgit, R., Chaisomboon, N., Pavasant, P. Apoptotic effect of alpha-mangostin on head and neck squamous carcinoma cells. Arch Oral Biol. 2011;56(5):483–90.

Kato, K., Umezawa, K., Funeriu, D.P., Miyake, M., Miyake, J., Nagamune, T. Immobilized culture of nonadherent cells on an oleyl poly(ethylene glycol) ether-modified surface. Biotechniques. 2003;35(5):1014–21.

Khismatullin, D. B. The Cytoskeleton and Deformability of White Blood Cells. Current Topics Membranes 2009, 64, 47–111.

Kihara, T., Haghparast, S.M., Shimizu, Y., Yuba, S., Miyake, J. Physical properties of mesenchymal stem cells are coordinated by the perinuclear actin cap. Biochem Biophys Res Commun. 2011;409(1):1–6.

Kihara, T., Nakamura, C., Suzuki, M., Han, S.W., Fukazawa, K., Ishihara, K., et al. Development of a method to evaluate caspase-3 activity in a single cell using a nanoneedle and a fluorescent probe. Biosens Bioelectron. 2009;25(1):22–7.

Kim, K.S., Cho, C.H., Park, E.K., Jung, M.H., Yoon, K.S., Park, H.K. AFM- detected apoptotic changes in morphology and biophysical prop- erty caused by paclitaxel in Ishikawa and HeLa cells. PLoS ONE. 2012;7(1):e30066.

Kunda, P., Pelling, A.E., Liu, T., Baum, B. Moesin controls cortical rigidity, cell rounding, and spindle morphogenesis during mitosis. Curr Biol. 2008;18(2):91–101.

Lau, A.W., Hoffman, B.D., Davies, A., Crocker, J.C., & Lubensky, T.C. Microrheology, stress fluctuations, and active behavior of living cells. Physical Review Letters. 91, 198101 (2003).

Lee, G. Y. H., Lim, C. T. Biomechanics Approaches to Studying Human Diseases. Trends Biotechnol. 2007, 25(3), 111–118

Lee, Y.B., Ko, K.C., Shi, M.D., Liao, Y.C., Chiang, T.A., Wu, P.F., et al. alpha-Mangostin, a novel dietary xanthone, suppresses TPA-medi- ated MMP-2 and MMP-9 expressions through the ERK signaling pathway in MCF-7 human breast adenocarcinoma cells. J Food Sci. 2010;75(1):H13–23.

Lee, C.H., Ying, T.H., Chiou, H.L., Hsieh, S.C., Wen, S.H., Chou, R.H., et al. Alpha-mangostin induces apoptosis through activation of reac- tive oxygen species and ASK1/p38 signaling pathway in cervical cancer cells. Oncotarget. 2017;8(29):47425–39.

Levental, I., et al. A simple indentation device for measuring micrometer-scale tissue stiffness. J. Phys-Condens. Mat. 22, doi:10.1088/0953-8984/22/19/194120 (2010).

Li, J., Lykotrafitis, G., Dao, M., Suresh, S. Cytoskeletal. Dynamics of Human Erythrocyte. Proc. Natl. Acad. Sci. U. S. A. 2007, 104(12), 4937–4942.

Liu, F. & Tschumperlin, D.J. Micro-mechanical characterization of lung tissue using atomic force microscopy. J. Vis. Exp. (54), e2911, doi:10.3791/2911 (2011).

Liu, J., et al. Microrheology probes length scale dependent rheology. Physical Review Letters. 96, 118104 (2006).

Liu, Y., Park, J.M., Chang, K.H., Chin, Y.W., Lee, M.Y. alpha- and gamma-mangostin cause shape changes, inhibit aggrega- tion and induce cytolysis of rat platelets. Chem Biol Interact. 2015;240:240–8.

Mahaffy, R.E., Park, S., Gerde, E., Kas, J., & Shih, C.K. Quantitative analysis of the viscoelastic properties of thin regions of fibroblasts using atomic force microscopy. Biophysical Journal. 86, 1777-1793, doi:10.1016/S0006-3495(04)74245-9 (2004).

Manjunath, N., Johnson, R.S., Stauton, D.E., et al., Targeted disruption of CD43 gene enhances T lymphocyte adhesion, J. Immunol. 151 (1993) 1528e1534.

Majstoravich, S., Zhang, J., Nicholson-Dykstra, S., Linder, S., Friedrich, W., Siminovitch, K.A., et al. Lymphocyte microvilli are dynamic, actin-dependent structures that do not require Wiskott-Aldrich syndrome protein (WASp) for their morphology. Blood. 2004;104(5):1396–403.

Maloney, J.M., Nikova, D., Lautenschlager, F., Clarke, E,, Langer, R., Guck, J., Van Vliet, K.J. 2010. Mesenchymal stem cell mechanics from the attached to the suspended state. Biophysical Journal 99:2479–2487 DOI 10.1016/j.bpj.2010.08.052.

Matzke, R., Jacobson K, Radmacher M. Direct, high-resolution measurement of furrow stiffening during division of adherent cells. Nat Cell Biol. 2001;3(6):607–10.

Moeendarbary, Emad; Harris, Andrew (2014). "Cell mechanics: principles, practices, and prospects". Wiley Interdisciplinary Reviews: Systems Biology and Medicine. 6: 371–388. doi:10.1002/wsbm.1275

Müller, D.J., Dufrêne, Y.F. Atomic force microscopy as a multifunctional molecular toolbox in nanobiotechnology. Nat Nanotechnol. 2008 May; 3(5):261-9.

Oh, M.J., Kuhr, F., Byfield, F., & Levitan, I. Micropipette Aspiration of Substrate-attached Cells to Estimate Cell Stiffness. J. Vis. Exp. (67), e3886, doi:10.3791/3886 (2012).

Ohnishi, H., Sasaki, H., Nakamura, Y., Kato, S., Ando, K., Narimatsu, H., et al. Regulation of cell shape and adhesion by CD34. Cell Adh Migr. 2013;7(5):426–33.

Pajerowski, J. D., Dahl, K. N., Zhong, F. L., Sammak, P. J., Discher, D. E. Physical Plasticity of the Nucleus in Stem Cell Differentiation. Proc. Natl. Acad. Sci. U. S. A. 2007, 104(40), 15619–15624.

Pedraza-Chaverri, J., Reyes-Fermin, L.M., Nolasco-Amaya, E.G., Orozco-Ibarra, M., Medina-Campos, O.N., Gonzalez-Cuahutencos, O., et al. ROS scavenging capacity and neuroprotective effect of alpha-mangostin against 3-nitropropionic acid in cerebellar granule neurons. Exp Toxicol Pathol. 2009;61(5):491–501.

Phan, T.K.T., Shahbazzadeh, F., Pham, T.T.H., Kihara, T. Alpha-mango- stin inhibits the migration and invasion of A549 lung cancer cells. PeerJ. 2018;6:e5027.

Radmacher, M., Tillamnn, R.W., Fritz, M., Gaub, H.E. From molecules to cells: imaging soft samples with the atomic force microscope. *Science*. 1992;257(5078):1900-1905. doi:10.1126/science.1411505

Radmacher, M., Fritz, M., Kacher, C.M., Cleveland, J.P., Hansma, P.K. Measuring the viscoelastic properties of human platelets with the atomic force microscope. Biophys J. 1996;70(1):556–67.

Radmacher, M. Measuring the elastic properties of biological samples with the AFM. IEEE Engineering in Medicine and Biology Magazine: The Quarterly Magazine of the Engineering in Medicine & Biology Society. 16, 47-57 (1997).

Ramos, J.R., Pabijan, J., Garcia, R., Lekka, M. The softening of human bladder cancer cells happens at an early stage of the malignancy process. Beilstein J Nanotechnol. 2014;5:447–57.

Rotsch, C., Braet, F., Wisse, E., Radmacher, M. AFM imaging and elasticity measurements on living rat liver macrophages. Cell Biol Int. 1997;21(11):685–96.

Shih, Y.W., Chien, S.T., Chen, P.S., Lee, J.H., Wu, S..H, Yin, L.T. Alpha- mangostin suppresses phorbol 12-myristate 13-acetate-induced MMP-2/MMP-9 expressions via alphavbeta3

integrin/FAK/ERK and NF-kappaB signaling pathway in human lung adenocarci- noma A549 cells. Cell Biochem Biophys. 2010;58(1):31–44.

Shimizu, Y., Haghparast, S.M., Kihara, T., Miyake, J. Cortical rigidity of round cells in mitotic phase and suspended state. Micron. 2012;43(12):1246–51.

Shimizu, Y., Kihara, T., Haghparast, S.M., Yuba, S., Miyake, J. Simple display system of mechanical properties of cells and their disper- sion. PLoS ONE. 2012;7(3):e34305.

Solon, J., Levental, I., Sengupta, K., Georges, P.C., & Janmey, P.A. Fibroblast adaptation and stiffness matching to soft elastic substrates. Biophysical Journal. 93, 4453-4461, doi:10.1529/biophysj.106.101386 (2007).

Sugitate, T., Kihara, T., Liu, X.Y., Miyake, J. 2009. Mechanical role of the nucleus in a cell in terms of elastic modulus. Current Applied Physics 9:e291–e293 DOI 10.1016/j.cap.2009.06.020.

Suresh, S. Biomechanics and Biophysics of Cancer Cells. Acta Biomaterialia 2007, 3(4), 413–438.

Suresh, S., Spatz, J., Mills, J. P., Micoulet, A., Dao, M., Lim, C. T., Beil, M., Seufferlein, T. Connections between SingleCell Biomechanics and Human Disease States: Gastrointestinal Cancer and Malaria. Acta Biomaterialia 2005, 1(1), 15–30.

Tao, M., Jiang, J., Wang, L., Li, Y., Mao, Q., Dong, J., et al. Alpha-mangostin alleviated lipopolysaccharide induced acute lung injury in rats by suppressing NAMPT/NAD controlled inflammatory reactions. Evid Based Complement Alternat Med. 2018;2018:5470187.

Trickey, W.R., Vail, T.P., Guilak, F. The role of the cytoskeleton in the viscoelastic properties of human articular chondrocytes. J Orthop Res. 2004;22(1):131–9.

Tachibana, K., Ohnishi, H., Ali Haghparast, S.M., Kihara, T., Miyake, J. Activation of PKC induces leukocyte adhesion by the dephosphorylation of ERM. Biochem Biophys Res Commun. 2020;523(1):177–82.

Watanapokasin, R., Jarinthanan, F., Nakamura, Y., Sawasjirakij, N., Jaratrungtawee, A., Suksamrarn, S. Effects of alpha-mangostin on apoptosis induction of human colon cancer. World J Gastroenterol. 2011;17(16):2086–95.

Wu, H.W., Kuhn, T., & Moy, V.T. Mechanical properties of l929 cells measured by atomic force microscopy: Effects of anticytoskeletal drugs and membrane crosslinking. Scanning. 20, 389-397 (1998).

von Andrian, U.H., Hasslen, S.R., Nelson, R.D., Erlandsen, S.L., Butcher, E.C. A central role for microvillous receptor presentation in leu- kocyte adhesion under flow. Cell. 1995;82(6):989–99.

Yamane, J., Ohnishi, H., Sasaki, H., Narimatsu, H., Ohgushi, H., Tachibana, K. Formation of microvilli and phosphorylation of ERM family proteins by CD43, a potent inhibitor for cell adhesion: cell detachment is a potential cue for ERM phosphorylation and organ- ization of cell morphology. Cell Adh Migr. 2011;5(2):119–32.

Yonemura, S., Hirao, M., Doi, Y., et al., Ezrin/radixin/moesin (ERM) proteins bind to a positively charged amino acid cluster in the juxta-membrane cytoplasmic domain of CD44, CD43, and ICAM-2, J. Cell Biol. 140 (1998) 885e895.

Figures

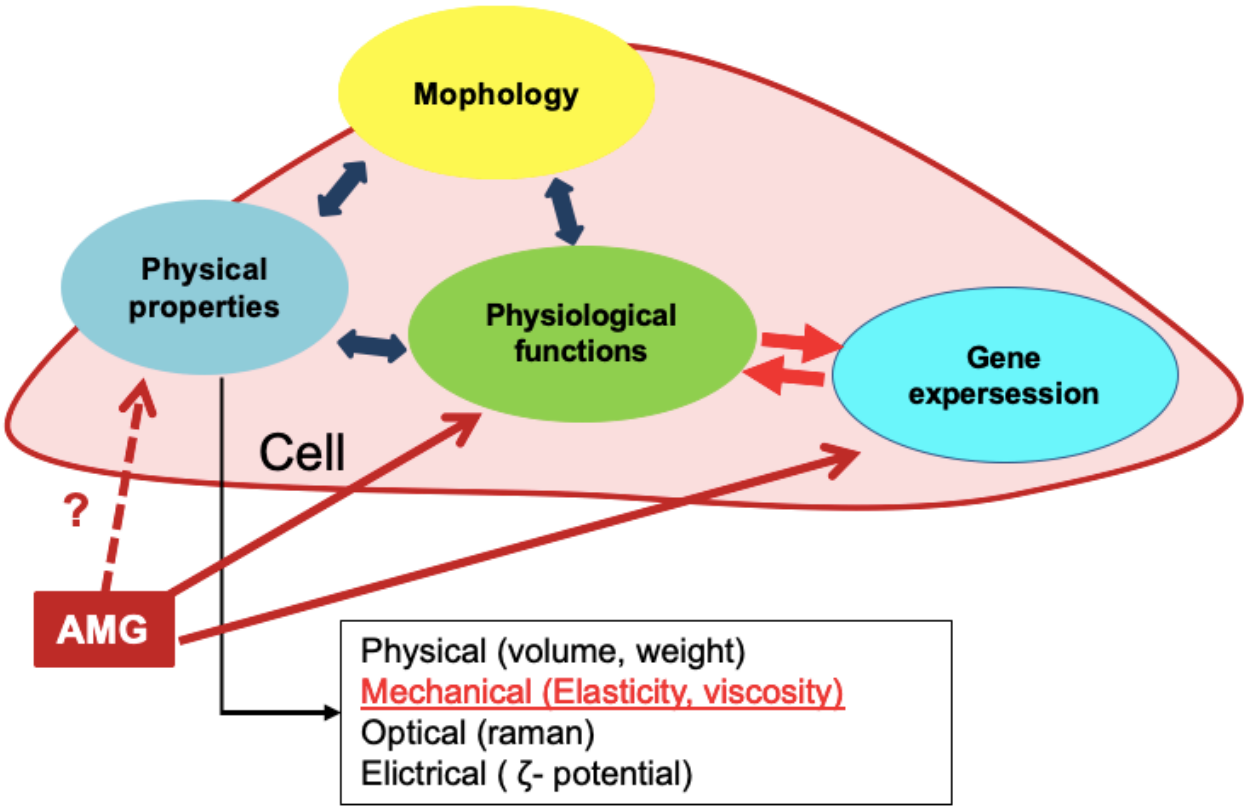

Figure 4.1: Cell phenotypes are determined via combinatorial factors. The cell phenotypes are remained through combination of physiological functions, physical properties, morphology and regulated by gene expression.

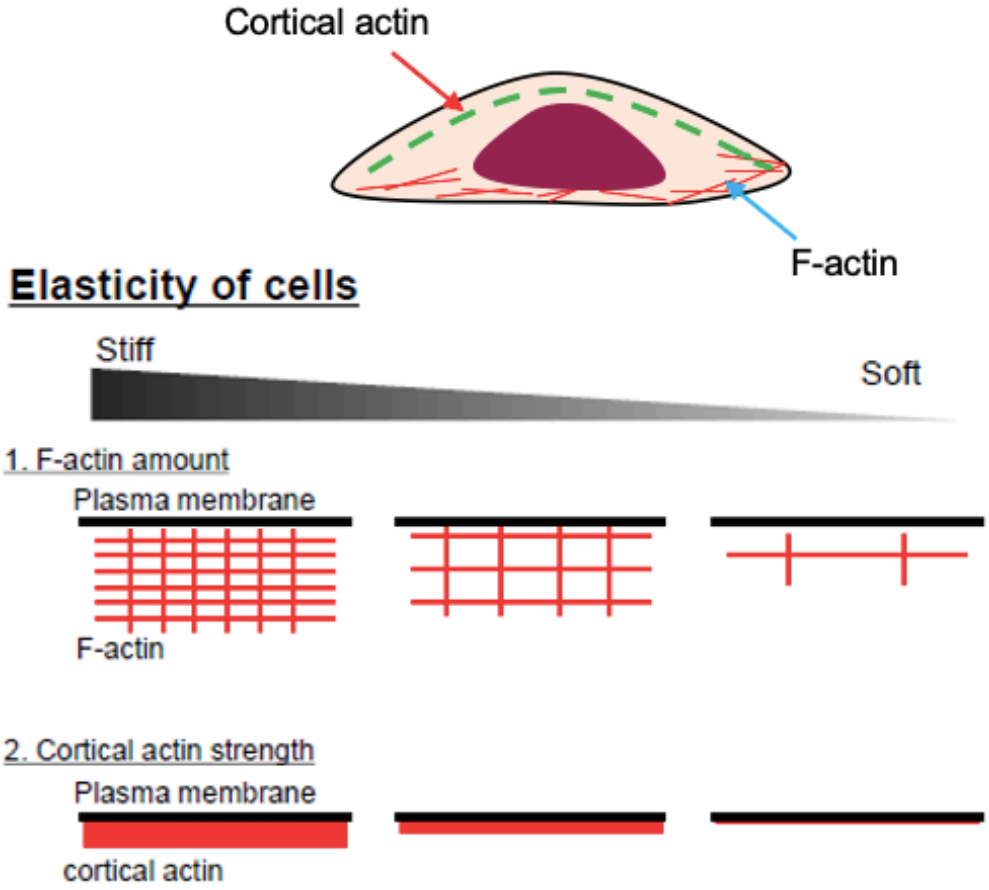

Figure 4.2: The elasticity of cells is attributed to actin cytoskeleton. The cell stiffness reflects the amount of F-actin and cortical actin strength inside the cell.

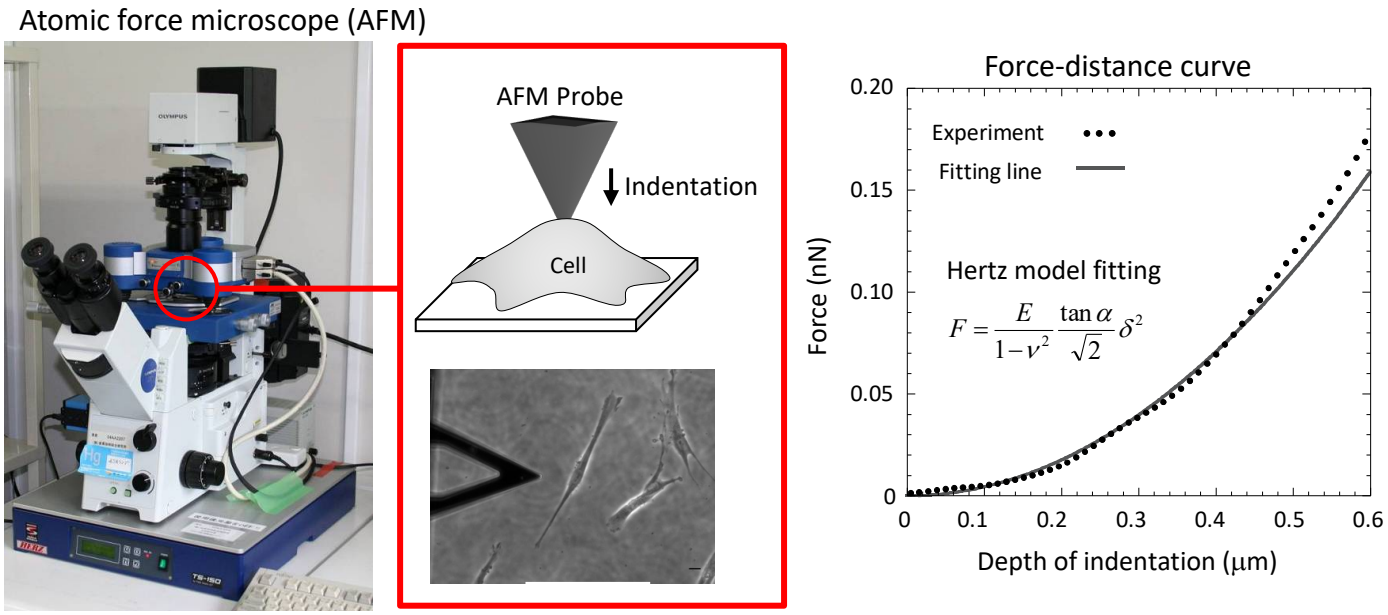

Figure 4.3. Atomic force microscope (AFM). The force for probe over the probe indentation can be directly measured. The elastic modulus (Young's modulus) of the surface of living cells can be calculate by using the force-distance curve for probe.

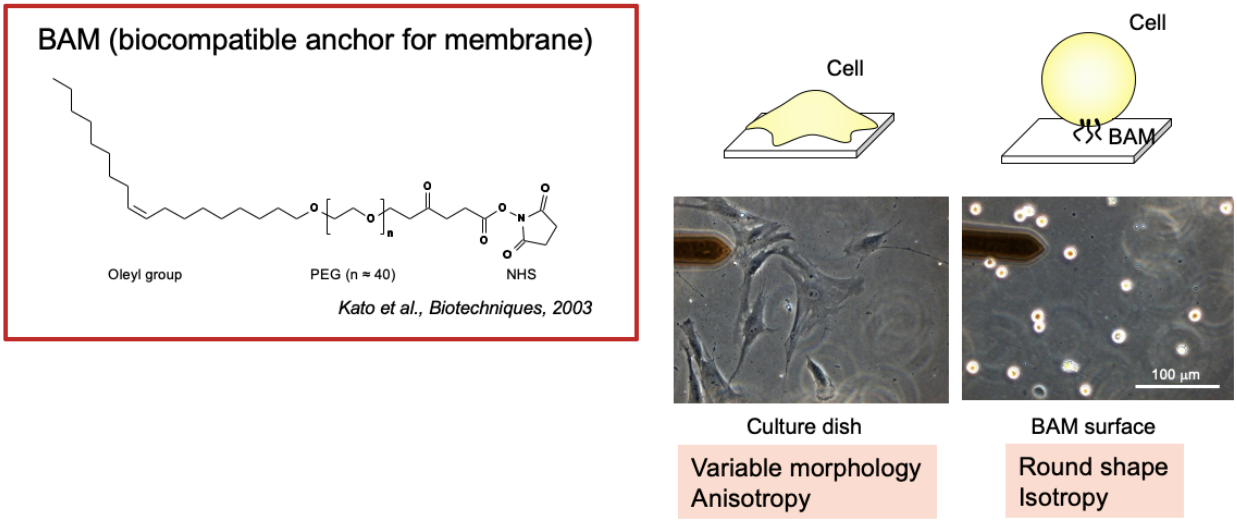

Figure 4.4: Preparing coating dish using BAM for suspended cells to measure AFM. BAM molecules covalently bind with BSA coated dish surface. The suspended round cells can be fixed on the BAM surface, then it can be measured the elasticity of floating cells by AFM using BAM surface.

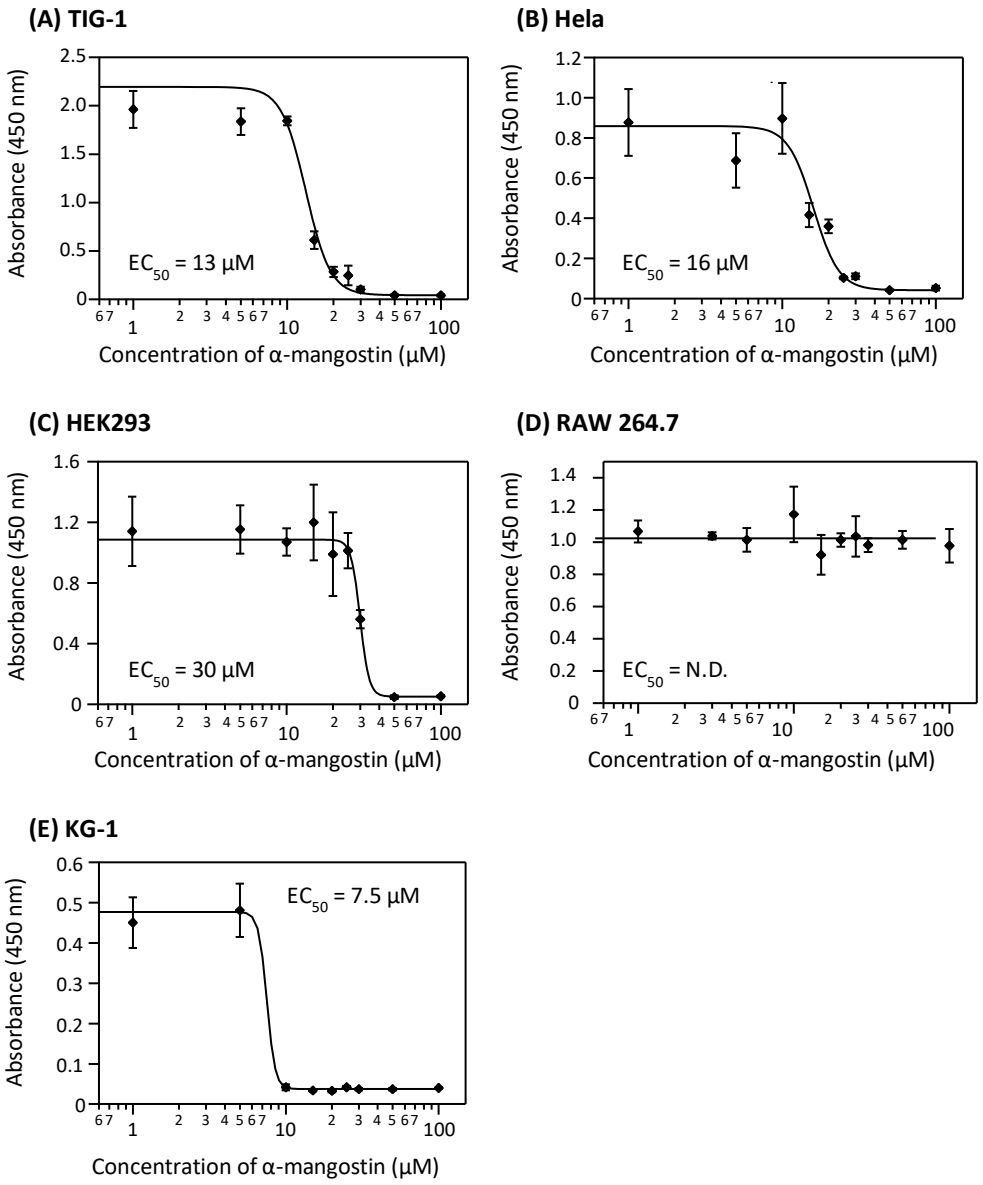

Figure 4.5. Cytotoxicity of α-mangostin on TIG-1, HeLa, HEK293, RAW 264.7, and KG-1 cells. These cells were treated with various concentrations of α-mangostin (0–100 μM) and incubated for 24 h. The viable cells were measured using the cell counting kit-8. The values were calculated from 3 experiments. The effective concentration (EC_{50}) is shown in each graph.

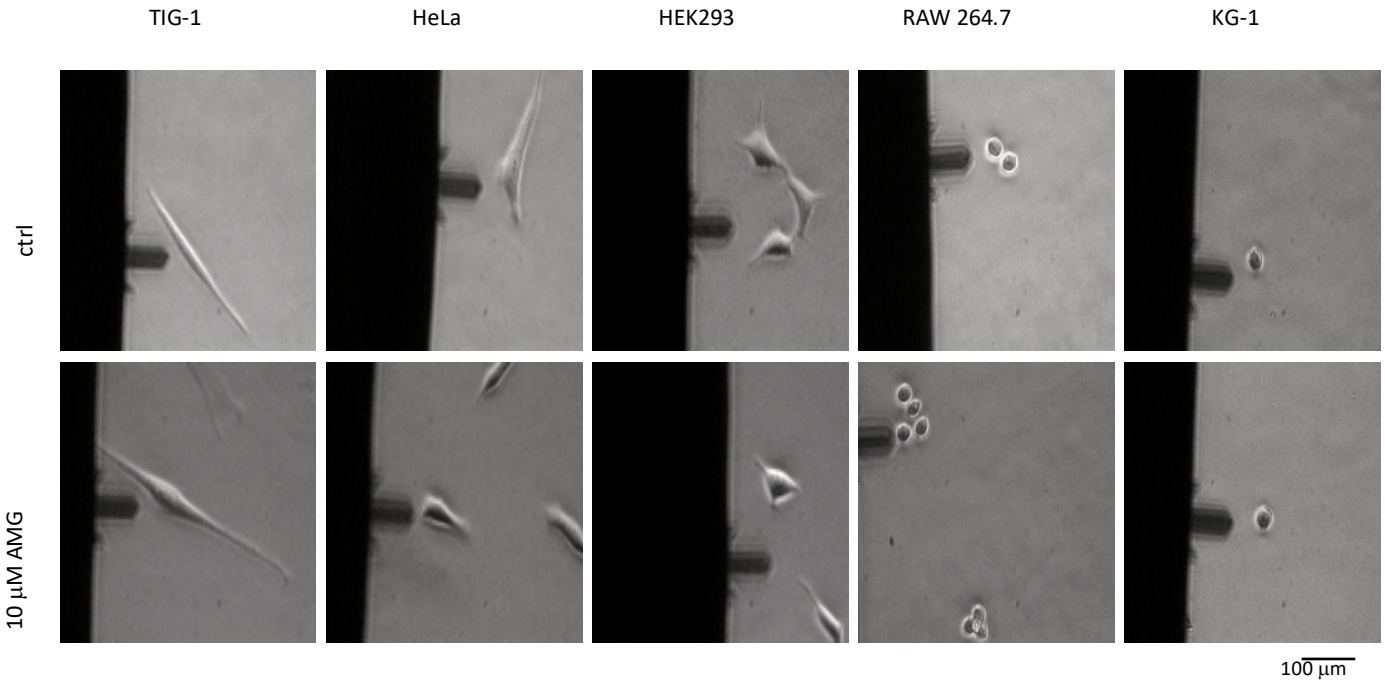

Figure 4.6. Phase-contrast micrographs of TIG-1, HeLa, HEK293, RAW 264.7, and KG-1 cells treated with α-mangostin. These cells were cultured with or without 10 μM of α-mangostin (AMG) for 6 h. The object at the left of each micrograph is the AFM cantilever. Bar 100 μm

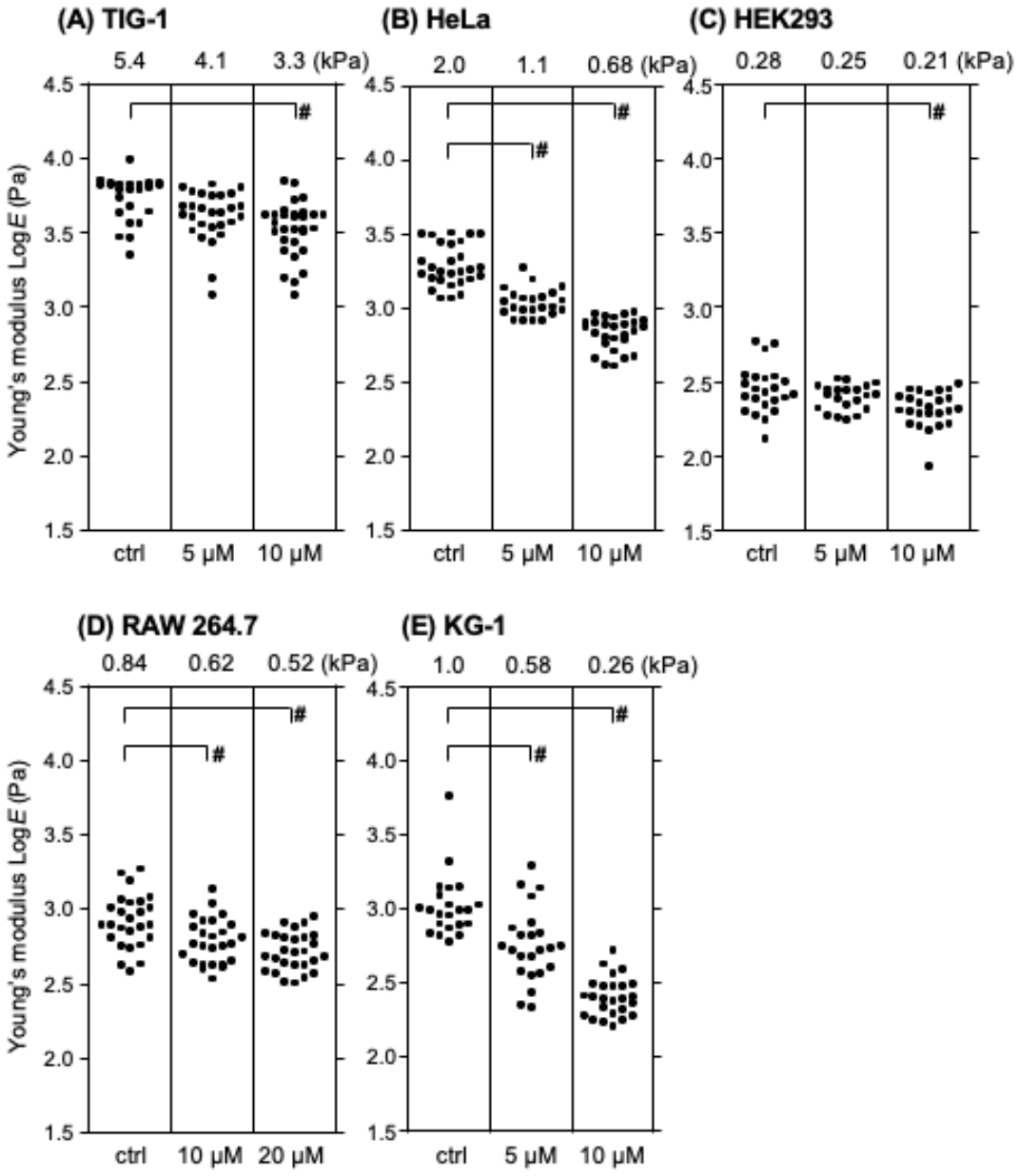

Figure 4.7. Young's modulus of cells treated with α-mangostin. Young's modulus of TIG-1, HeLa, HEK293, RAW 264.7, and KG-1 cells were examined by AFM. The distribution of the Young's modulus of cells treated with α-mangostin for 6 h is represented by scatterplots. Each point represents the median value of 25 measuring points in each cell, and the Young's modulus in each condition is represented in more than 21 independent cells.

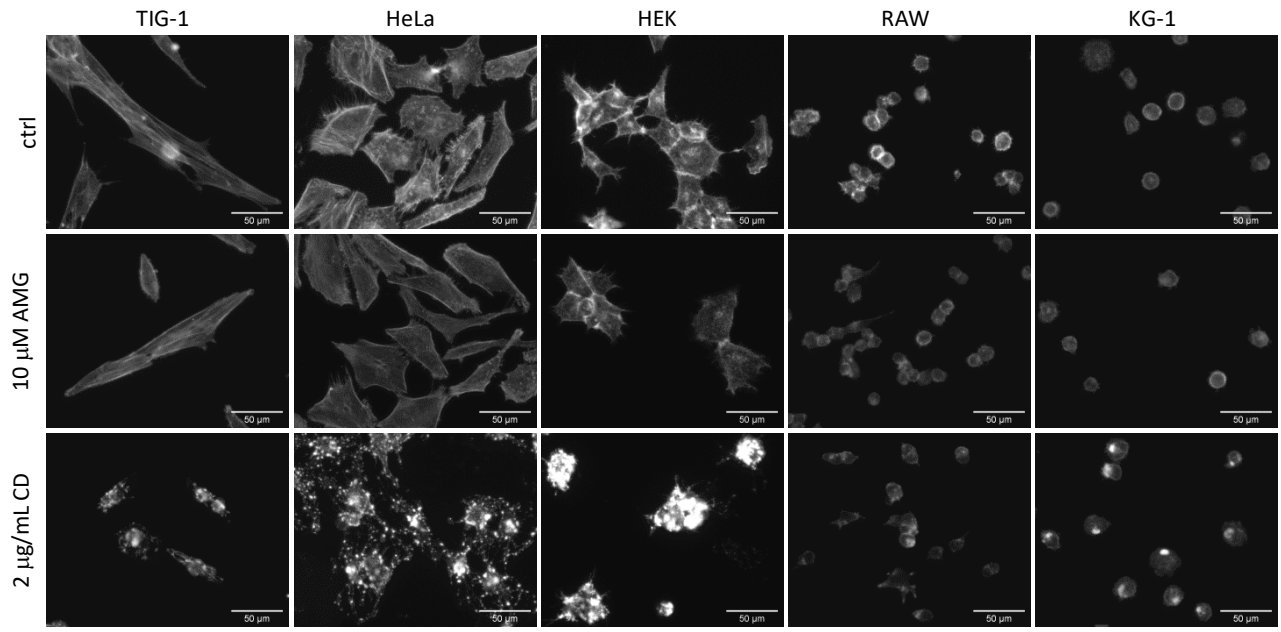

Figure 4.8. Fluorescence microscopy images of F-actin of cells treated with α-mangostin. TIG-1, HeLa, HEK293, RAW 264.7, and KG-1 cells were treated with 10 μM of α-mangostin for 6 h or 2 μg/mL of cytochalasin D (CD) for 1.5 h, and then stained with rhodamine labeled-phalloidin. Bar 50 μm.

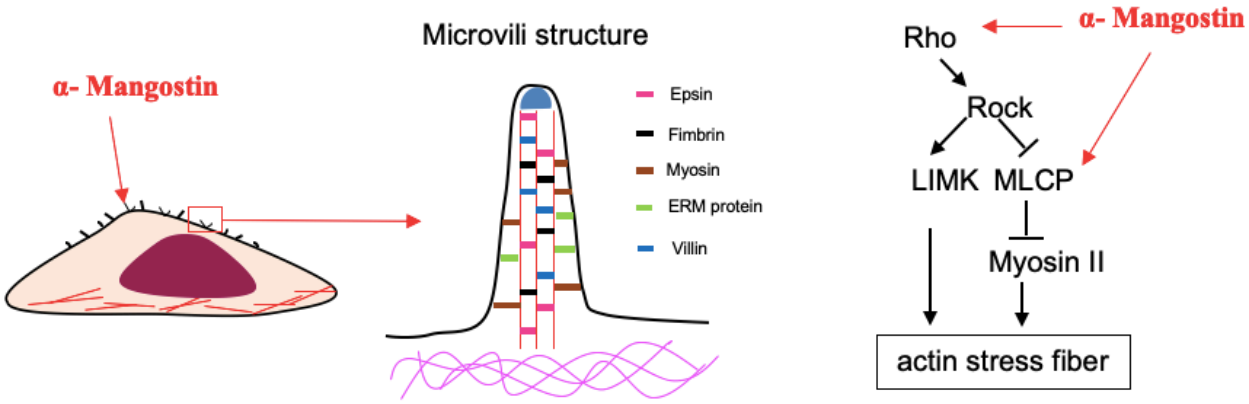

Figure 4.9: α-Mangostin is sensitive with microvilli structure. Microvilli are weak actin structures, they distribute high consistence the cell surface of Hela cells and KG-1 cells. The stiffness of these cells are significantly effected α-mangostin, so microvilli are sensitive with α-mangostin. Moreover, α-mangostin was found to change actin modulation molecules (such as MLC), so it may cause the change to the actin stress fiber.

Chapter 5: α – Mangostin induces the cell adhesion and activates the leukocytes

5 – 1. Overview

Leukocytes, as well known as white blood cells, are a central part of the immune system who help to protect the body against foreign substances, microbes, and infectious diseases. Almost leukocytes are non-adhesion/or suspended cells, they travel through the body, moving between the organs and nodes and monitoring any potentially problematic germ or infection. However, leukocytes are possible to transform to adherent state, the adhesion of leukocytes to vascular endothelium is a hallmark of the inflammatory process. In previous research, I found that α-mangostin reduced the cell surface stiffness of human myelomonocytic KG-1 cells, and it also found that α-mangostin induced cell adhesion in KG-1 to substratum. Therefore, in this study, I investigated to clarify mechanism of α-mangostin in change the cell surface stiffness and inducing cell adhesion of leukocyte.

Leukocytes have spherical shape with cortical actin cytoskeleton on their cortex; which is almost the only mechanical structures of the cells. In addition, the mechanical properties are linked to the leukocytes activation, and all these events are linked to dephosphorylation of Erin/Radixin/Moesin (ERM) protein. The results showed α-mangostin decreased the cell surface stiffeness and induced cell adhesion in myelomonocytic KG-1 cells. However, PKC inhibitors, phosphatase inhibitor prevented α-mangostin reduce the surface stiffness and induce cell adhesion. Taken together, these findings strongly suggest α-mangostin decreased the stiffness through activating PKC, protein phosphatase then regulated the signal which relates the ERM-dephosphorylation to activate cell adhesion in leukocytes.

5 – 2. Introduction

White blood cells are floating cells that exist in the blood and have the role of attacking and eliminating foreign substances that have entered the body. When the tissue is damaged, the recruitment of leukocytes to adhere to the damaged vascular endothelial cells through adhesion molecules, and after rolling on the cells, migrate from the interstitial spaces of the vascular endothelial cells into the damaged tissue. Damaged cells caused the release of TNF-α and IL-1, and the vascular endothelial cells express the adhesion molecule selectin. This recruitment process and the requirement for (and participation of) specific adhesion glycoproteins in the binding of leukocytes to endothelial cells have been elegantly demonstrated using a variety of experimental approaches. The initial adhesive interactions between the leukocytes and venular endothelium are tethering (capture) and rolling. These low-affinity (weak) interactions are subsequently strengthened as a result of leukocyte activation (mediated by chemokine-dependent and chemokine-independent mechanisms). Consequently, the leukocytes attach to the endothelium and remain stationary. The current paradigm for leukocyte (neutrophil) recruitment in the inflamed microvasculature is summarized in Figure 5.1 The adhesive determinants are known to vary between vascular beds and between different leukocyte populations.

The adhesion of leukocytes is regulated by adhesion-inhibitory sialomucin such as CD43 (leukosialin) and CD34 (a cell surface sialomucin). CD43 is expressed in most of leukocytes (Fukuda, 1999), while CD34 is enriched in hematopoietic progenitor cells (Krause, 1996), and they are considered as inhibitor for cell adhesion (Drew, 2005). Gene disruption of CD43 and/or CD34 increased cell adhesion, while overexpression of CD43 or CD34 inhibited cell adhesion in adherent cells (Manjunath et al., 1993; Drew et al., 2005). In addition, the phosphorylation of Ezrin/Radixin/Moesin (ERM) are located at the surface of leukocytes and it could also inhibit cell

adhesion which express of Moesin-T558D, a phospho-mimetic Moesin mutant, inhibited cell adhesion to both substratum or other cells (Tachibana, 2015, 2019). The engagement of T cell receptor induced decrease of phosphorylated-ERM in correspondence with the re-distribution of CD43 and formation of immunological synapse (Delon et al., 2001; Allenspach et al., 2001). Combined with the binding of CD43 with phosphorylated-ERM (Yonemura et al., 1998), this decrease of phosphorylated-ERM is the likely mechanism of CD43 exclusion from attachment sites to promote cell adhesion in T lymphocytes. Moreover, stromal cell-derived factor 1 (SDF-1), a CXC chemokine, has been found to quickly induces decrease of phosphorylated-ERM as well as microvillus collapse in T lymphocytes (Brown et al., 2003).

The cell surface mechanicals are altered following the alteration in bioactivities and transformation of cells. The cell surface stiffness is largely attributed to the actin cytoskeleton and display the cell surface actin architectures (Dai, 1995; Collinsworth, 2002; Guilak, 2002; Trickey, 2004). The surface stiffness alteration reflects the remodeling of actin cytoskeleton in respective the cellular events and states (Matzke, 2001; Kunda, 2008). Thus, by analyzing the mechanical properties of cells, it may provide us to understand changes of cell characteristics. In addition, the surface stiffness measurement may evaluate the strength of the actin cytoskeleton network near cell surface and may provide better understanding about regulatory mechanism of cell surface actin skeleton. The cell surface rigidity is involved to the change of cell shape to adhesion states. Leukocytes have cortical actin placed on plasma membrane which mechanically supports their surface rigidity (Ohnishi, 2013). Their actin cortical is very special with very thin and uniform structure, it is different with intermittent cortical actin structures seen in other cells (Bray, 1986). The actin cytoskeleton at cellular cortex play important role in the maintenance of leukocyte's spherical shape and microvilli (Chhabra, 2007), and contributes to cell surface rigidity (Shimizu,

2012). In addition, a decrease of phosphorylated-ERM has been shown to diminish cell surface rigidity (Tachinana, 2015), by linking cell surface molecules with cortical actin skeleton (Fiéver, 2007; Niggli, 2008). Decrease the cell surface stiffness caused increase deformability of cell, so it is possibility enhance cell adhesion.

Atomic force microscopy (AFM) is proved that is one of the most sensitive method in several method to detect the cell stiffness and mechanical properties under physiological conditions (Radmacher, 1996). This method has been indicated an effective method that can measure the stiffness of both adherent and suspended cells (Haga, 2000; Kihara, 2011; Kagiwada, 2010). Leukocytes were previously measured the stiffness by using AFM and a biocompatible anchor for membrane (BAM) substrate for anchoring the suspended cells (Kagiwade, 2010; Shimizu, 2012) (Fig. 4.2). Thus, this method AFM can be a suitable tool to analyze the mechanical stiffness of leukocytes.

In this study, I investigated the mechanism of α-mangostin reduced the cell surface stiffness and induced cell adhesion in leukocytes, and activated PKC was found as the key event for the induction of leukocytes' adhesion by external stimuli.

5 – 3. Experimental result

5 – 3.1. α – Mangostin reduces the cell surface stiffness of leukocytes

I previously found that α-mangostin decreased the mechanical properties of various cells including A549 lung cancer cells and CCD-14Br lung normal cells (Phan, 2018), human fibroblast TIG-1 cells, human cancerous Hela cells, human embryonic kidney HEK293 cells, mouse macrophage RAW 264.7 cells, and human myeloblasts KG-1 cells after 6 h treatment with α-mangostin using the cone probe (BL-AC-40TS-C2) for AFM measurement (Phan, 2020). In this study, I change the cantilever to the pyramid probe (SN-AF01S-NT) to measure the AFM and KG-1 cells were exposed with various concentration of α-mangostin for 6 h. KG-1 cells were fixed on cell anchoring culture dishes, then treated with 5, 10, 15 μM of α-mangostin for 6 h and surface stiffness was examined using AFM. The distribution of the Young's modulus of KG-1 treated with α-mangostin is shown in Fig. 5.3. The results are consistent with my previous research event using different cantilever to measure the stiffness. The results indicated α-mangostin reduced the distribution of the Young moduli in KG-1 cells after short time treatment. Particularly, the Young's modulus of KG-1 cells significantly decreased by treatment with 10 μM of α-mangostin, and it was almost exactly the same as at 15 μM.

5 – 3.2. α – Mangostin alters leukocytes' surface and cortical actin

According to many published researches, the mechanical properties is largely attributed to the actin cytoskeleton (Dai, 1995; Collinsworth, 2002; Guilak, 2002; Trickey, 2004). Therefore, the actin filaments of KG-1 cells were stained with rhodamine labeled-phalloidin and DAPI to label nuclei, then observed under the confocal laser scanning microscopy. KG-1 cells showed the cortical F-actin and short fine microvilli on their plasma membrane in Fig. 5.4. They are spherical

land have abundant microvilli of varying lengths and high density. However, within short time of α-mangostin stimulation have undergone dramatic changes in surface features. The cells are observed that remain nearly spherical but show a marked reduction in microvilli exposing with α-mangostin. In addition, α-mangostin slightly blurred the actin cortical and appeared blebbing on the surface. Bleb expansion occurs when the membrane detaches from the actin cortical cytoskeleton (Guillaume, 2006), so α-mangostin caused an impact to cortical actin and re-arrangement f-actin binding membrane and cortical actin. The actin cytoskeleton of KG-1 cells is structured only by the actin cortical under plasma, so this results matched with the decrease of the stiffness caused by α-mangostin.

5 – 3.3. α – Mangostin induces cell adhesion of leukocytes

Most of leukocytes are non-adhesion cells which are spherical and do not attach to substrate, but they are possible to adhere to the other cells or substratum in response to external stimuli (Dustin, 1989; Van KooyK, 1989; Shimizu, 1991; Hynes, 1992; Hemler, 1993). KG-1 cells derived from acute myelogenous leukemia are non-adherent cells and express α4β1 integrin, but they hardly adhere to substrate even coated with Fibronectin, a ligand for α4β1 integrin (Ohnishi, 2013). However, I found that α-mangostin treatment intensified KG-1 cell adhesion to Fibronectin-coated substrate. In the control group, there are about 121.18 cells/mm^2 of KG-1 cells adhered to the Fibronectin-coated substrate (Fig. 5.5). Meanwhile, percentage of KG-1 cell adhesion was significantly increased by treatment with α-mangostin at 5, 10, 15 μM in short time into 186.59, 196.56, 287.96 cells/mm^2, respectively (Fig. 5.5). This result indicated that α-mangostin augmented KG-1 adhesion mediated by integrin.

5 – 3.4. Activation of PKC is essential for α – Mangostin-activated-leukocytes

Cell undergo the adhesion process is regulated by variable adhesion molecules. Activation of leukocytes adhesion is recently improved that related to dephosphorylation of Ezrin/Radixin/Moesin (ERM) protein which mediated by activation PKC and it also involves to protein phosphatase 1 and/or 2A (Tachibana, 2019). In order to clarify how α-mangostin induce adhesion of KG-1 cells, I further used phosphatase inhibitor Calyculin A and PKC inhibitor BIM I. KG-1 cells were treated with α-mangostin and Calyculin A/BIM I, then adherent cells were calculated, and results were shown in Fig. 5.6. As the results, the amount of α-mangostin induced adherent KG-1 cells were estimated around 300 cells/mm^2, but it decreased when added Calyculin A and BIM I together with α-mangostin. Adding BIM I with α-mangostin caused a loss of adhered cells in dose-dependent, adherent KG-1 cells decreased to 293.49, 214.422, 198.866 cells/mm^2 at BIM I concentration of 0.5, 1, 3 μM, respectively. Especially, Calyculin A significantly prevented α-mangostin induced KG-1 cell adhesion, the ratio of adhesion cells dropped to 171.71, 127.39, 134.55 cells/mm^2 by treatment with Calyculin A at 0.5, 1, 3 μM, respectively. Calyculin A and BIM I showed they inhibited α-mangostin induced KG-1 cell adhesion. Therefore, these results indicated that α-mangostin induced KG-1 cell adhesion related to activated PKC and protein phosphatase 1 and/or 2A.

α-Mangostin induced adhesion of KG-1 cells was inhibited by PKC inhibitor and protein phosphatase inhibitor, so can it affect to α-mangostin reduced KG-1 cell mechanical? I further examine the surface stiffness of KG-1 cells treatment with α-mangostin adding BIM I or Calyculin A. As demonstrated in Figure 5.7, average surface stiffness of Calyculin A/BIM I-treated KG-1 cells were higher than untreated cells, meanwhile KG-1 cells were significantly softened by treatment with 10 μM of α-mangostin. However, adding Calyculin A/ BIM I together with 10 μM of α-mangostin increased the average surface stiffness of KG-1 cells. The Young's modulus of

Calyculin A and α-mangostin-treated KG-1 cells were markedly increased into 0.8, 1.2 and 5.8 kPa by adding 0.3, 1 and 3 nM of Calyculin A. The results were also the same in adding BIM I together with 10 μM of α-mangostin, it's Young modulus drastically raised to 1.9 kPa at 0.5 μM of BIM I, and around 3 kPa at 1μM and 3 μM of BIM I. These results showed, Calyculin A and BIM I prevent α-mangostin-reduced KG-1 cell rigidity, or activated PKC and protein phosphatase related/necessary for α-mangostin-reduced cell surface mechanical.

In this study, I demonstrated that α-mangostin reduced the cell stiffness of leukocytes which are improved that related to induce the adhesion of leukocytes and activate leukocytes via the activation of PKC and protein phosphatase.

5 – 4. Conclusion and Discussion

In this study, I investigated the mechanism of α-mangostin-reduced mechanical of KG-1 cells, and the results indicated that α-mangostin has ability to activate the leukocytes due to turn on some main events which appear in activation process. In addition, activation of PKC was critical for α-mangostin-reduced stiffness and induced adhesion in leukocytes, because PKC inhibitor inhibited these processes. Previously, α-mangostin was reported that activated the expression of PKC (Yuan Fang, 2016). Therefore, PKC activated by α-mangostin results in decrease of the surface stiffness and inducing cell adhesion. Besides PKC inhibitor, Calyculin A also inhibited α-mangostin-reduced stiffness and induced adhesion, that indicated the involvement of protein phosphatase 1 and/or 2A in these impacts.

Leukocytes adhesion to endothelium is a multistep process in which chemokines play an important role of inducing strong adhesion by activating integrin. The chemokines SDF-1 induced T lymphocytes adhesion (Martin et al., 2003) and PMA activated KG-1 adhesion (Tachibana et al., 2020) which are all regulated by ERM- dephosphorylation via activation of PKC. Since SDF-1 engagements activate PLCs, these stimuli likely activate PKC via PLC-diacylglycerol-PKC pathway. Besides PKC inhibitors, Calyculin A inhibited PMA-induced ERM-dephosphorylation, indicating the involvement of protein phosphatase 1 and/or 2A in this dephosphorylation. However, the ERM-dephosphorylation has been not observed in KG-1 after treatment with α-mangostin (Fig. 5.8), the most optimized treatment condition of α-mangostin has not been indicated in which induces the dephosphorylation of ERM. What is the next target regulated by α-mangostin to turn on the events of leukocytes activation? In addition, α-mangostin was indicated that elevated the contents of reactive oxygen species (ROS), which can activate protein kinases. Thus, the activation of PKC by α-mangostin may be involve to ROS (Fig. 5.9).

Microvilli are cell surface thin protrusion, composed of cytoplasmic membrane and parallel bundles of actin filaments. Microvilli are observed on the surface of lymphocytes and other hematopoietic cells (Mooseker et al., 1975; Chhabra et al., 2007). Contradictory roles in cell adhesion were proposed for leukocyte microvilli. Several adhesion receptors are specifically localized on microvilli, and such localization may be critical for the binding to vascular endothelium (von Andrian et al., 1995; Berlin et al., 1995; Singer et al., 2001). Reduction of microvilli also affect to the cell adhesion. Microvilli are actin-rich protruding structures located at the cell surface. Functions of microvilli are to expanse cell surface area, molecule presentation and inhibit of cell adhesion (Chhabra, 2007). Because of their thin protruding structure, microvilli restrict attachment area, so it leads to inhibit cell adhesion. In addition, microvilli are collapsed by the stimulation of chemokines which was suggested for inhibition of cell adhesion (Brown, 2003). Therefore, α-mangostin caused an elimination of microvilli followed by inducing the cell adhesion of KG-1. Furthermore, most of leukocytes are suspended with spherical shape and surrounded with microvilli, so the cell surface stiffness plays important role in remaining their spherical shape. However, in adhesion process, leukocytes are essential to alter their shape and make some flat attachment sites by deforming cell shape which caused from reduction of the cell surface stiffness.

The impacts of α-mangostin on leukocytes were observed which are some similar to leukocyte treated with PMA or T lymphocytes stimulated with SDF-1. In leukocytes treated with PMA or T lymphocytes treated with PMA, SDF-1 all induced dephosphorylation of ERM which were regulated by activation of PKC. α-Mangostin also reduced the cell surface stiffness and induced the cell adhesion of KG-1, and the activation of PKC and protein phosphatase are essential for these processes. However, the dephosphorylation was not observed in the process of α-

mangostin-induced KG-1 cell adhesion. Therefore, the mechanism how does α-mangostin-activated PKC induce KG-1 adhesion is further subject.

To conclusion, in this study α-mangostin was found in decreases the cell surface rigidity which related to induce the cell adhesion and the activation of leukocytes via of activation of PKC and protein phosphatase.

5 – 5. Materials and experimental methods

Materials

Human leukemia myeoblast KG-1 cells were purchased from Riken Cell Bank (Ibaraki, Japan). α-Mangostin, rhodamine labeled phalloidin, DAPI (4′,6-diamidino-2-phenylindole), cytochalasin D, calyculin A, DMEM, and RPMI1640 medium were purchased from Wako Pure Chemical Industries Ltd. (Osaka, Japan). Bisindolylmaleimide I (BIM I) was obtained from Cayman Chemical (Michigan, USA). Cell anchoring molecule, SUNBRIGHT OE-020CS, was purchased from NOF Corporation (Tokyo, Japan). The pyramid probe (SN-AF01S-NT; spring constant: around 0.06 N/m) was purchased from Olympus (Tokyo, Japan). Fetal bovine serum (FBS) was purchased from Life Technologies Japan Ltd. (Tokyo, Japan). Antibiotics, phorbol 12-myristate 13-acetate (PMA) were purchased from Sigma-Aldrich (St. Louis, MO). Glass-based culture dishes were purchased from Matsunami Glass (Osaka, Japan). 6 Channel μ-Slide was purchased from ibidi, Germany. Other reagents were purchased from Sigma-Aldrich, Wako Pure Chemical Industries Ltd., or Life Technologies Japan Ltd.

Preparation of cell anchoring dishes

The culture dishes were coated with cell anchoring molecule, SUNBRIGHT OE-020CS, as described previously (Haghparast, 2013). Briefly, the polystyrene tissue culture dishes were coated with BSA, and then the surfaces were coated with SUNBRIGHT OE-020CS. Floating cells are caught at oleyl group at one end of SUNBRIGHT OE-020CS in coated dishes (Kato, 2003). Therefore, the anchored cells were fixed and then the cell surface stiffness can be measured by AFM (Shimizu, 2012; Shimizu, 2012).

Cell culture

KG-1 cells were cultured in RPMI1640 medium containing 10% FBS and the antibiotics (100 units/mL penicillin G and 100 μg/mL streptomycin sulfate) in humidified atmosphere of 95% air and 5% CO_2 at 37°C.

AFM measurements

The cell stiffness was measured by AFM (Nanowizard III; JPK Instruments AG, Berlin, Germany) at room temperature. KG-1 cells were plated on the cell anchoring culture dishes for 1.5 h in serum free medium, then washed with PBS to remove unattached cells, and cultured for 6 h in α-mangostin containing complete culture medium. The cone shaped AFM probe was indented 25 different points within 1 μm × 1 μm of cell top with a loading force of up to 0.5 nN and velocity of 5 μm/s. Then the Young's modulus of the cell surface was calculated with the Hertz model (Hertz, 1881); the force-indentation curve for a region up to about 1 μm of indentation was fitted using JPK data processing software (JPK instruments AG) as:

$$F = \frac{E}{1-\nu^2}\frac{2\tan\alpha}{\pi}\delta^2$$

Where F = force, δ = depth of the probe indentation, ν = Poisson's ratio (0.5), α = half-angle of the cone probe (9°), and E = Young's modulus. The median value adopted for the Young's modulus of each cell (Kihara, 2011). More than 21 cells and 525 force-distance curves were analyzed in each condition.

Actin filaments staining

KG-1 cells were seeded on the cell anchoring glass base dishes for 1.5 h in serum free medium, then washed with PBS to remove floating cells, and cultured for 6 h in 10 μM α-mangostin or for 1.5 h in 2 μg/mL cytochalasin D containing complete culture medium. Then the culture cells were fixed with 4% paraformaldehyde, permeabilized with 0.3% TritonX-100, and

then stained with rhodamine labeled-phalloidin for actin filaments and DAPI for nucleus. Specimens were observed by fluorescence microscopy (IX81, Olympus).

Adherent assay

The 6 Channel μ-Slide were incubated with PBS containing 50 μg/mL of Fibronectin for 1 h in room temperature, and then washed three times with PBS. Suspended KG-1 cells in medium at 1 x 10^6 cells/mL with α-mangostin or PMA, or BIM I were incubated in fibronectin coated Slide for 3 h in 37^0C. For counting, the Slides were washed three times with medium to remove floating cells, then specimens were taken photos by using phase contrast microscopy. The data were analyzed by ImageJ software (NIH, Bethesda, MD).

Western blot analysis

KG-1 cells were treated with α-mangostin then washed with ice-cold PBS and lysed in ice-cold RIPA buffer (1mM Tris-HCl pH 8.8, 150mM NaCl, 1% SDS, 1mM EDTA, 1M phosphatase , MiliQ water) with a protease inhibitor cocktail tablet (Roche, Germany) for 30 min at 4^0C. Protein from cell lysates were quantified using BCA Assay Kit (Thermo Fisher scientific), and equivalent amounts of proteins were loaded on sodium dodecylsulfate polyacrylamide gels. Separated proteins were transferred to a 0.45-μm nitrocellulose membrane (GE Healthcare Life Sciences), then the membrane was blocked with blocking buffer (1% BSA, 1X PBST) for overnight at 4^0C. After blocking, the membrane was incubated with primary antibodies, then with HRP-conjugated anti-rabbit IgG. The complex with the HRP-linked secondary antibody was detected using DAB (3,3'-Diaminobenzidine). Densitometry analysis of Western blot data was carried out using Image J software.

References

Bray, D. et al. (1986) The membrane-associated 'cortex' of animal cells: its structure and mechanical properties. J. Cell Sci. 71–88

Berlin, C., Bargatze, R.F., Campbell, J.J., von Andrian, U.H., Szabo, M.C., Hasslen, S.R., et al. α4 integrins mediate lymphocyte attachment and rolling under physiologic flow. Cell 1995; 80:413-22.

Brown MJ, Nijhara R, Hallam JA, Gignac M, Yamada KM, Erlandsen SL, et al. Chemokine stimulation of human peripheral blood T lymphocytes induces rapid dephosphorylation of ERM proteins, which facilitates loss of microvilli and polarization. Blood. 2003;102:3890–3899.

Chen, G., Li, Y., Wang, W., Deng, L. Bioactivity and pharmacologi- cal properties of alpha-mangostin from the mangosteen fruit: a review. Expert Opin Ther Pat. 2018;28(5):415–27.

Chhabra, E.S., Higgs, H.N. The many faces of actin: matching assembly factors with cellular structures. Nat Cell Biol 2007; 9:1110-21.

Collinsworth AM, Zhang S, Kraus WE, Truskey GA. Apparent elastic modulus and hysteresis of skeletal muscle cells throughout differentiation. Am J Physiol Cell Physiol. 2002;283(4):C1219–C12271227.

Drew E., Merzaban J.S., Seo,W. et al., CD34 and CD43 inhibit mast cell adhesion and are required for optimal mast cell reconstitution, Immunity 22 (2005) 43e57.

Fang Y, Su T, Qiu X, Mao P, Xu Y, Hu Z, Zhang Y, Zheng X, Xie P, Liu Q. Protective effect of alpha-mangostin against oxidative stress induced-retinal cell death. Sci Rep. 2016 Feb 18;6:21018. doi: 10.1038/srep21018. PMID: 26888416; PMCID: PMC4757868.

Dai J, Sheetz MP. Mechanical properties of neuronal growth cone membranes studied by tether formation with laser optical twee- zers. Biophys J. 1995;68(3):988–96.

Dustin M.L., Springer T.A., T-cell receptor cross-linking transiently stimulates adhesiveness through LFA-1, Nature 341 (1989) 619e624.

Fiéver B., Louvard D., Arpin M., ERM proteins in epithelial cell organization and functions, Biochem. Biophys. Acta 1773 (2007) 653e660.

Fukuda M., Tsuboi S., Mucin-type O-glycans and leukosialin, Biochem. Biophys. Acta 1455 (1999) 205e217.

Guilak F, Erickson GR, Ting-Beall HP. The effects of osmotic stress on the viscoelastic and physical properties of articular chon- drocytes. Biophys J. 2002;82(2):720–7.

Guillaume T. Charras, Chi-Kuo Hu, Margaret Coughlin, Timothy J. Mitchison; Reassembly of contractile actin cortex in cell blebs . J Cell Biol 6 November 2006; 175 (3): 477–490.

Haghparast, S.M., Kihara, T., Shimizu, Y., Yuba, S., Miyake, J. Actin- based biomechanical features of suspended normal and cancer cells. J Biosci Bioeng. 2013;116(3):380–5.

Haghparast SM, Kihara T, Miyake J. Distinct mechanical behavior of HEK293 cells in adherent and suspended states. PeerJ. 2015;3:e1131.

Haga H, Sasaki S, Kawabata K, Ito E, Ushiki T, Sambongi T. Elasticity mapping of living ffibroblasts by AFM and immunofluorescence observation of the cytoskeleton. Ultramicroscopy. 2000;82(1–4):253–8.

Haghparast SM, Kihara T, Shimizu Y, Yuba S, Miyake J. Actin-based biomechanical features of suspended normal and cancer cells. J Biosci Bioeng. 2013;116(3):380–5.

Hertz, H. Über die berührung fester elastischer Körper. J Reine Angewandte Math. 1881;92:156–71.

Hemler M.E., Mihich E., Cell Adhesion Molecules, Plenum Press, NY, 1993.

Hynes R.O., Integrins: versatility, modulation, and signaling in cell adhesion, Cell 69 (1992) 11e25.

Kagiwada H, Nakamura C, Kihara T, Kamiishi H, Kawano K, Nakamura N, et al. The mechanical properties of a cell, as determined by its actin cytoskeleton, are important for nanoneedle insertion into a living cell. Cytoskeleton (Hoboken). 2010;67(8):496–503.

Kato K, Umezawa K, Funeriu DP, Miyake M, Miyake J, Nagamune T. Immobilized culture of nonadherent cells on an oleyl poly(ethylene glycol) ether-modified surface. Biotechniques. 2003;35(5):1014–21.

Kihara T, Haghparast SM, Shimizu Y, Yuba S, Miyake J. Physical properties of mesenchymal stem cells are coordinated by the perinuclear actin cap. Biochem Biophys Res Commun. 2011;409(1):1–6.

Kihara T, Haghparast SM, Shimizu Y, Yuba S, Miyake J. Physical properties of mesenchymal stem cells are coordinated by the perinuclear actin cap. Biochem Biophys Res Commun. 2011;409(1):1–6.

Krause D.S., Fackler M.J., Civin C.I., May W.S., CD34: structure, biology, and clinical utility, Blood 87 (1996) 1e13.

Kunda P, Pelling AE, Liu T, Baum B. Moesin controls cortical rigidity, cell rounding, and spindle morphogenesis during mitosis. Curr Biol. 2008;18(2):91–101.

Matzke R, Jacobson K, Radmacher M. Direct, high-resolution measurement of furrow stiffening during division of adherent cells. Nat Cell Biol. 2001;3(6):607–10. 36.

Mooseker, M.S., Tilney, L.G. Organization of an actin filament-membrane complex: Filament polarity and membrane attachment in the microvilli of intestinal epithelial cells. J Cell Biol 1975; 67:725-43.

Niggli V., Rossy J., Ezrin/radixin/moesin: versatile controllers of signaling molecules and of the cortical cytoskeleton, Int. J. Biochem. Cell Biol. 40 (2008) 344e349.

Ohnishi H, Sasaki H, Nakamura Y, et al. Regulation of cell shape and adhesion by CD34. *Cell Adh Migr*. 2013;7(5):426-433. doi:10.4161/cam.25957.

Phan TKT, Shahbazzadeh F, Pham TTH, Kihara T. Alpha-mangostin inhibits the migration and invasion of A549 lung cancer cells. PeerJ. 2018;6:e5027.

Phan, T.K.T., Shahbazzadeh, F. & Kihara, T. Alpha-mangostin reduces mechanical stiffness of various cells. Human Cell 33, 347–355 (2020).

Radmacher M, Fritz M, Kacher CM, Cleveland JP, Hansma PK. Measuring the viscoelastic properties of human platelets with the atomic force microscope. Biophys J. 1996;70(1):556–67.

Shimizu Y., Newman W., Gopal T.V., et al., Four molecular pathways of T cell adhesion to endothelial cells: roles of LFA-1, VCAM-1, and ELAM-1 and differ activation conditions, J. Cell Biol. 113 (1991) 1203e1212.

Shimizu, Y., Haghparast, S.M., Kihara, T., Miyake, J. Cortical rigidity of round cells in mitotic phase and suspended state. Micron. 2012;43(12):1246–51.

Shimizu, Y., Kihara, T., Haghparast, S.M., Yuba, S., Miyake, J. Simple display system of mechanical properties of cells and their dispersion. PLoS ONE. 2012;7(3):e34305.

Singer II, Scott S, Kawka DW, Chin J, Daugherty BL, DeMartino JA, et al. CCR5, CXCR4 and CD4 are clustered and closely apposed on microvilli of human macrophages and T cells. J Virol 2001; 75:3779-90.

Tachibana K., Haghparast S.M.A., Miyake J., Inhibition of cell adhesion by phosphorylated Ezrin/Radixin/Moesin, Cell Adhes. Migrat. 9 (2015) 502e512.

Tachibana K., Yamane J., Haghparast S.M.A., Miyake J., Sialomucin and phosphorylated-ERM are inhibitors for cadherin-mediated aggregate formation, Biochem. Biophys. Res. Commun. 520 (2019) 159e165.

Tachibana K, Ohnishi H, Ali Haghparast SM, Kihara T, 565 Miyake J. Activation of PKC induces leukocyte adhesion by the 566 dephosphorylation of ERM. Biochem Biophys Res Commun. 567 2020;523(1):177–82.

Trickey WR, Vail TP, Guilak F. The role of the cytoskeleton in the viscoelastic properties of human articular chondrocytes. J Orthop Res. 2004;22(1):131–9.

van Kooyk Y., van de Wiel-van Kemenade P., Weder P., et al., Enhancement of LFA-1-mediated cell adhesion by triggering through CD2 and CD3 on T lym- phocytes, Nature 342 (1989) 811e813.

von Andrian UH, Hasslen SR, Nelson RD, Erlandsen SL, Butcher EC. A central role for microvillous recep- tor presentation in leukocyte adhesion under flow. Cell 1995; 82:989-99.

Yamane J, Ohnishi H, Sasaki H, Narimatsu H, Ohgushi H, Tachibana K. Formation of microvilli and phosphorylation of ERM family proteins by CD43, a potent inhibitor for cell adhesion: cell detachment is a potential cue for ERM phosphorylation and organization of cell morphology. Cell Adh Migr. 2011;5(2):119-132. doi:10.4161/cam.5.2.13908

Figures

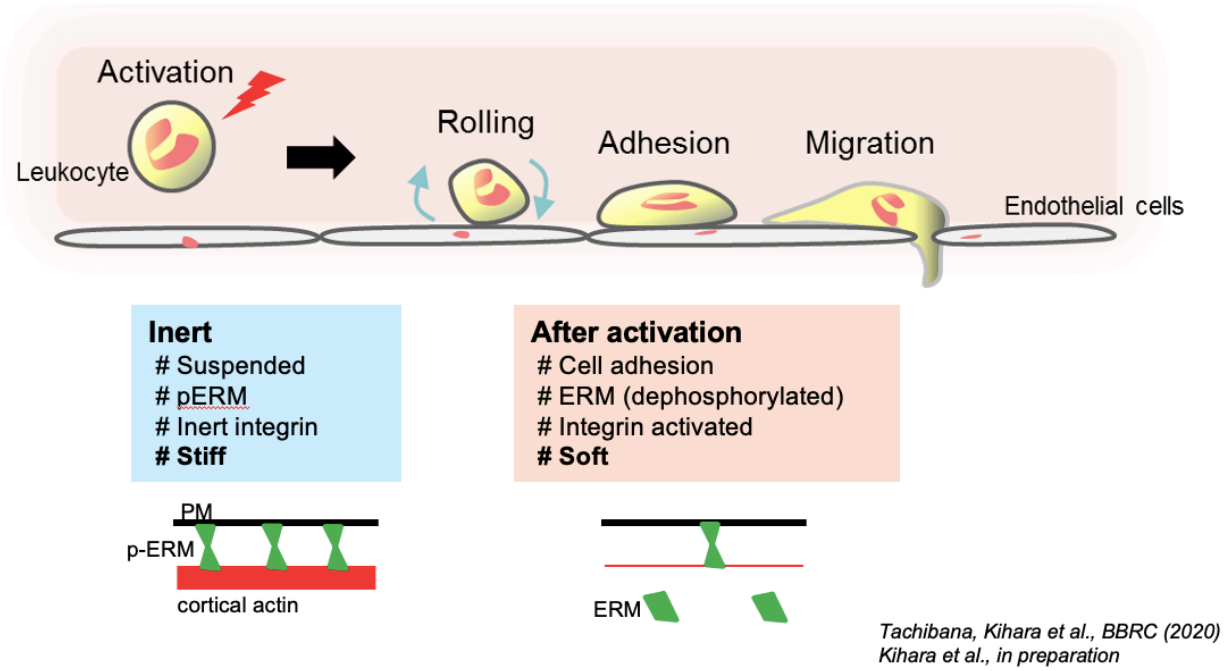

Figure 5.1. The leukocyte adhesion cascade. Progress has been made in defining steps: capture (or tethering), slow rolling, adhesion strengthening and spreading, and transcellular transmigration.

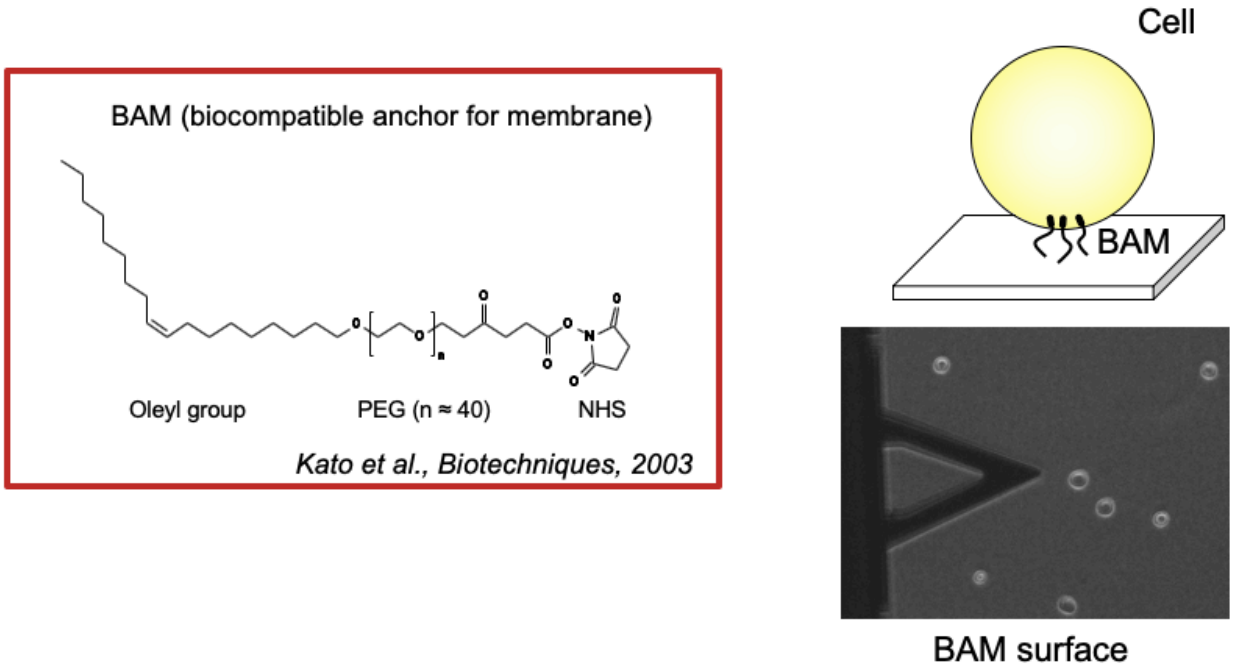

Figure 5.2. BAM molecules covalently bind with BSA coated dish surface. The suspended round cells can be fixed on the BAM surface. I can measure the elasticity of floating cells by AFM using BAM surface.

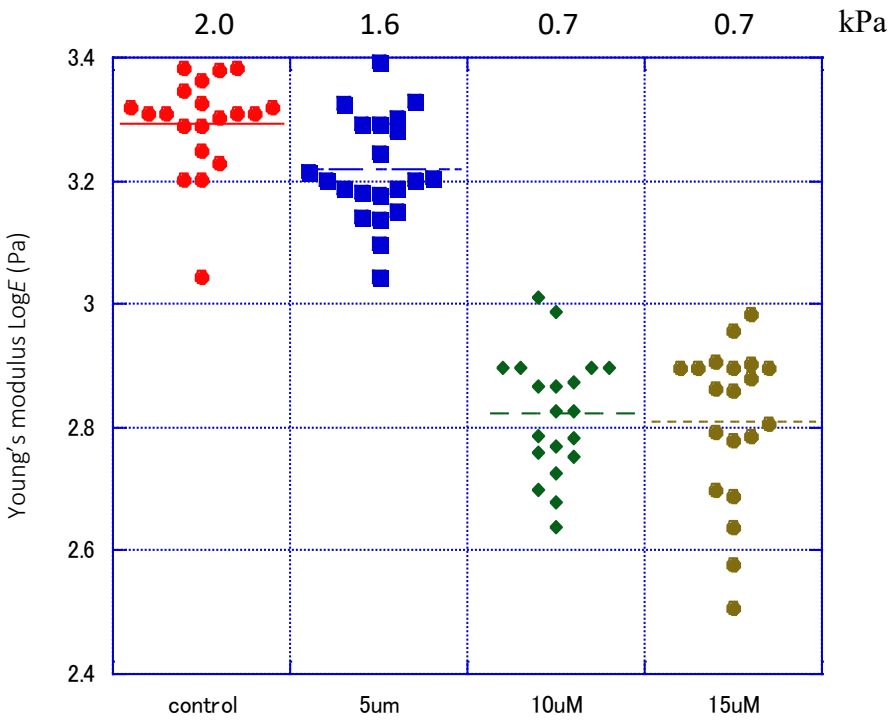

Figure 5.3. Young's modulus of KG-1 cells treated with α-mangostin, then examined by AFM. The distribution of the Young's modulus of cells treated with α-mangostin for 6 h is represented by scatterplots. Each point represents the median value of 25 measuring points in each cell, and the Young's modulus in each condition is represented in more than 21 independent cells.

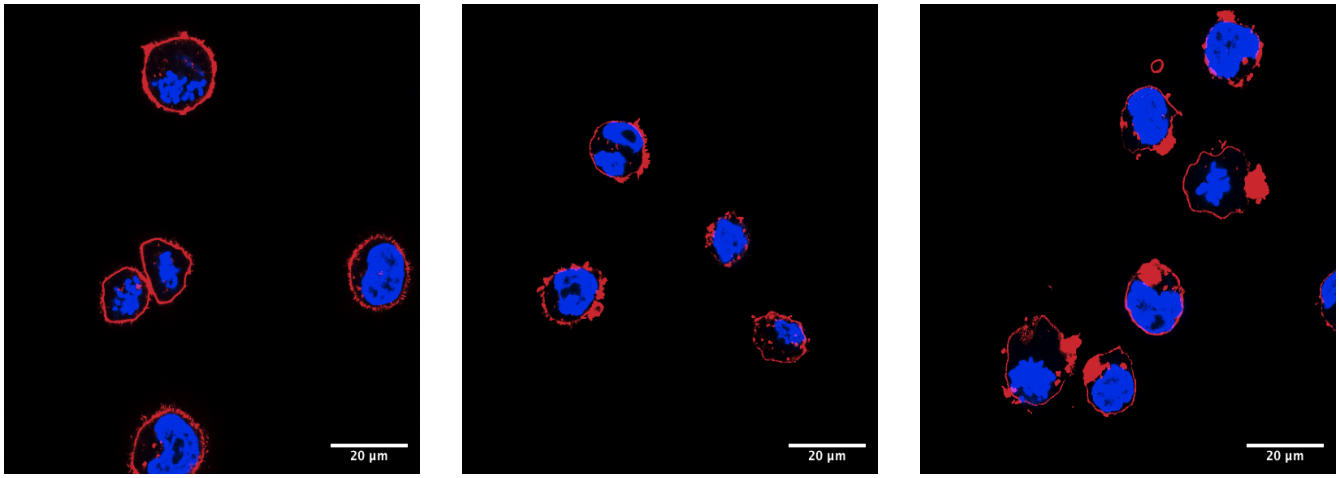

Figure 5.4. The cortical actin of KG-1 after treatment with α-mangostin. KG-1 cells were exposed with α-mangostin for 6 h or 2 µg/mL of cytochalasin D (CD) for 1.5 h, and then the actin filaments stained with rhodamine labeled-phalloidin, and DAPI (4′,6-diamidino-2-phenylindole) labeled the nucleus.

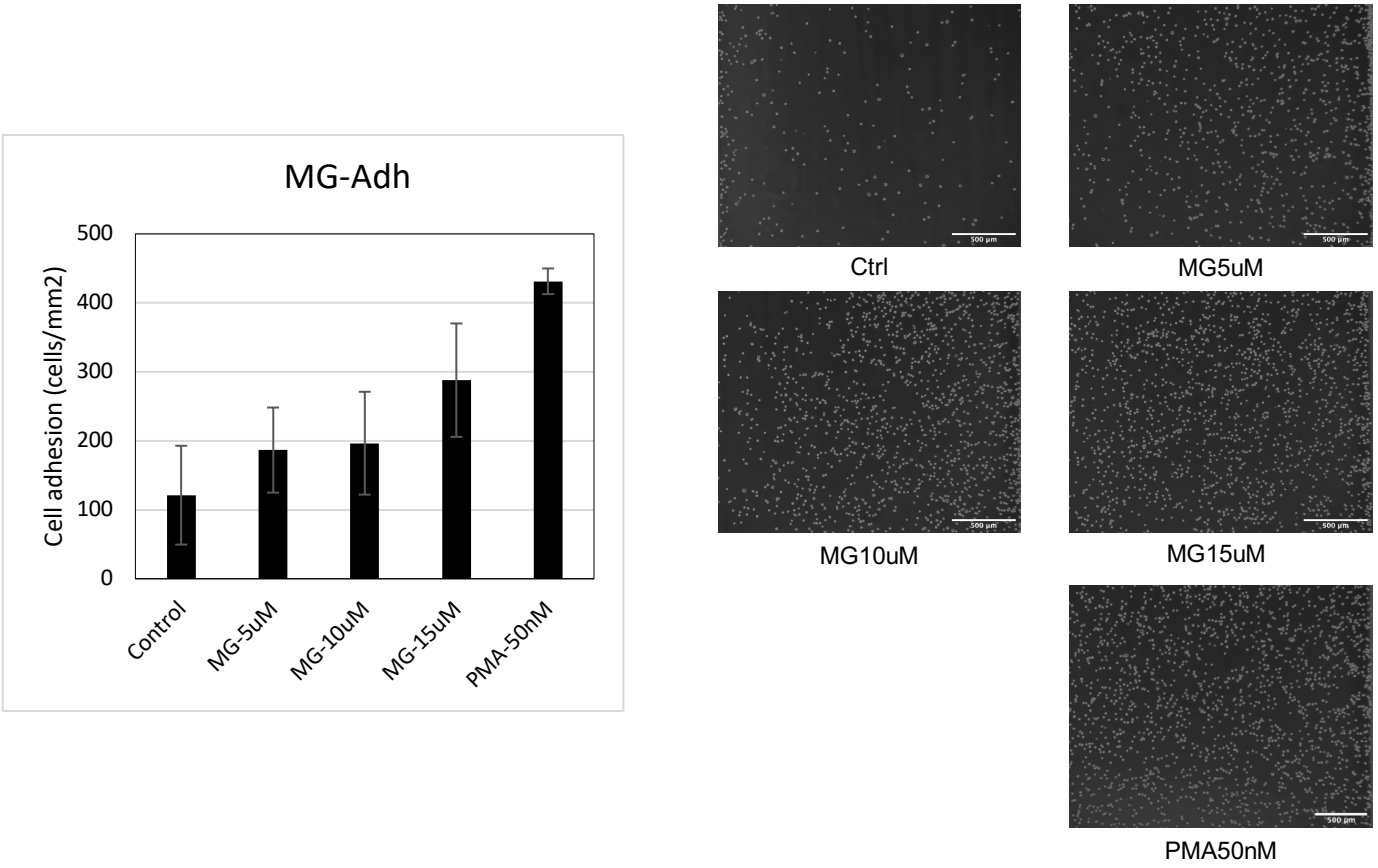

Figure 5.5. α-Mangostin induced KG-1 cell adhesion to Fibronectin-coated dish. Cell culture dishes were coated with Fibronectin for 1h, then KG-1 cells were seeded with/without α-Mangostin (5, 10, 15 μM) or with PMA for 3 h incubation.

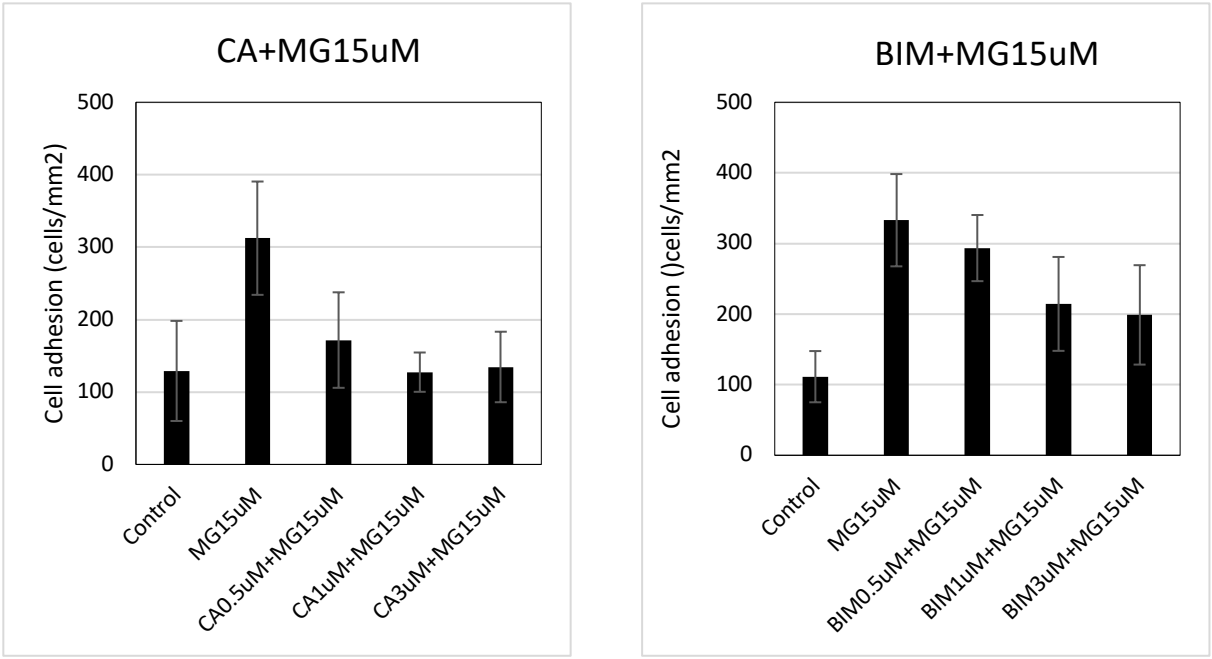

Figure 5.6. α-Mangostin induced KG-1 cell adhesion to Fibronectin-coated dish. Cell culture dishes were coated with Fibronectin for 1h, then KG-1 cells were seeded with α-Mangostin 15 μM plus Calyculin A (CA) or Bisindolylmaleimide I (BIM) for 3 h incubation.

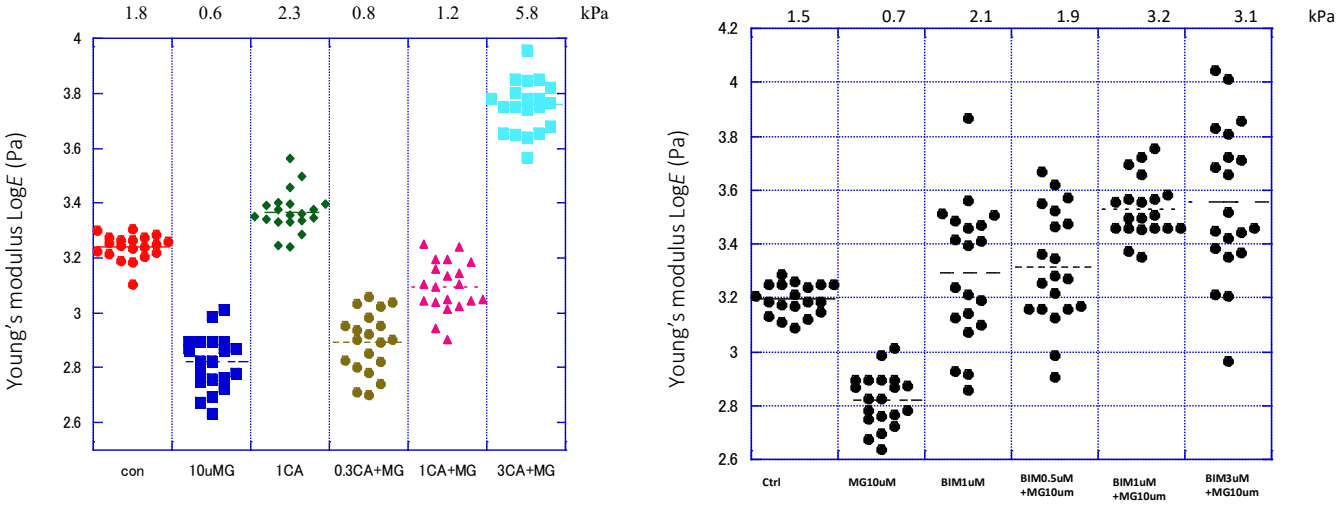

Figure 5.7. Young's modulus of KG-1 cells treatment with α-Mangostin plus Calyculin A or Bisindolylmaleimide I. The distributions of the Young's moduli of cells are shown as scatter plots in different concentration treatment of α-mangostin plus CA or BIM for 6 h. Each condition displays the Young's modulus of more than 20 individual cells.

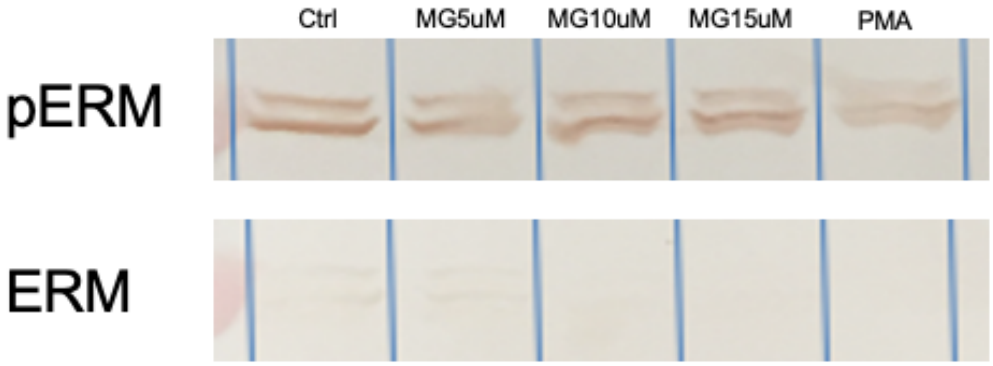

Figure 5.8: The ERM protein expression level after treatment with α-mangostin. KG-1 cells were pre-incubated with α-mangostin for indicated time, then the cells were subjected with western blot.

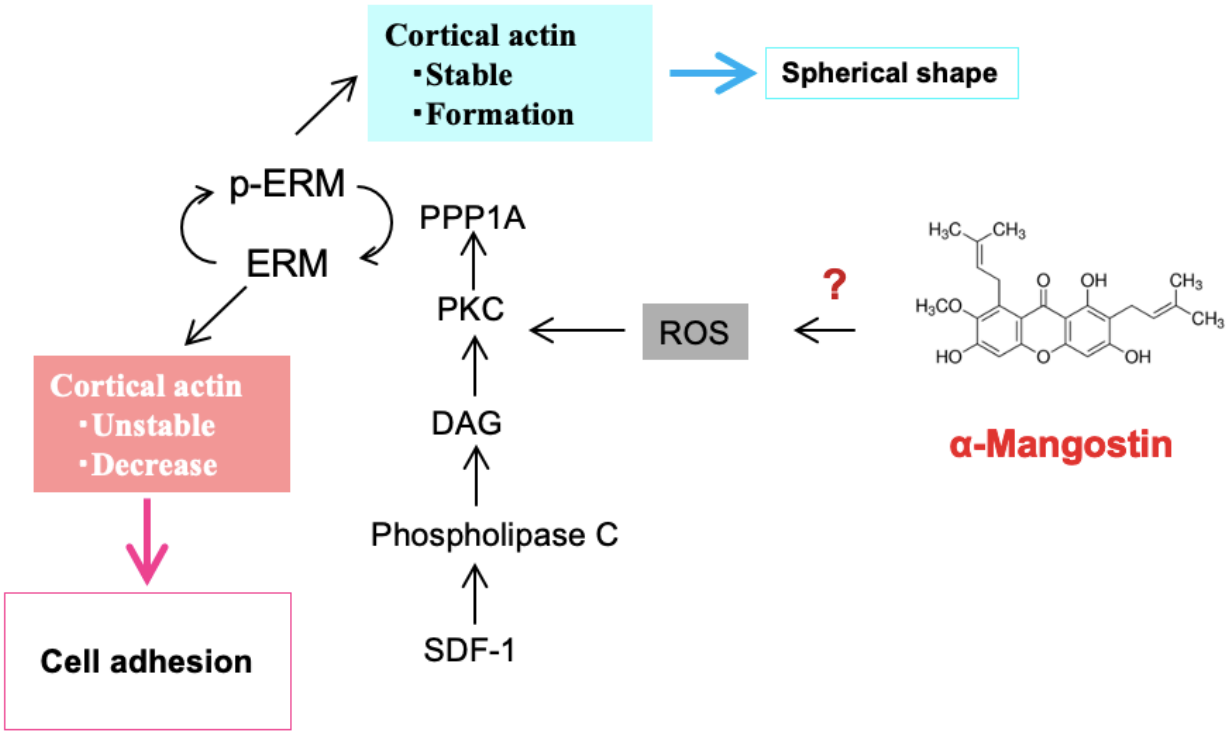

Figure 5.9: Schema of potential signaling pathways for α-mangostin-activated-KG1 cells. As for the mechanism by which α-mangostin induces KG-1 cell adhesion, activated PKC and protein phosphatase are one of important factors that α-mangostin regulated through to activate leukocytes. In addition, I hypothesize that α-mangostin induces ROS which activates PKC and regulate the protein phosphatase, so ROS may also play role in this signalling pathway.

Chapter 6: General Discussion and Conclusion

In this study, the various functions of α-mangostin from pericarp of mangosteen fruit *Garcinia Mangostana* Linnincluding "α-mangostin inhibits metastasis" (Chapter 3), "α-mangostin reduces the cell surface mechanical of various cell types" (Chapter 4), and "α-mangostin induces cell adhesion and activates leukocytes" (Chapter 5) has been demonstrated. As mentioned in the General Introduction, α-mangostin has been explored with various biological function and also pharmacological properties. The anticarcinogenic properties of α-mangostin attracts the most interesting from sicientists. However, almost studies about the anticarcinogenic activities of α-mangostin were examined on the mono-culture which are lack of interaction between normal cell and cancer cells. Therefore, I designed the co-culture system in order to mimic the communication of cancer cell and normal cell which also reflects the invasion process. The function of α-mangostin on cancer cells were found that it did not only kill cancer cells at high dose, but also inhibit the migration and invasion of cancer cells. In addition, there are two new biological functions of α-mangostin on the cell stiffness and leukocyte which have not published, it has been described in the Chapter 4 and 5 in my studies. Therefore, my studies provided more evidences support for the multi-biological functions of α-mangostin.

6 – 1. The variety function of α-mangostin on cancer cells

Several potential natural compounds are expected to develop chemotherapeutic agent with high efficiency and less side effects. α-Mangostin has been indicated as a potential candidate through hundred researches about anticancer activities. In my study, it is demonstrated that α-mangostin can kill cell at high concentration treatment. Besides, α-mangostin has been improved that can prohibited the metastasis process of cancer cells. However, these researches are mainly

performed by detecting of cancer cells in mono-culture which lack the cell-cell interaction existing in the body. Therefore, in order to indicated more accurate result of the effect of α-mangostin on cancer metastasis, a co-culture system of cancer cells and normal cells are need to be establish.

In this study, I developed one simple co-culture system by culture both cancer cells and normal cells together, then α-mangostin was exposed and observed its impacts. In co-culture system, lung cancer cells presented their strong growth and damaged to lung normal cells with the percentage of cancer cells taking places in culture dish (Fig. 3.7). Comparison to mono-culture, cancer cells still grow well, but it is not strong like it in co-culture (Fig. 3.6). In addition, by treatment with α-mangostin significant inhibited the suffusion of cancer cells by increasing the area of normal cells on co-culture dish (Fig. 3.7). However, cancer cells in mono-culture were almost disappeared at them same concentration of α-mangostin and culture periods.

Therefore, in this study I found the multi-function of α-Mangostin on cancer cells including cause of the cytotoxicity on cancer cells, inhibition of the cancer cell migration. Especially, thanks to using the co-culture system which provides chance for cancer cells and normal cells make communication, α-Mangostin was found that inhibited the invasive activities of cancer cell and also support the survival of normal cells in this co-culture system.

6 – 2. α-Mangostin reduces the stiffness of various cell types.

According many studies, alternations in biological activities and transformation of cells states often entail a change in the mechanical behavior of cells. The change in cell stiffness has emerged as a marker for cellular phenotypic events and diseases. Malignant cancer cells exhibit lower stiffness than normal cells. The mechanical properties are mainly attributed to the cytoskeleton components, especially actin microstructures. Therefore, the stiffness alternations reflect the remodeling process of the actin and other cytoskeletal elements in the respective cellular

events and disease states. α-Mangostin has been discovered inhibited the migration and invasion of cancer cells, so whether α-mangostin change the stiffness of cells.

Different cell types including normal human fibroblast TIG-1 cells, human cervical cancer HeLa cells, human embryonic kidney HEK293 cells, mouse leukemia macrophage RAW 264.7 cells, and human leukemia myeloblasts KG-1 cells were used for this study. TIG-1, HeLa, HEK293, and RAW 264.7 cells are adherent cells and KG-1 cells are suspension cells. The morphologies of these cells vary, and the features of the actin cytoskeleton vary in these cell types. TIG-1 cells have an elongated morphology; HeLa and HEK293 cells have a shortly extended morphology; RAW 264.7 cells have weakly adhering morphology; and KG-1 cells are suspended and spherical shape. These cells are varied phenotypes and cytoskeleton structure, but their cell surface stiffness is reduced by treatment with α-mangostin.

The stiffness of TIG-1 cells, HEK293 cells and RAW 264.7 cells are slightly reduced comparison to KG-1 cells and Hela cells. TIG-1 cells show the well-developed actin stress fiber and their stiffness is also high due to the developed actin stress fiber. While the HEK293 cells contains immature actin cytoskeletons, and their stiffness are also slightly decreased by α-mangostin. The cytoskeleton structures of RAW 264.7 cells contain of F-actin at the cell-cell border and cortical region along with protrusion. RAW 264.7 cells resistance the cytotoxicity of α -mangostin, but its stiffness was little changed. α-Mangostin also did not change the actin cytoskeleton structures of these cells (Fig. 4.8).

The stiffness of KG-1 cells and Hela cells were largely reduced by α-mangostin. KG-1 cells had cortical actin, Hela cells obtained many fine fibers inside the cells, and both types of cells have many short microvillus and protrusion on their surface. At the base of each microvillus, the actin filaments are anchored into a specialized region known as the terminal web. This contains a

concentrated network of spectrin molecules and a layer of intermediate filaments. It is thought that spectrin imparts rigidity to the cell cortex; because the actin filaments are anchored to the terminal web, this keeps the microvilli orientated perpendicularly to the apical surface of the cell. The actin filaments are attached to the plasma membrane by lateral bridges composed of myosin-I and several other molecules including the Ca^{2+} and the Ca^{2+} binding protein, Camodulin. Therefore, α-mangostin is sensitive with microvilli for the reduction of the stiffness.

α-Mangostin has been found reduced the cell surface stiffness but did not change the cytoskeleton actin structures. However, α-mangostin was improved that has contradictory functions on the molecules that impacts the actin cytoskeleton, such as it increases MLCP, reduces Ca^{2+} elevation, inhibits MLCK. Therefore, the results indicated α-mangostin regulate the signal cascades of the actin cytoskeleton inside these cells and it is needed to the further study to confirm.

6 – 3. α-Mangostin reduces the cell stiffness related to the adhesion and activation of leukocytes.

In the above study, KG-1 cells were mentioned that is sensitive with α-mangostin in reduction of the cell surface stiffness. In addition, KG-1 had only cortical actin on plasma membrane and short microvillus on the cell surface. The mechanical properties and surface microvilli are involvement with KG-1 cells adhesion and stimulation. Therefore, in this study we continue to use KG-1 in order to reveal the molecules involved with the reduction of the stiffness caused by α-mangostin.

KG-1 cells were exposing with α-mangostin for 6 h and result in decrease of the cell surface stiffness. In addition, KG-1 cells just obtain a simple cytoskeleton structure – cortical actin and microvilli, so after treatment with α-mangostin they were stained with rhodamine phalloidin. The

results presented α-mangostin decreased significantly number of microvilli on KG-1 surface. In addition, it appeared the blebbing on surface which blurred the actin cortical. Therefore, these results indicated the actin microvilli is sensitive targeting of α-mangostin in changing the mechanical properties of leukocytes.

In addition, the decreased of leukocytes stiffness has been indicated that relates to leukocytes activation. KG-1 cells are non-adhesion cells in maintenance culture, but in the present of α-mangostin, KG-1 cells adhered to Fibronectin-coated dish. α-Mangostin-induced KG-1 cell adhesion occurred in very short time, so it is the results of signal transduction, not the results of differentiation.

The induction of cell adhesion and reduction of stiffness of KG-1 by α-mangostin is prevented by Calyculin A (protein phosphatase 1/2A inhibitor) and BIM (PKC inhibitor). Therefore, the activation of PKC and protein phosphatase 1/2A (PPP1A) are the target signaling of α-mangostin in activation of leukocytes. The leukocytes are activated by PMA, SDF-1 which also regulated via PKC and PPP1A involved with dephosphorylation of ERM protein.

In previous researches indicate α-mangostin induces Ca^{2+} influx in platelets; it inhibits Ca^{2+}-ATPase in the sarcoplasmic reticulum; and it reduces Ca^{2+} elevation by suppressed Ca^{2+}influx. The Ca^{2+} influx is involved with regulate stress fiber and result in change the cell surface stiffness. Therefore, further study examining Ca^{2+} influx might reveal the signal cascade related in the processes of the mechanical change caused by α-mangostin.

6 – 4. Conclusion

The figure 6.1 shows a summary of the multi-biological function of α-mangostin discovered in my studies. α-Mangostin presented its cytotoxicity for different cell types at high concentration treatment excepted RAW cells. In addition, α-Mangostin also present its anti-metastasis activities by disturbing the communication between cancer cells and normal cells. The secret proteins, cytokines and growth factors in cancer cells are declined by α-mangostin, it prevented cancer cells send "message" to normal cells. Thus, α-mangostin protects the normal cells from cancer cells and prohibited the invasion of cancer cells on normal cells.

Whiles α-mangostin inhibited the migration of cancer cells, it is found that α-mangostin decreased the cell surface stiffness of various cells. α-Mangostin has been found that changed the cell surface stiffness not only cancer cells, but also different types of cells including human fibroblast cells, human cancerous cells, human embryonic kidney cells, mouse macrophage cells, and human myeloblasts cells. α-Mangostin dose not impact to change the actin cytoskeleton in these cells, but its target in the process of changing the cell stiffness is microvilli – a weak structure of actin filaments. In addition, α-mangostin is firstly investigated on the leukocytes and found that reduces the cell stiffness related to the cell adhesion and activation of leukocytes via activation of PKC and protein phosphatase 1/2A.

To conclusion, my findings will provide more evidences for the use of complex- and multi-biological functional α-mangostin in future pharmaceutical application.

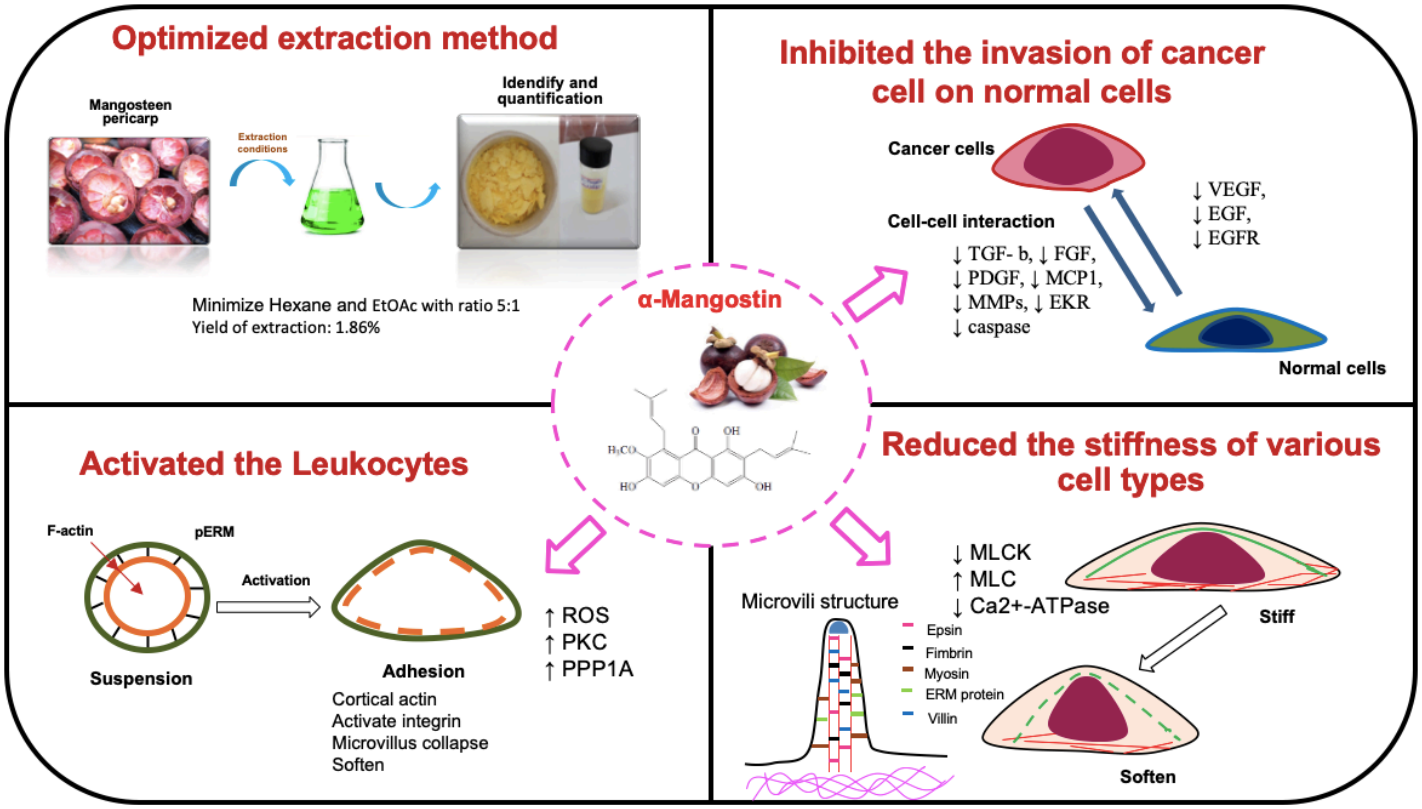

Figure 6.1: Summary the multi-biological function of α-mangostin.

Acknowledgement

I would like to express the most gratitude and appreciation to my supervisor Ass.Prof. Takanori Kihara for your kindly supporting, teaching and inspiring me in scientific research. I am very lucky and proud to be your student, you are not only my supervisor, but you are also very important with me like a “father” in all time I lived in Japan. You teach me many things about research, kindly help me to resolve trouble in my research and give me many useful advices.

Besides my supervisor, I also would like to be very grateful to Prof. Hidenari Yasui and Prof. Kazuo Sakurai for very precious supporting me in order to have more comfortable life in here and pursue my dream with research.

My PhD thesis will not be completed without the support from all reviewers. Therefore, I am very grateful to Prof. Hidenari Yasui, Prof. Kazuo Sakurai, Prof. Nakazawa and Ass.Prof.Dr. Takehito Hayami for giving me very useful, meaning comments to my thesis.

I also want to give a million thanks to all Kihara lab’s members who are always be side by me whenever I have trouble, and we were working together before deadlines, and had a lot of fun memories together. You supported me very much to complete my research and also my life in here.

I thank my all Vietnamese friends in here, you are very important for me because you are the same as a “medicine” for me when I am stressed or homesick.

I would like to thank my two very important “friends”, my mother and my father for always supporting me spiritually throughout almost 5 year that I pursued my research in Japan.

Last but not the least, I would like to send a three thousand thanks to my very special person PhD. Thanh Duong Nguyen who are not by side me but are always ready to support me in life and research.